DNMT1 IN INTESTINAL DEVELOPMENT AND CANCER

Ellen N. Elliott

A DISSERTATION

in

Cell and Molecular Biology

Presented to the Faculties of the University of Pennsylvania

in

Partial Fulfillment of the Requirements for the

Degree of Doctor of Philosophy

2015

Supervisor of Dissertation

_____

Klaus H. Kaestner, Ph.D.

Thomas and Evelyn Suor Butterworth Professor in Genetics

Graduate Group Chairperson

_____

Daniel S. Kessler, Ph.D.

Associate Professor of Cell and Developmental Biology

Dissertation Committee

Marisa S. Bartolomei, Ph.D., Professor of Cell and Developmental Biology

John P. Lynch, M.D., Ph.D., Associate Professor of Medicine

Jonathan P. Katz, M.D., Associate Professor of Medicine

Christopher J. Lengner, Ph.D., Assistant Professor of Biomedical Sciences

Acknowledgements

There are many people I would like to thank, who have aided and supported me over the past five years. First and foremost, I want to thank Klaus Kaestner, my thesis mentor, and also a dear friend. Thank you for taking me into your lab, providing an excellent scientific training environment, and encouraging me in each step of my Ph.D. Klaus continues to challenge me, and has made me a true scientist. He was also incredibly understanding and supportive of my life outside of the lab. Thank you for giving me the confidence to pursue scientific research as a career. I will miss you, and the Kaestner lab family, so much.

I also want to thank Karyn Sheaffer, with whom I have worked from the very beginning of graduate school, during my rotation in the Kaestner lab. I also collaborated with her for Chapter 4 of this thesis, which would not exist without her tenacity and curiosity. She taught me everything I know about the intestinal epithelium, and is so much fun to work with. You are a great scientist, and an amazing, hilarious, sarcastic person, and I wish you all the best going forward.

Of course, I also want to thank the Kaestner Lab Gut Club, including Karyn Sheaffer, Julia Kieckhaefer, Rinho Kim, Michal Shoshkes-Carmel, and Reina Aoki, who taught me numerous experimental techniques, edited and critiqued my papers, and helped me troubleshoot experiments. A special thank you to Julia, who taught me organoid culture, and to Karyn, who trained me in next-generation sequencing techniques.

For their technical assistance and advice on all things related to sequencing, I want to thank the Functional Genomics Core, especially Jonathan Schug, Olga Smirnova, Joe Grub, Haleigh Zilges, and Shilpa Rao. The FGC were invaluable in my sequencing experiments and data analysis. I especially want to thank Olga, who advised me during my RNA-Seq experiments, and Jonathan, who worked with me in RNA-Seq analysis and aligned all of my bisulfite sequencing data.

There are many other members of the Kaestner lab that I need to thank. I especially want to acknowledge Tia Bernard-Banks, who took care of all my mice the past four years; thank you so much, the lab would fall apart without you. I also want to thank Diana Bernstein and Vasu Kameswaran, for your help with countless sequencing projects, and for providing much needed

emotional support when necessary. I would like to thank everyone else in the Kaestner lab, because if I haven't mentioned you, I should have. Thank you for being a bunch of great people. I will miss you all.

I particularly want to recognize and thank the GI Tissue and Morphology Core, including Adam Bedenbaugh, Daniela Budo, and Roxana Hasan. Thank you for the hundreds of serial sections, and for your cooperation in all of the tissues I needed sectioned for laser-capture microdissection. You are the best at what you do. Thank you Thaddeus Stappenbeck for inviting me to the Stappenbeck lab at Washington University in Saint Louis, and to Kelli VanDussen for training me on the Arcturus LCM equipment. I also want to acknowledge John Seykora and Stephen Prouty, of the Dermatology Department, for allowing me to use their Leica LCM equipment and providing technical support.

Thank you to my committee members, Marisa Bartolomei, Chris Lengner, John Lynch, and Jonathan Katz, for serving on my committee and providing support and advice over the last four years. I also want to thank Catherine Lee May, a mentor and friend who has given me much guidance over the past four years. I am so happy you are back in the Kaestner lab!

I have several close friends I would also like to recognize as well. My roommates, Jenessa Smith and Julia Kieckhaefer, are amazing people that I will miss tremendously. Thank you for being such good friends. I will miss watching all the TV with you both. Julia, thank you so much for reading the last few chapters of my thesis. Thank you Crystal Wilcox, for being a great friend, listening to me complain, troubleshooting experiments, and reading my prelim exam. I also want to give a special thanks to Jeff Raum and Scott Soleimanpour, who were bay mates for several years, and have both given me good advice over the years. Jeff, thank you for reading and editing my monster of an introduction chapter. And Scott, thank you so much for your help during the post-doc interview process. I hope to stay in touch with you both!

I would like to recognize my family as well, who unceasingly supported and loved me during graduate school, even when I was cranky. Kevin Elliott, my husband; I would be lost without you, and I love you. Boop. My Mom and Dad, and sisters Leah and Pam: I know that what

I do makes little sense to you, but you listen to me talk and complain anyway. I love you, and thank you so much for your help and support during graduate school.

ABSTRACT

DNMT1 IN INTESTINAL DEVELOPMENT AND CANCER

Ellen N. Elliott

Klaus H. Kaestner

Patterns of DNA methylation are established and maintained by DNA methyltransferases (Dnmts), which have traditionally been subdivided into the '*de novo*' methyltransferases, Dnmt3a and Dnmt3b, and the 'maintenance' methyltransferase, Dnmt1. Dnmt1 maintains DNA methylation patterns and genomic stability in several *in vitro* cell systems, but its function in tissue-specific development, homeostasis, and disease *in vivo* is only beginning to be investigated.

Recently, the Kaestner lab demonstrated that loss of *Dnmt1* in the adult intestinal epithelium causes a two-fold expansion of the proliferative crypt zone, indicating that Dnmt1 and DNA methylation regulate proliferative processes in the intestine. I hypothesized that loss of *Dnmt1* may impart similar effects during intestinal development and tumorigenesis, and employed distinct Cre-*loxP* mouse models to ablate *Dnmt1* in progenitor cells during intestinal development and in the mature intestinal epithelium of cancer-prone $Apc^{Min/+}$ mice.

In the first part of my thesis, I show that loss of *Dnmt1* in intervillus progenitor cells in the developing intestine causes global hypomethylation, DNA damage, premature differentiation, and apoptosis. I confirm this novel role for Dnmt1 during crypt development using the *in vitro* organoid culture system, and illustrate a differential requirement for Dnmt1 in immature versus mature organoids. These results demonstrate an essential role for Dnmt1 in maintaining genomic stability during intestinal development and the establishment of intestinal crypts.

DNA methylation is thought to drive CRC progression by the repression of tumor suppressor genes via promoter methylation. In the second part of my thesis, I utilize inducible intestinal epithelial-specific gene ablation to determine the requirement of Dnmt1 in intestinal

tumorigenesis. Surprisingly, I find that loss of *Dnmt1* in cancer-prone $Apc^{Min/+}$ mice results in accelerated, not decreased, intestinal tumor development. *Dnmt1* deletion precipitates an acute response in mature intestinal epithelium characterized by hypomethylation of repetitive elements, genomic instability, and apoptosis, which is followed by remethylation with time. This recovery is entirely dependent on the activity of the *de novo* methyltransferase Dnmt3b. In light of these data, the current dogma regarding the role of DNA methylation in colon cancer needs to be revisited.

TABLE OF CONTENTS

LIST OF TABLES

Chapter 2

Chapter 3

LIST OF FIGURES

Chapter One

Introduction

Epigenetic regulation of the intestinal epithelium

Introduction

Waddington coined the term “epigenetics” in 1942 to describe the burgeoning field of developmental biology, and the mechanisms underlying development from the undifferentiated embryo to the mature adult organism (Waddington 1942). In the modern context, epigenetics is defined as mitotically heritable phenotypes that are mediated by mechanisms other than alteration of DNA sequences (Berger, Kouzarides et al. 2009). These mechanisms affect chromatin organization, i.e. the three-dimensional structure of DNA within the nucleus, which in turn influences gene expression patterns and resulting phenotypic traits among distinct cell types.

Epigenetic modifications are classified into three general categories: DNA methylation, histone modifications, and nucleosome positioning. Although the term “epigenetic” refers to the inheritance of the mark through at least one mitotic cycle, all of the described epigenetic modifications are dynamic to some extent (Berger 2007). We know that DNA methylation patterns are first erased and then re-established during early embryonic development, and we understand the molecular mechanism of their trans-mitotic inheritance. In contrast, the processes underlying the maintenance of histone modifications and nucleosome arrangements through the cell cycle are not well understood. In these instances, the marks are termed “epigenetic” due to their capabilities to alter gene expression patterns, which are maintained in specific cell lineages.

Histone modifications and nucleosome positioning

Histones are the core proteins that comprise nucleosomes, and form the structural basis underlying chromatin architecture. Nucleosomes consist of 147 base pairs of DNA wrapped around a histone octamer, which contains two copies of each core histone protein (H2A, H2B, H3, and H4) (Luger, Mäder et al. 1997). The placement and density of nucleosomes determines the relative accessibility of DNA to different transcription factors and enzymes, and thus can directly impact gene expression (Jenuwein and Allis 2001).

Histone proteins can be altered by covalent posttranslational modifications to their charged tails, which protrude from the histone and are thus accessible to various modifying

enzymes. These modifications alter the electrostatic charge of the histone tails to induce changes in the chromatin structure. Repressive histone modifications create a more compact chromatin environment, while activating modifications allow DNA binding factors and other proteins to interact with DNA and increase gene expression (Kouzarides 2007). In addition, specific histone modifications allow binding of 'reader' proteins, which can transmit the charged histone state into altered gene actions. There are many types of histone modifications and corresponding enzymes. For the purpose of this review, we have chosen the most commonly profiled modifications described in the current literature.

Activating histone modifications

There are multiple histone modifications that distinguish active areas of chromatin, but the most commonly found at actively transcribed genes are tri-methylation of H3K4 (H3K4me3) at their transcription start sites (Kim, Barrera et al. 2005), and H3K36 (H3K36me3) within gene bodies (Barski, Cuddapah et al. 2007). The H3K4me3 mark is established by SET-domain proteins, including the well-characterized MLL protein (Krivtsov and Armstrong 2007). MLL is a mammalian homologue of the *Drosophila* Trithorax complex, and is a target for translocations in acute myeloid leukemia (Thirman, Gill et al. 1993, Krivtsov and Armstrong 2007). MLL contains a SET domain responsible for methylation of H3K4 to the mono-, di-, and trimethylated state (H3K4me1, me2, me3), and associates with the WDR5, RBPB5, and ASH2L proteins, which are necessary for MLL targeting and function (Krivtsov and Armstrong 2007). H3K36me3 marks exons within actively transcribed genes, and specifically functions to prevent aberrant RNA polymerase activity within active genes (Venkatesh, Smolle et al. 2012). In addition, the H3K36me3 intergenic mark contributes to DNA mismatch repair (Li, Mao et al. 2013) and alternative splicing (Luco, Pan et al. 2010).

Enhancers are distal *cis*-regulatory elements that can be bound by sequence-specific DNA-binding transcription factors to activate a given target gene, and are also associated with multiple histone modifications. Active enhancers are characterized by H3K27 acetylation

(H3K27Ac) (Creyghton, Cheng et al. 2010), which is established by both the CREB binding protein (CBP) and p300 acetyltransferases (Tie, Banerjee et al. 2009). H3K4me1and H3K4me2 also mark *cis*-regulatory elements such as enhancers and promoters, but do not necessarily denote active transcription (Ong and Corces 2011). Interestingly, enhancers are also frequently sites of reduced DNA methylation (Lister, Pelizzola et al. 2009, Stadler, Murr et al. 2011, Ziller, Gu et al. 2013, Sheaffer, Kim et al. 2014), indicative of cross-talk between histone modifications and DNA methylation machinery (see below).

Repressive histone modifications

The two most commonly profiled repressive histone methylation marks are H3K27me3 and H3K9me3. H3K27me3 is established by the Polycomb repressive complex 2 (PRC2), comprised of the catalytic subunits EZH1 and EZH2, in addition to core subunits SUZ12, EED and RBBP7/4 (Margueron and Reinberg 2011). H3K27me3 is regarded as a stable histone modification (Zee, Levin et al. 2010), and is widely distributed in ES cell chromatin (Peters, Kubicek et al. 2003). PRC2 and H3K27me3 are responsible for silencing key lineage-specific regulators in mouse ES cells to repress differentiation processes and maintain pluripotency (Boyer, Plath et al. 2006). Depletion of EZH2 and EED in mouse ES cells impairs mesendoderm differentiation (Shen, Liu et al. 2008), and deletion of SUZ12, EZH2, or EE causes severe gastrulation defects during embryogenesis (Faust, Schumacher et al. 1995, O'Carroll, Erhardt et al. 2001, Pasini, Bracken et al. 2007), demonstrating the critical function of PRC2 in developmental and differentiation processes.

The H3K9me3 mark is considered a hallmark of constitutive heterochromatin and is regulated by the SUV39H family of methyltransferases, including G9a, SUV39H1/2, and SETDB1/2. SUV39H1/2 establish the H3K9me3 mark in heterochromatin (Peters, Kubicek et al. 2003), where its interaction with heterochromatin protein 1 (HP1) recruits additional SUV39H1/2 methyltransferases to promote gene silencing (Margueron and Reinberg 2010). SETDB1 is highly

expressed in ES cells, and is required to maintain pluripotency and self-renewal capabilities *in vitro* (Bilodeau, Kagey et al. 2009).

Nucleosome Positioning

Nucleosome remodeling complexes can completely alter the three-dimensional structure of chromatin by the addition, subtraction, or remodeling of nucleosome subunits. These dynamic activities are regulated by four families of proteins: SWI/SNF, ISWI, CHD, and INO80 (Portela and Esteller 2010). These families of proteins assemble into large complexes, allowing them to alter nucleosome position within the larger context of histone modifications and DNA methylation patterns. All four types of complexes interact with multiple proteins, including nucleosomes, specific histone modifications, chromatin remodeling enzymes, and transcription factors. In addition, these remodelers all contain a catalytic subunit with a DNA-dependent ATPase domain, which uses the energy from ATP hydrolysis to remodel nucleosomes (Portela and Esteller 2010).

The ATPases BRM and BRG1 are members of the SWI/SNF family, and share sequence homology with the *Drosophila* Trithorax genes (Schuettengruber, Martinez et al. 2011). BRM and BRG1 form multi-protein BAF remodeling complexes, which show a surprising amount of tissue and cell-type specificity via differential inclusion of BAF protein subunits (Lessard and Crabtree 2010). Neural progenitors require BAF45a/53a subunits to support proliferation, while differentiation to postmitotic neurons necessitates BAF45b/45c/53b (Lessard, Wu et al. 2007). The SWI/SNF family is widely known as a master regulator of gene expression, having roles in various pathways related to cell adhesion, alternative splicing, cell cycle regulation and differentiation (Reisman, Glaros et al. 2009). Several members, including BRG1 and SNF5, are frequently mutated or silenced in various types of cancers, pointing to a possible function as a tumor suppressor (Clapier and Cairns 2009).

The CHD family of nucleosome remodelers is defined by ATPase proteins with chromodomains, which bind methylated lysine residues in histone tails (Lessard, Wu et al. 2007). CHD3/4 ATPases are essential for nucleosome remodeling activity in the Mi-2/NuRD complex.

Mi-2/NuRD also contains the MBD3 protein, which binds methylated DNA, and histone deacetylases HDAC1 and HDAC2, which deacetylate histones and tighten local chromatin structure (Xue, Wong et al. 1998, Wade, Gegonne et al. 1999, Zhang, Ng et al. 1999). In ES cells, Mi-2/NuRD deacetylates H3K27 to promote PRC2-mediated transcriptional repression, which is required for ES cell pluripotency and differentiation (Kaji, Caballero et al. 2006, Reynolds, Salmon-Divon et al. 2012). Overall, Mi-2/NuRD regulates transcriptional activity by coupling histone deacetylation with increased nucleosome density, which alters interactions with other histone modifying proteins.

DNA methylation

DNA methylation refers to the covalent addition of a methyl group to a cytosine base, referred to as 5-methylcytosine (5mC), and commonly occurs in the context of a CpG dinucleotide. CpG dinucleotides are underrepresented in the mammalian genome due to the spontaneous deamination of 5mC to thymine. As a result of these processes, only 1% of the human genome consists of CpG sites as opposed to the ~4 percent expected by chance, and approximately 60-80% of these CpG sites are methylated, depending on the cell type (Smith and Meissner 2013). The remaining unmethylated CpGs are predominantly located in regions of increased CpG frequency, termed CpG islands (CGIs). CGIs, as defined by Takai and Jones (2002), are ≥ 500 base pairs in length, have a CpG observed/expected ratio ≥0.65, and have at least 55% GC content. CGIs are generally unmethylated, and are located at 72% of annotated promoters in the human genome (Saxonov, Berg et al. 2006). Interestingly, regions of low CpG methylation can also be found for distal CGIs in enhancers (Lister, Pelizzola et al. 2009, Stadler, Murr et al. 2011, Ziller, Gu et al. 2013).

The enzymes that establish DNA methylation patterns are DNA methyltransferases (DNMT). There are three DNMTs encoded in the mammalian genome, divided into two categories based on their sequence similarities and DNA methyltransferase activities *in vitro*. The "*de novo*" methyltransferases, DNMT3A and DNMT3B, have low affinity for hemi-methylated compared to

unmethylated DNA *in vitro* (Okano, Xie et al. 1998), and can establish novel patterns of DNA methylation. The second type of DNMT is the "maintenance" methyltransferase DNMT1. DNMT1 associates with factors at the replication fork to copy patterns of methylation onto newly synthesized strands of DNA, thereby faithfully maintaining the pattern of DNA methylation across multiple cell divisions (Leonhardt, Page et al. 1992). It has recently been suggested that the categories of "maintenance" and "de-novo" are too simplistic to describe the complex interplay of DNMT activity *in vivo* (Jones and Liang 2009). For example, deletion of *Dnmt1* in mouse ES cells causes only a 66% decrease in DNA methylation levels (Li, Bestor et al. 1992), suggesting that DNMT3A and DNMT3B have some maintenance methyltransferase activity.

DNA methylation and therefore DNMTs are crucial for mammalian development. *Dnmt1*- or *Dnmt3b*-null mouse embryos arrest at E.9.5, and *Dnmt3a*-null newborn mice are runted and die within the first two weeks of life (Li, Bestor et al. 1992, Okano, Bell et al. 1999). Intriguingly, triple *Dnmt*-knockout (TKO) mouse ES cells have normal morphology and survival *in vitro*, but undergo apoptosis when induced to differentiate (Jackson, Krassowska et al. 2004, Tsumura, Hayakawa et al. 2006). In contrast, recent studies have shown that human ES cells require DNMT1 even during maintenance culture (Liao, Karnik et al. 2015). These results support the notion that mouse and human ES cells denote distinct pluripotent states, with human ES cells representing a later stage of epiblast development relative to mouse ES cells (Nichols and Smith 2009). Overall, these data strongly implicate a critical role for DNA methylation in early embryonic development and differentiation processes.

Differential methylation patterns distinguish specific tissue and cells types, with differential methylation occurring at CGI shores and enhancer elements (Irizarry, Ladd-Acosta et al. 2009, Stadler, Murr et al. 2011, Ziller, Gu et al. 2013). DNA methylation acts primarily as a repressive epigenetic modification in chromatin, downregulating expression of genes associated with regions of increased DNA methylation. There are two broad means by which DNA methylation can repress gene expression: direct inhibition of DNA binding transcription factors, and interactions with other chromatin remodeling enzymes to promote a repressive chromatin

environment. Although several examples of direct inhibition of transcription factor binding to methylated DNA are known, including for CREB, AP-2, and E2F (Tate and Bird 1993), the majority of studies have focused on how DNA methylation patterns influence global chromatin organization. The effects of DNA methylation on chromatin may be indirect, such as through the methyl CpG binding proteins MeCP2, MBD2, or MBD3. MeCP2 recruits histone deacetylases to methylated DNA, which promotes heterochromatin formation and stable gene repression (Jones, Veenstra et al. 1998, Nan, Ng et al. 1998). Additionally, the DNMTs directly interact with several chromatin-remodeling complexes, such as Polycomb group protein EZH2, to facilitate heterochromatin formation (Viré, Brenner et al. 2006).

Histone modifications, such as the repressive H3K9me, can be recognized by DNMTs to influence heterochromatin formation and nucleosome remodeling. G9a dimethylates H3K9, which creates a binding site for heterochromatin protein 1 (HP1). HP1 then recruits DNMT1, which methylates CpGs to support permanent transcriptional repression (Estève, Chin et al. 2006, Smallwood, Estève et al. 2007). Interestingly, binding to DNMT1 also stabilizes localization of HP1, allowing HP1 to recruit other chromatin remodeling complexes to form highly structured heterochromatin (Estève, Chin et al. 2006, Smallwood, Estève et al. 2007). In cancer, both HP1 and DNA methylation levels are globally reduced, signifying the importance of epigenetic cross talk in disease progression (Feinberg and Vogelstein 1983, Gama-Sosa, Slagel et al. 1983, Dialynas, Vitalini et al. 2008).

DNA methylation has long been considered the most “stable” of the epigenetic modifications. The earliest studies of DNA methylation and DNMT function described the processes of imprinting and X-chromosome inactivation during development (Holliday and Pugh 1975, Venolia and Gartler 1983, Bartolomei, Zemel et al. 1991). Imprinting refers to the phenomenon of monoallelic gene expression in a parent-of-origin specific manner. One of the best-understood examples of imprinting occurs at the *H19/IGF2* locus, in which differential methylation at the imprinting control region (ICR) located between the two genes determines monoallelic *H19* and *IGF2* expression. The ICR is methylated on the paternal allele, which results

in *IGF2* expression from the paternal chromosome and *H19* expression from the maternal chromosome (Li, Beard et al. 1993). Imprints are maintained in all mature somatic cells types, and are only erased during primordial germ cell development in embryogenesis (Plasschaert and Bartolomei 2014).

The mammalian intestinal epithelium

One of the aims of epigenetic research is to elucidate how the various marks interact with one another, and which components are essential to disease progression and prevention. To study chromatin dynamics *in vivo*, during development as well as homeostasis and disease progression, requires a model system that closely parallels its human counterpart but is still genetically tractable. The mouse intestinal epithelium fits these requirements, and is an excellent model for the study of chromatin in modulating gene expression and disease. The structural components of the mouse intestinal epithelium are strikingly similar to those of the human intestine. Models for human intestinal disease, including colorectal cancer and inflammatory bowl disease, are well established in the mouse, which permits studies of chromatin marks and complexes in disease progression. The precise mechanisms that regulate intestinal epithelial homeostasis and disease have remained elusive, and it is possible that epigenetic marks play a crucial role in such processes.

The adult intestinal epithelium consists of a single layer of columnar cells lining the lumen of the intestine. The epithelium is structured into crypts that invaginate into the underlying mesenchyme, and villi that project into the intestinal lumen (Figure 1.1). In intestinal homeostasis, the crypt-based columnar (CBC) stem cells give rise to rapidly dividing transit-amplifying crypt cells. As the transit amplifying cells exit the crypt, they differentiate into one of five major cell types: absorptive cells, called enterocytes, goblet cells, enteroendocrine cells, Paneth cells (Cheng and Leblond 1974), and Tuft cells (Gerbe, Legraverend et al. 2012). Paneth cells are retained at the base of the crypt, while the other types of differentiated cells migrate up the villi. Differentiated cells migrate in ordered cohorts along the villi as more cells are produced, and

reach the top of the villus after 3-5 days, at which point the cells apoptose and are shed into the intestinal lumen. This high rate of cellular turnover indicates tight regulation of cell proliferation and differentiation processes. Indeed, misregulation of intestinal crypt proliferation is the hallmark of intestinal and colorectal cancer (Fearon 2011).

The intestinal stem cell niche and Wnt signaling

Crypts form the intestinal stem cell niche, and harbor two well-characterized populations of stem cells (Figure 1.1). The first are the crypt-based-columnar (CBC) stem cells, which express the markers Lgr5 and Olfm4, and give rise to all cell types in the intestinal epithelium (Barker, van Es et al. 2007, van der Flier, Haegebarth et al. 2009). CBCs are considered the active population of intestinal stem cells, and divide approximately once every 24 hours. The second population of stem cells are the quiescent "+4 stem cells," marked by Bmi1, Tert, and Hopx (Barker, van Oudenaarden et al. 2012). The +4 stem cells constitute a reserve population; upon ablation of the CBC population in mice, +4 stem cells can give rise to new CBC stem cells and repopulate the intestinal epithelium (Tian, Biehs et al. 2011). In separate studies, it was also shown that the CBC cells can give rise to +4 stem cells (Takeda, Jain et al. 2011). As a result, it is difficult to make a clear distinction between the two interconverting stem cell populations. It is possible that the crypt base contains a equipotent population of intestinal stem cells, and that the cell position within the crypt determines whether the cell is a fast- or slow-dividing stem cell. Evidence supporting this equipotent stem cell hypothesis comes from studies of irradiated mice, in which $Dll1^+$ secretory precursors can convert to $Lgr5^+$ CBCs to compensate for epithelial loss (van Es, Sato et al. 2012).

The main signaling pathway that supports proliferation in the crypt, both *in vivo* and *in vitro*, is the canonical Wnt signaling pathway. Briefly, canonical Wnt signaling depends on cytoplasmic stabilization of β-catenin, via disassociation of the Gsk3β-APC-Axin destruction complex. Accumulation of stable β-catenin protein in the cytoplasm results in its translocation to the nucleus, where it interacts with Tcf/Lef DNA binding effector proteins at target genes to

activate transcription. Wnt activity is required to maintain proliferation in the adult intestinal crypt; overexpression of the secreted Wnt antagonist Dkk1 in mouse intestinal epithelium inhibits proliferation, and blocks formation and maintenance of crypts (Pinto, Gregorieff et al. 2003, Kuhnert, Davis et al. 2004). Deletion of *Tcf4*, the main β-catenin nuclear effector in mouse intestinal epithelium, causes complete loss of proliferation and stem cell identity in the adult intestine, and mice die ~9 days following ablation (Korinek, Barker et al. 1998).

Paneth cells are proposed to have an active role in maintaining the CBC stem cells through their secretion of Wnt ligands (Sato, van Es et al. 2011). This hypothesis was supported by observations that single $Lgr5^+$ cells grow more efficiently *in vitro* when paired with a Paneth cell (Sato, van Es et al. 2011). However, ablation of Paneth cells has no deleterious effects on CBC homeostasis or crypt architecture in adult mice (Durand, Donahue et al. 2012), suggesting there are redundant mechanisms to maintain proliferation and Wnt signaling *in vivo*. Inhibiting Wnt ligand secretion concurrently in Paneth cells and subepithelial myofibroblasts did not alter crypt proliferation or crypt-villus architecture in adult mice (San Roman, Jayewickreme et al. 2014). However, there is some evidence that supports a critical role for the mesenchyme in maintaining the intestinal stem cell niche. Kabiri and colleagues inhibited epithelial Wnt secretion, and demonstrated that epithelial Wnt ligands are not required for crypt maintenance during development, homeostasis, or following injury (2014). Interestingly, *ex vivo* organoid cultures from these mice illustrated a dependence on exogenous Wnt sources. The authors reported that co-culture with wild-type intestinal stromal cells negated the requirement for supplementation with Wnt factors, strongly suggesting that the niche supporting cells exist within the intestinal stroma (Kabiri, Greicius et al. 2014). Thus, there are many populations of distinct mesenchymal cells surrounding the intestinal epithelium, and it is likely that one of these cell types is supporting the intestinal crypt.

Differentiation in the intestinal epithelium

There are five main types of differentiated cells in the intestinal epithelium: absorptive enterocytes, goblet cells, Paneth cells, enteroendocrine cells, and Tuft cells (Figure 1.1). Although enterocytes comprise ~90% of the intestinal villi cell population (Cheng and Leblond 1974), the other types of differentiated cells secrete proteins that are crucial to intestinal function and survival. Goblet cells secrete mucin, the main component of mucus and the intestinal epithelial barrier, and are important to protect against potential pathogens in the lumen. Mucus coats the entire intestinal epithelium, acting as a lubricant to promote digestion, and preserves the structure of the epithelium upon physical force or injury (van der Flier and Clevers 2009). Enteroendocrine cells secret various hormones, including glucagon-like peptides 1 and 2 (GLP-1, -2), cholecystokinin (CCK), Glucose-dependent insulinotropic peptide (GIP), and somatostatin (SST) (Lee and Kaestner 2004). There are ~15 types of enteroendocrine cells, and their secreted hormones have important functions in feeding behavior, satiation, and glucose homeostasis (Cummings and Overduin 2007). For instance, GLP-1 is released in the small intestine following food intake, and promotes glucose uptake by stimulating pancreatic β-cell insulin secretion (Kreymann, Williams et al. 1987, Mojsov, Weir et al. 1987).

Paneth cells are distinct from the other types of differentiated cells. As they differentiate from the transit-amplifying pool, they migrate to the base of the crypt and reside interspersed between the CBC stem cells (Figure 1.1). Paneth cells are long-lived relative to villus cell populations, surviving for approximately one month in the crypt epithelium (Troughton and Trier 1969). Their main function is to secrete lysozyme and other defensin proteins that protect against bacterial infection in the epithelium (Porter, Bevins et al. 2002).

Another type of endocrine cell, the Tuft cell, comprises 0.4% of the intestinal epithelium (Gerbe, Legraverend et al. 2012) and has garnered much attention over the past five years due to the discovery of their distinct cell lineage. Although they require the pan-endocrine transcription factor Atoh1 for differentiation, Tuft cells do not require the other factors necessary for enteroendocrine, goblet, or Paneth cell specification (Gerbe, van Es et al. 2011). Tuft cells are

marked by expression of Dclk1, and have been shown to contribute to intestinal recovery following injury (Gerbe, Brulin et al. 2009, Westphalen, Asfaha et al. 2014). Dclk1 is also a putative cancer stem cell marker, and loss of Dclk1^{+} cells abrogates tumorigenesis on the *Apc*$^{Min/+}$ colorectal cancer mouse model (May, Riehl et al. 2008, Nakanishi, Seno et al. 2013).

Notch signaling regulates differentiation and stem cells

Notch is one of the most important signaling pathways in the intestinal epithelium, and has crucial roles in regulating both intestinal proliferation and differentiation processes. The Notch signaling pathway works via lateral inhibition, in which one cell expressing the Delta ligand activates the Notch receptor on an adjacent cell. Activation of the Notch receptor causes cleavage of its intracellular domain, which subsequently translocates to the nucleus and forms a complex with the DNA-binding transcription factor CSL (CBF-1/RBP-Jκ, Su(H), Lag-1). CSL normally acts to repress gene expression, but binding of the Notch intracellular domain (NICD) converts CSL to a transcriptional activator. In the intestinal epithelium, secretory precursors expressing the Delta ligand (Dll) activate Notch signaling in neighboring cells. NICD activity increases expression of the bHLH transcription factor Hes1, which supports enterocyte differentiation via its repression of *Atoh1* (Jensen, Pedersen et al. 2000, Zheng, Tsuchiya et al. 2011). Atoh1 is a bHLH transcription factor necessary (Yang, Bermingham et al. 2001, Shroyer, Helmrath et al. 2007) and sufficient (VanDussen and Samuelson 2010) for all secretory lineages in the intestinal epithelium. Notch signaling opposes Atoh1 activation to direct cell fate into the enterocyte lineage. Loss of Notch signaling causes increased secretory cell differentiation along the crypt-villus axis, either through use of γ-secretase inhibitors (van Es, van Gijn et al. 2005, VanDussen, Carulli et al. 2012), or by ablation of Notch receptors (Riccio, van Gijn et al. 2008, Carulli, Keeley et al. 2015), Dll ligands (Pellegrinet, Rodilla et al. 2011), or CSL/RBP-Jκ (van Es, van Gijn et al. 2005). Combined loss of Notch signaling and *Atoh1* expression blocks secretory cell fate conversion and induces global enterocyte differentiation (Kazanjian, Noah et al. 2010, van Es, de Geest et al. 2010, Kim and Shivdasani 2011, VanDussen, Carulli et al. 2012),

establishing that Notch acts specifically through that Atoh1 to regulate secretory cell fate, and that active Notch is not required for enterocyte differentiation. Conversely, mice with forced over-expression of Notch ICD display severe reduction of secretory cell types and increased enterocyte differentiation (Fre, Huyghe et al. 2005, Stanger, Datar et al. 2005).

Interestingly, over-expression of the NICD causes increased crypt cell proliferation (Fre, Huyghe et al. 2005, Stanger, Datar et al. 2005), whereas loss of Notch signaling blocks proliferation and converts crypt cells to secretory cell fates (van Es, van Gijn et al. 2005, Riccio, van Gijn et al. 2008, Pellegrinet, Rodilla et al. 2011, VanDussen, Carulli et al. 2012). Notch pathway inhibition decreases expression of CBC stem cell marker genes, including *Olfm4* and *Lgr5* (Pellegrinet, Rodilla et al. 2011, VanDussen, Carulli et al. 2012, Carulli, Keeley et al. 2015). VanDussen and colleagues found that the NICD directly activates expression of Olfm4, demonstrating the crucial function of Notch signaling in maintaining the CBC stem cell population (2012).

Notch signaling components are expressed in the crypt, and interact with Wnt signaling to support stem cell renewal, proliferation, and differentiation processes (Noah and Shroyer 2013). In fact, Wnt activation strongly favors a secretory cell fate by its positive regulation of Atoh1 and Sox9 (Pinto, Gregorieff et al. 2003, Blache, van de Wetering et al. 2004), important for Paneth cell fate, and mouse models with decreased Wnt signaling display reduced numbers of secretory cells (Korinek, Barker et al. 1998, Pinto, Gregorieff et al. 2003). Activation of Notch in the *Tcf4*-null, non-proliferative developing intestinal epithelium fails to restore progenitor cell division (Fre, Pallavi et al. 2009). A recent report from Tian et al. (2015) used Notch-inhibiting antibodies to illustrate that Notch inhibition allows increased Wnt-activation of secretory genes, such as *lysozyme*, at the expense of crypt cell proliferation. Concurrent treatment with both Wnt- and Notch-blocking antibodies restored CBC proliferation and normal cell differentiation, suggesting that Notch mediates its effects in part through Wnt pathway inhibition (Tian, Biehs et al. 2015). These experiments demonstrate that cooperation between Notch and Wnt signaling is crucial to maintain proliferation and differentiation processes in the intestinal epithelium.

Crypt-villus organization: Hedgehog and BMP

The architecture of the intestinal epithelium is tightly regulated, and misregulation of crypt-villus organization is a step in disease progression. There are several signaling pathways essential for maintaining the crypt-villus axis demarcation. Many of these signals are active during intestinal development, and require cross talk between the intestinal epithelium and the surrounding mesenchymal tissue.

The Hedgehog ligands Sonic hedgehog (Shh) and Indian hedgehog (Ihh) are expressed in developing epithelium, and become restricted to proliferative regions as development progresses (Ramalho-Santos, Melton et al. 2000). The Hedgehog receptors, Patched, and their effectors, the Gli transcription factors, are expressed in the underlying mesenchyme (Ramalho-Santos, Melton et al. 2000). Hedgehog signaling during intestinal development becomes active upon binding of epithelial Hh ligands to Patched receptors expressed in intestinal mesenchyme. Hedgehog (Hh) ligand binding to Patched relieves inhibition of Smoothened, which activates Gli transcription factors; Gli then translocates to the nucleus, where it regulates expression of Hh target genes. Expression of the pan-*Hh* inhibitor *Hhip* in the developing intestinal epithelium impairs villus morphogenesis and increases Wnt signaling, resulting in flattened hyper-proliferative intestinal epithelium (Madison, Braunstein et al. 2005).

The *Hhip*-mice also display disorganization of myofibroblasts normally associated with crypt epithelium, and significantly decreased BMP ligand expression within the intestinal mesenchyme (Madison, Braunstein et al. 2005). Similar to Hedgehog, BMP signaling also requires crosstalk between the mesenchyme and epithelium. In this situation, however, the BMP ligands are expressed in the mesenchyme, and the receptors are expressed in the epithelium (Haramis, Begthel et al. 2004). During intestinal development, the BMP ligands are expressed in clusters of mesenchymal cells underlying putative villi (Karlsson, Lindahl et al. 2000), and the highest levels of BMP signaling are observed in villi (Madison, Braunstein et al. 2005). When the BMP antagonist Noggin is overexpressed in intestinal epithelium (Haramis, Begthel et al. 2004, Batts, Polk et al. 2006), or if the BMP receptor is ablated (He, Zhang et al. 2004), irregular hyper-

proliferative crypt structures appear throughout the epithelium, confirming a role for BMP in supporting villus formation and repressing crypt development. It has been posited that epithelial Hedgehog signals promote mesenchymal BMP activation, and that both pathways antagonize one another to ensure proper crypt and villus formation (Roberts, Johnson et al. 1995, Roberts, Smith et al. 1998, Sukegawa, Narita et al. 2000, Ishizuya-Oka, Hasebe et al. 2006). However, direct activation of BMP signaling by Hedgehog has not been demonstrated in the mammalian intestinal epithelium *in vivo*.

The Foxl1 transcription factor is highly expressed in intestinal mesenchyme (Kaestner, Bleckmann et al. 1996), and regulates the transition from pseudostratified to columnar epithelium during intestinal epithelial development. Ablation of *Foxl1* results in delayed crypt-villus morphogenesis, and abnormal proliferation patterns in late fetal stages and the first two weeks of life (Kaestner, Silberg et al. 1997). Foxl1 is also a bona-fide Hedgehog target gene, and contains several highly conserved Gli binding sites near its promoter (Madison, McKenna et al. 2009). Interestingly, BMP ligand expression is decreased in developing *Foxl1*-mutant intestinal mesenchyme (Kaestner, Silberg et al. 1997), suggesting that Foxl1 may be the link modulating BMP and Hedgehog signals between epithelial and mesenchymal cells (Madison, McKenna et al. 2009).

Transcriptional and Epigenetic Regulation of the Intestinal Epithelium

The genetics of key DNA binding transcription factors in the intestinal epithelium has been extensively studied, but less is known about the role of chromatin marks and mediators in the processes of intestinal homeostasis. Two conflicting viewpoints have emerged over the past decade (Figure 1.2). The first is the concept that the chromatin of the intestinal epithelium is largely permissive, and that transcription factor activity is the defining characteristic that alters gene expression patterns (Figure 1.2 A-B). The second posits that the chromatin itself plays an important role in regulating gene expression, and that chromatin states are not necessarily dependent on transcription factor activity (Figure 1.2 C-D).

Transcription factors regulate open chromatin and intestinal homeostasis

There are several transcription factors that are globally important for intestinal epithelial development, maintenance, and proliferation. Cdx2 is master-regulator of intestinal epithelial differentiation, and is essential for the specification of all intestinal epithelia during mouse endoderm development (Gao, White et al. 2009). Cdx2 ablation in mouse endoderm prevents colon and rectum morphogenesis and causes global defects in differentiation and proliferation transcriptional programs (Gao, White et al. 2009). Cdx2 is also required for normal activation of pro-intestine transcription factors, including Hnf1α, Hnf4 α, and Cdx1, and regulates Hedgehog ligand secretion from the epithelium to the underlying mesenchyme (Gao, White et al. 2009). Loss of Cdx2 at mid-gestation perturbs apical-basolateral polarity of the developing epithelium, causing deficient enterocyte development and maintenance (Gao and Kaestner 2010). In addition, inducible deletion of *Cdx2* in the adult gut reduces villus length and the numbers of enterocytes, causing nutrient malabsorption and death within three weeks (Verzi, Shin et al. 2010, Verzi, Shin et al. 2011). Each of these studies demonstrated that Cdx2 is capable of both transcriptional repression and activation, based on gene expression changes following *Cdx2* loss (Gao, White et al. 2009, Gao and Kaestner 2010, Verzi, Shin et al. 2011).

To study the CDX2 binding dynamics during intestinal cell differentiation, Verzi and colleagues first utilized the Caco-2 human cell line, which can be manipulated to produce homogeneous populations of proliferative and differentiated intestinal cells. They performed H3K4me2, H3K27ac, and CDX2 ChIP-Seq to demonstrate that CDX2 binds distinct *cis*-regulatory sites in differentiated and proliferative cell states (Figure 1.2 A-B) (Verzi, Shin et al. 2010). In the same model system, they showed that CXD2 preferentially co-localizes with GATA6 at enhancer-marked chromatin in proliferative cells, and HNF4α at different enhancer elements in differentiated cell populations (Figure 1.2 B) (Verzi, Shin et al. 2010). In differentiated mouse villi, Verzi and colleagues found that Cdx2 co-localized with Hnf4α at many distal enhancer elements, which they defined as 450-600 bp regions flanked by H3K4me2-marked nucleosomes (Figure 1.2 B) (2013). Loss of Cdx2 in mouse intestinal villi reduced HNF4α binding at co-bound sites (Verzi,

Shin et al. 2013), in agreement with previous data showing that Cdx2 regulates Hnf4α expression (Gao, White et al. 2009). Interestingly, they also discovered that Cdx2-bound sites displayed reduced H3K4me2 nucleosome occupancy in *Cdx2*-deficient villi, and conclude that Cdx2 is required to maintain open chromatin in differentiated cells (Verzi, Shin et al. 2010, Verzi, Shin et al. 2013). These findings build upon previous work that established Cdx2 as the master-regulator of intestinal epithelial differentiation (Gao, White et al. 2009, Gao and Kaestner 2010), and suggest that Cdx2 exerts this function both by its ability to control chromatin compaction and through its interactions with multiple transcription factors.

Based on the above data, it appears that Cdx2 maintains the intestinal epithelium in a largely active chromatin state (Figure 1.2 A-B). These conclusions are supported by additional studies that more thoroughly analyzed histone marks during *in vivo* differentiation. Through advanced genetic and cell sorting techniques it is possible to isolated various populations of cells from the adult mouse intestine, including the $Lgr5^{+}$ stem cells, secretory progenitors, and enterocyte progenitors. Kim and colleagues performed H3K4me2 and H3K27ac ChIP-Seq, DNAseI mapping, and RNA-Seq to define the different cell populations by their open chromatin states and associated gene expression (2014). Although the stem cells, secretory progenitors, and enterocytes display distinct transcript profiles, the enterocyte and secretory progenitor populations have remarkably similar H3K27ac, H3K4me2, and DNAseI profiles, which indicate active enhancer elements and globally open chromatin structure (Kim, Li et al. 2014). The authors propose that DNA-binding factors influence chromatin activity during the differentiation process, and that the labile chromatin structure renders progenitors capable of reacting to the available set of transcription factors. To test this hypothesis, they attempted to direct progenitor cell fate *in vivo* by genetic manipulation of lineage-specific transcription programs. Acute inhibition of Notch signaling forces progenitors to adopt a secretory cell fate within two days. Following global conversion of progenitors to secretory cell fate, the authors induced loss of *Atoh1*, which is completely required for secretory lineages. As the authors predicted, secretory progenitors present at the outset of *Atoh1* deletion convert to enterocyte fates (Kim, Li et al. 2014). They

concluded that the dynamic abilities of progenitor cells to convert lineages is due to their similar chromatin profiles, and that expression of distinct transcription factors specifies cell fate.

Additional work has characterized the function of the H3K79 methyltransferase DOT1L in the mouse intestinal epithelium. H3K79me2 is associated with both heterochromatin and euchromatin in model organisms and has known functions in transcriptional elongation, cell cycle checkpoints, and DNA repair (Nguyen and Zhang 2011). DOT1L-mediated gene activation is commonly employed in human leukemias with MLL translocations, making DOT1L an attractive target in disease research (Okada, Feng et al. 2005). Two recent studies analyzed the requirements for DOT1L and H3K79me, and reported strikingly different results.

Mahmoudi and colleagues originally identified Mllt10/Af10 in a screen for proteins that bind directly to the Tcf4/Wnt-signaling complex in the mouse intestinal epithelium (2010). MLLT10/AF10 directly interacts with the DOT1L methyltransferase to promote transcriptional activation, and is the primary mechanism by which DOT1L is activated in human leukemia (Okada, Feng et al. 2005, Nguyen and Zhang 2011). The authors report that DOT1L and the Mllt10/Af10 mediators are essential for Wnt target activation in intestinal crypts (Mahmoudi, Boj et al. 2010). However, these conclusions were only validated at *Axin* and *C-myc*, two canonical Wnt target genes.

A comparable study from an independent research group also evaluated the function of DOT1L in the intestinal epithelium, with different results (Ho, Sinha et al. 2013). They profiled H3K79me2 and RNA expression levels in villi and crypts isolated from adult mouse intestine. Surprisingly, the authors demonstrate similar levels of H3K79me2 at various Wnt targets in both crypt and villus compartments. They do note that H3K79me2 generally correlates with increased expression of associated genes, for both Wnt and non-Wnt target genes. Ablation of DOT1L in the intestinal epithelium caused global loss of H3K79me, but did not have any deleterious effects on differentiation or crypt-villus morphology. Indeed, Wnt targets were expressed at normal levels in the absence of DOT1L, indicating that the H3K79me2 mark is not essential for intestinal epithelial gene activation (Ho, Sinha et al. 2013). Ho and colleagues clearly demonstrate that

DOT1L-mediated H3K79me2 associates with transcribed genes both in crypts and villi, and is not required for Wnt target gene activation in intestinal crypt cells (2013).

Overall, these studies suggest that the chromatin landscape of the intestinal epithelium is largely accessible, particularly at enhancer and regulatory elements. This enhancer chromatin is amenable to changes induced by transcription factors, such as Cdx2 and Hnf4α, and allows progenitor cells to quickly adapt to specific cell fates. These statements align well with reports of plasticity within the intestinal epithelium upon tissue damage (van Es, Sato et al. 2012). However, a comprehensive study comparing various repressive and activating histone modifications in intestinal epithelial cell sub-populations has not been reported. In the future, it will be important to profile multiple histone marks in the stem cell, progenitor, and differentiated cell types in order to fully understand the function of chromatin during intestinal homeostasis and disease.

DNA methylation regulates enhancers and intestinal proliferation

The second view within the current literature introduced above is that chromatin and its associated modifications play a significant role in regulating proliferation and differentiation in the intestinal epithelium. This premise closely aligns with the two reports profiling genome-wide methylation levels in intestinal $Lgr5^+$ CBC stem cells and differentiated villus cells. Both studies reported similar methylomes between stem and differentiated cells, and focused their analyses specifically on enhancer regions that have altered DNA methylation between the two cell populations.

In the first published study, the authors note low levels of DNA methylation at the majority of transcription start sites, which they suggest primes cells for the process of differentiation. Their data analysis required a 40% change in DNA methylation between the two cell populations for identification as a differentially methylated region (DMRs), resulting in the discovery of only 50 DMRs (Kaaij, van de Wetering et al. 2013). The majority of these DMRs lost DNA methylation from stem to differentiated cell. Interestingly, these DMRs were positive for H3K4me1 and H3K27ac enhancer marks, and several of these putative enhancers loop and make contact with

the transcription start site of differentially expressed genes (Kaaij, van de Wetering et al. 2013). Many DMRs were also located near Tcf4 binding sites, indicating possible regulation by Wnt signaling. Unfortunately, the authors provided only limited *in vivo* data testing of their hypothesis that loss of Tcf4 correlates with higher methylation levels at several DMRs in villi, and suggest that Wnt signaling interacts with chromatin to promote DNA demethylation during the differentiation process (Kaaij, van de Wetering et al. 2013).

A second study employed vastly different bioinformatics approaches, resulting in identification of considerably more DMRs (Sheaffer, Kim et al. 2014). The authors note that modest DNA methylation levels of 13.9-50% identify most enhancer regions (Stadler, Murr et al. 2011), and suggest that a 40% change in methylation for DMR identification is too strict a limitation. Sheaffer and colleagues report that the average change in methylation at DMRs was 15%, and that these changes were enriched at CGIs and CGI shores (2014). These data align with the observations that alterations in CG methylation affecting tissue and cell-specific gene expression often occur in CGIs and shores (Irizarry, Ladd-Acosta et al. 2009, Stadler, Murr et al. 2011, Ziller, Gu et al. 2013). They performed parallel H3K27ac ChIP-Seq and RNA-Seq, and also utilized available Cdx2 and Hnf4α ChIP-Seq data (Verzi, Shin et al. 2013)(Verzi, Shin et al. 2013)(Verzi, Shin et al. 2013)(Verzi, Shin et al. 2013)(Verzi, Shin et al. 2013)(Verzi, Shin et al. 2013), to correlate DMRs with active enhancer elements during the differentiation process. Many DMRs that gained methylation during differentiation associate with highly expressed ISC genes, and demonstrate increased H3K27ac and Cdx2 binding in the Lgr5^{+} population relative to villus cells (Figure 1.2 C-D). DMRs that lost methylation from the stem to differentiated cell state corresponded with increased expression of the associated gene, which were enriched for metabolism and enterocyte-specific transcripts. Interestingly, they discovered that these differentiation-DMRs also gained H3K27ac, and displayed increased Cdx2 and Hnf4α binding in differentiated cells versus Lgr5^{+} ISCs (Sheaffer, Kim et al. 2014). These data indicate that DNA methylation works in combination with transcription factors to activate enhancers and modulate gene expression programs during intestinal differentiation.

The authors also employed genetic means to demonstrate that DNA methylation has significant effects on cell proliferation and differentiation *in vivo*. Inducible deletion of *Dnmt1* in the adult mouse intestine caused an approximately two-fold expansion of the crypt compartment, and increased expression of *Lgr5* and *Olfm4*, markers of active CBC stem cells (Sheaffer, Kim et al. 2014). Targeted bisulfite sequencing upstream of these stem cell genes revealed demethylation at putative enhancer elements, implicating a role for Dnmt1 and DNA methylation in promoting cell differentiation and restricting crypt cell proliferation (Figure 1.2 C-D) (Sheaffer, Kim et al. 2014). The above experimental results strongly suggest a role for DNA methylation in regulating enhancer activation and controlling processes relating to cell proliferation.

Epigenetic Modifications and Aberrations in Intestinal Disease

Colorectal cancer (CRC) is the third most common type of cancer in the United States, with a lifetime incidence of approximately 5% in both men and women (Siegel, Desantis et al. 2014). The risk of developing colorectal cancer increases with age, as 60% of CRC diagnoses and 70% of deaths relating to CRC occur in patients at 65 years or older (Siegel, Desantis et al. 2014).

The adenoma to carcinoma progression is well characterized in human CRC, and it may take several decades for a malignant tumor to fully form. Cancers begin as hyper-proliferative crypts that have accumulated mutations in tumor suppressor genes, such as *APC*, a Wnt inhibitor that is mutated in 80% of sporadic CRCs (Fearon 2011). Loss of APC causes constitutive Wnt activation and increased proliferation, resulting in dysplastic crypts. Over time, these hyper-proliferative foci develop into adenomatous polyps, or adenomas. Adenomas are generally benign, but a small percent progress to carcinoma, and adenomatous polyps are the main precursor to invasive colorectal cancers (Jass 2007).

Development from adenoma to carcinoma requires multiple gene mutations; primary tumors harbor up to 80 distinct somatic mutations, and as many as 7 major genetic translocations or duplications (Wood, Parsons et al. 2007, Leary, Lin et al. 2008). Tumor suppressor proteins,

including *p53* and *PTEN* in addition to *APC*, accumulate inactivating mutations that allow unrestrained proliferative activity. Typically, both alleles of a tumor suppressor gene must be inactivated to cause a phenotype, following Knudson's two-hit rule (Fearon 2011). Thus, germline inheritance of a heterozygous allele at these genes renders patients sensitive to cancer initiation by a loss-of-heterozygosity (LOH) mutation mechanism. Loss of tumor suppressor gene function is important in promoting genomic instability, a key feature of most invasive carcinomas. For instance, nearly 70% of CRCs display mutations in chromosome 18q (Vogelstein, Fearon et al. 1988). These mutations inactivate TGF-β signaling, which normally acts to restrict intestinal cell proliferation to the crypt. Oncogenic mutations are common in CRC as well, with approximately 40% of CRCs demonstrating activating mutations at *KRAS* to support cell division via the EGFR pathway (Fearon 2011).

Sporadic CRCs are separated into two general categories: those with microsatellite instability and mismatch repair deficiencies, and those that are microsatellite stable but display chromosomal aneuploidy and large-scale genomic alterations (Network 2012). Microsatellite instability (MSI) refers to changes in the length of microsatellite repeat elements, and is usually caused by defects in the DNA mismatch repair (MMR) machinery. MSI is significantly associated with the human heredity nonpolyposis colorectal cancer (HNPCC) syndrome (Fearon 2011). The gene most commonly inactivated in MSI^+ cancers is *Mlh1*, although other MMR proteins including *MSH2*, *PMS1*, and *PMS2* account for a significant subset of gene mutations (Vilar and Gruber 2010). The incidence of MSI is nearly 100% in HNPCC patients, but occurs in only ~15% of sporadic CRC (Aaltonen, Peltomäki et al. 1993).

The remaining 85% of sporadic CRCs are microsatellite stable, but show a high degree of chromosomal instability (CIN) (Rajagopalan, Nowak et al. 2003). CIN tumors display increased rates of aneuploidy, such as the translocations frequently cited on chromosome 18q, and high levels of LOH at tumor suppressor genes (Fearon 2011). The CIN phenotype is considered dominant; when CIN cells are fused with non-CIN cells, a CIN phenotype is transferred. When two non-CIN cells are fused, the mere presence of 4 copies of each chromosome does not

induce CIN, indicating the cancer cells harbor a specific phenotype (Lengauer, Kinzler et al. 1997). CIN tumors also associate with mutations in the genes encoding spindle-related proteins, such as BUB1 and MAD2 (Cahill, Lengauer et al. 1998, Michel, Liberal et al. 2001). However, there has been continued speculation that the CIN phenotype is simply an artifact of cancer progression, and this argument will likely continue until a molecular mechanism for CIN is found (Pino and Chung 2010).

There are also several human genetic syndromes that predispose to CRC. Familial adenomatous polyposis (FAP) patients have germ-line *APC* mutations, leaving them with only one functional copy of this crucial tumor suppressor protein (Fearon 2011). Thus, the likelihood of loss of heterozygosity at the *APC* locus is dramatically increased in FAP patients, and nearly 100% of cases develop CRC by 36 years of age (Galiatsatos and Foulkes 2006). Typical treatment for FAP involves resection of the colon in early adulthood to prevent development of metastatic CRC (Lynch and de la Chapelle 2003). Although FAP accounts for only 0.5% of CRC cases (Fearon 2011), its genetic basis has made it attractive for use in model organisms. The $Apc^{Min/+}$ mouse model is based on the human FAP syndrome, and is the main model for studies of CRC development and progression (Su, Kinzler et al. 1992). Tumors in $Apc^{min/+}$ mice are Apc-negative, demonstrating that loss of heterozygosity (LOH) is required for tumor development (Luongo, Moser et al. 1994). Interestingly, $Apc^{Min/+}$ mice form tumors predominantly in the small intestine, as opposed to human FAP, which develops adenomas in the colon (Su, Kinzler et al. 1992). The cause for this different anatomical site is not well understood, although it has been noted that several markers of human CRC, such as the CBC stem cell marker Olfm4, are not expressed in the murine colonic epithelium (van der Flier, Haegebarth et al. 2009). Nevertheless, $Apc^{Min/+}$ mice have proven to be a useful tool in understanding both intestinal and colorectal tumorigenesis.

The epigenetic contribution to CRC has been studied extensively over the past thirty years, but there is still much we do not understand about its role in carcinogenesis. The majority of these studies focused on the function of DNA methylation, because colorectal cancers

generally display genome-wide hypomethylation that occurs early in the adenoma-carcinoma progression sequence (Goelz, Vogelstein et al. 1985, Feinberg, Gehrke et al. 1988). Below, we outline the proposed function of altered epigenetics in human CRC, and the information we have gleaned from studies of DNA methyltransferase mutations in mouse models of intestinal and colorectal cancer.

DNA methylation patterns in human colorectal cancer

The precise function of hypomethylation in human CRC progression is not well understood. The earliest epigenetic profiling of cancer cells noted genome-wide hypomethylation in malignant human colorectal tumors (Feinberg and Vogelstein 1983, Gama-Sosa, Slagel et al. 1983). In later studies, it was discovered that even benign polyps and precancerous adenomas were substantially demethylated, with a reduction of 8-10% compared to histologically normal adjacent tissue (Goelz, Vogelstein et al. 1985, Feinberg, Gehrke et al. 1988). These results were striking, and implicated a role for DNA methylation in colorectal tumorigenesis. Global genomic hypomethylation may cause activation of proliferation-associated genes, and leads to increased mutation rates based on *in vitro* data (Chen, Pettersson et al. 1998). Analyses of human CRC cell lines indicates that hypomethylation causes expression of previously silenced genes (Nakamura and Takenaga 1998), and correlated with increased genomic instability (Lengauer, Kinzler et al. 1997). Ablation of *DNMT1* in a human CRC cell line caused hypomethylation, DNA replication defects, cell cycle arrest, and apoptosis (Chen, Hevi et al. 2007).

Notably, in CRC tumor suppressor genes often display decreased expression, few genetic alterations, and increased promoter or CGI methylation. This promoter hypermethylation has been studied extensively, and is a defining characteristic of the CpG Island Methylator Phenotype, or CIMP (Toyota, Ahuja et al. 1999). CIMP-high (CIMP-H) tumors display increased DNA methylation at CGIs of tumor suppressors including *CDKN2A* (*p16*), *THBS1*, and *Mlh1*. CIMP-H tumors account for nearly all CRCs containing oncogenic *BRAF*/MAPK-pathway mutations (Weisenberger, Siegmund et al. 2006), and is also common among tumors displaying

MSI (Issa 2004). In sporadic MSI^{+} tumors, DNA mismatch repair (MMR) genes are often inactivated via promoter hyper-methylation. The association of MSI with CGI hypermethylation at multiple tumor suppressor genes strongly implicates CIMP as the underlying cause of genomic instability in MSI (Weisenberger, Siegmund et al. 2006). MSI also correlates with loss of genomic imprinting (Cui, Horon et al. 1998), and mutations at the SWI/SNF chromatin-remodeling gene *ARID1A* (Jones, Li et al. 2012).

With the advent of next-generation sequencing, there have been multiple studies aiming to profile the epigenome of human CRC (Irizarry, Ladd-Acosta et al. 2009, Berman, Weisenberger et al. 2012, Network 2012). The Cancer Genome Atlas Network published an extensive study profiling DNA methylation and RNA expression from hyper-mutated versus non-hypermutated categories of tumors (2012). They observed that non-hypermutated tumors, regardless of CIMP status, displayed similar DNA methylation and gene expression patterns. In accordance with previous studies, they found that hyper-mutated cancers were enriched for hypermethylation and CIMP-H status, as well as *BRAF* mutations (Network 2012).

The mechanism underlying CIMP is not known. Several studies have reported that DNMT overexpression underlies this phenotype (Nosho, Shima et al. 2009), but numerous reports have refuted this mechanism (Eads, Danenberg et al. 1999). One study suggests that aberrant DNA methylation in CRC may involve the repressive Polycomb complex. Widschwendter et al. reported a 12-fold enrichment for Polycomb target sequences among hypermethylated regions in CRC (2007). Polycomb repressive complexes interact with DNMTs in human cell lines, and the EZH2 subunit of Polycomb is required to recruit DNMTs to H3K27-methylated CpGs (Viré, Brenner et al. 2006). Thus, in cancer, EZH2 activity may attract DNA methylation to permanently silence target genes, predisposing to cancer development.

Irizarry and colleagues performed genome-wide bisulfite sequencing in human colorectal tumors to assess exactly where hypermethylation occurs relative to CGIs and transcription start sites (2009). Interestingly, they found that hypermethylation in CRCs is enriched at CGI shores, defined as the regions 2KB upstream and downstream of a respective CGI. The CGI enrichment

data for CRCs are similar to the distribution they found for tissue-specific differentially methylated regions (DMRs) in normal tissues (Irizarry, Ladd-Acosta et al. 2009). Furthermore, they found nearly equal amount of hypo- and hyper-methylated CGI shores in CRC compared to normal colon, suggesting that both types of methylation aberrations are involved in cancer formation. Many of these so-called cancer DMRs were enriched for tissue-specific DMRs, such as spleen, liver and brain, and gene ontology of the cancer-specific DMRs identified gene categories involved in pluripotency and development (Irizarry, Ladd-Acosta et al. 2009). Thus, many of the same pathways and tissues involved in development are altered in human CRC. This idea forms the basis for the epigenetic progenitor model of cancer, in which aberrant activity of differentiation pathways causes cancer (Jones and Baylin 2007).

DNA methylation in CRC: Lessons from Mouse models

The *Apc*$^{Min/+}$ model, based on human FAP, forms the basis for *in vivo* studies of intestinal carcinogenesis. The *Apc*$^{Min/+}$ mice develop multiple tumors throughout the intestinal epithelium, with microadenomas visible by 3 months of age (Moser, Pitot et al. 1990, Su, Kinzler et al. 1992, Laird, Jackson-Grusby et al. 1995). The earliest reports of the effects of DNA hypomethylation on tumorigenesis in *Apc*$^{Min/+}$ mice utilized a combination of *Dnmt1* hypomorphic alleles and the pharmacological Dnmt inhibitor 5-aza-deoxycytidine (5-aza). Laird and colleagues produced *Apc*$^{Min/+}$;*Dnmt1*$^{S/+}$ hypomorphic mice, and treated them with 5-aza from one week of age to induce DNA hypomethylation. At 100 days, they observed that the *Apc*$^{Min/+}$;*Dnmt1*$^{S/+}$ 5-aza treated mice had only two intestinal polyps, compared to 113 in the *Apc*$^{Min/+}$ no 5-aza control. They concluded that DNA hypomethylation is not a causative factor in intestinal tumor development, and that DNA methylation is required for intestinal carcinogenesis.

Further studies enhanced this hypothesis, using varying *Dnmt1* hypomorphic alleles on the *Apc*$^{Min/+}$ background. Cormier and Dove (2000) used *Apc*$^{Min/+}$;*Dnmt1*$^{N/+}$ mice to show that Dnmt1 regulates both intestinal tumor incidence and size, and noted that tumor suppression in this model was not dependent on p53. Eads and colleagues built on these data by constructing a

Apc$^{Min/+}$;*Dnmt1*$^{N/R}$ mouse line, which displayed severe hypomethylation and no polyp formation (2002). They also found that these mice display reduced CGI hypermethylation at tumor suppressor genes, and conclude that CGI hypermethylation is required for intestinal tumor development (Eads, Nickel et al. 2002).

The most recent report more closely analyzes the varying stages of colonic tumor development in the absence of Dnmt1 (Yamada, Jackson-Grusby et al. 2005). *Apc*$^{Min/+}$;*Dnmt1*$^{chip/c}$ mice exhibit reduced DNA methylation and colon macroadenoma formation, as expected. Interestingly, *Apc*$^{Min/+}$;*Dnmt1*$^{chip/c}$ mice displayed increased numbers of colonic microadenomas, suggesting that Dnmt1 is not required to initiate tumors, but is required for their sustained growth. It should be noted that *Apc*$^{Min/+}$ mice typically do not develop colonic tumors; unlike human FAP, *Apc*$^{Min/+}$ mice develop primarily intestinal tumors. Yamada et al.'s *Apc*$^{Min/+}$ colon controls only contain ~1 tumor per mouse, as opposed to the 100^{+} tumors an *Apc*$^{Min/+}$ intestine would produce (Yamada, Jackson-Grusby et al. 2005). As a result, it is difficult to draw precise conclusions from this model.

Due to the impact of the CIMP phenotype in human CRC research, the function of *de novo* Dnmts in mouse tumor development has also been a significant area of research. Inducible overexpression of *Dnmt3a* had no effect on colon tumorigenesis on the *Apc*$^{Min/+}$ background (Linhart, Lin et al. 2007). In the same study, inducible overexpression of Dnmt3b increased the number of colonic and intestinal macroscopic adenomas. Linhart and colleagues also report that Dnmt3b overexpression increased *de novo* methylation at *Sfrp2*, *Sfrp4*, and *Sfrp5*, which are endogenous suppressors of Wnt signaling (2007). *Sfrp* genes are common targets of promoter hypermethylation in human CRCs (Suzuki, Watkins et al. 2004). In related studies in human colorectal cancer cell lines, demethylation of *Sfrp* gene promoters reactivated the associated genes, halting cell proliferation and inducing apoptosis (Suzuki, Watkins et al. 2004).

Additionally, Dnmt3b overexpression in *Apc*$^{Min/+}$ mice causes hypermethylation of similar gene sets in both colonic tumors and adjacent normal epithelium. Dnmt3b had no effect on the typical CIMP tumor suppressors, such as *Mlh1* or *Mgmt*, implying that Dnmt3b targets specific

genes for hypermethylation (Linhart, Lin et al. 2007). Overall, these results suggest that Dnmt3b may promote the formation of colorectal cancers, and has a transformative effect on normal colonic epithelium.

The same group also published a study assessing the requirement for Dnmt3b in *Apc*$^{Min/+}$ tumor development. They used the Cre-*loxP* recombination system to produce a colon-specific *Dnmt3b* deletion on the *Apc*$^{Min/+}$ background. Lin and colleagues did not report any variation in normal wild-type mucosa in the absence of Dnmt3b (2006). In *Apc*$^{Min/+}$ mice, loss of Dnmt3b led to a significant decrease in the number of macroscopic colonic tumors, but did not affect microadenoma initiation. The *Dnmt3b* deletion was fairly mosaic; only about half of microadenomas demonstrated loss of Dnmt3b protein. All mature tumors, however, contained patches of Dnmt3b^{+} cells, indicating an active selection against Dnmt3b-null microadenomas in tumor development (Lin, Yamada et al. 2006). These results suggest that Dnmt3b is crucial for progression to adenoma, but may not be essential to maintain a fully formed tumor.

Based on the above studies, one could conclude that DNA hypomethylation is unimportant for tumor development. However, there are several problems with these studies that remain to be addressed in the future. The above experimental models employed hypomorphic *Dnmt1* alleles, which caused hypomethylation in all tissues from early development onward. As a result, the observed phenotypes may be due to developmental defects or intestine-independent effects of hypomethylation. For instance, mesenchyme-specific transcription factors, such as Foxl1, are important modifiers of the *Apc*$^{Min/+}$ phenotypes (Perreault, Sackett et al. 2005), and may be affected in *Dnmt1*-hypmorphic mice. Dnmt1 is also required for embryonic development (Li, Bestor et al. 1992), and may play an important role in organogenesis as well (Georgia, Kanji et al. 2013). Although the role of Dnmt1 in the developing intestinal epithelium is unknown, in the mature epithelium Dnmt1 supports differentiation processes and restricts the proliferative stem cell zone (Sheaffer, Kim et al. 2014). Indeed, loss of Dnmt1 in the adult intestinal epithelium causes a two-fold expansion of the crypt compartment (Sheaffer, Kim et al. 2014), suggesting that methylation plays essential roles in regulating proliferative processes. Thus, it would be

valuable to reassess the role of Dnmt1 in the *Apc*$^{Min/+}$ colorectal cancer model using epithelial specific and/or inducible Cre-*loxP* mouse models. In this work, I describe the function of Dnmt1 during perinatal intestinal development and *Apc*$^{Min/+}$ intestinal cancer progression.

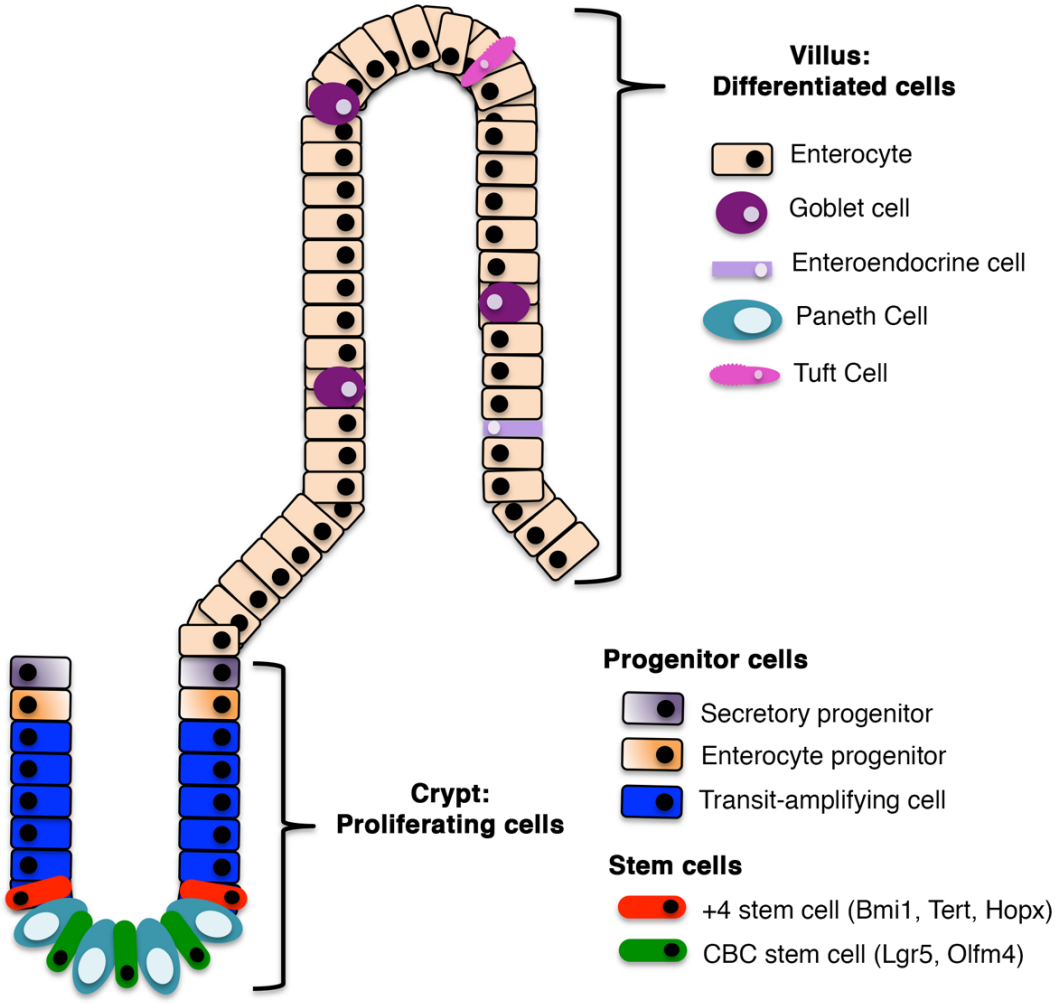

Figure 1.1. The mammalian intestinal epithelium

Figure 1.1. The mammalian intestinal epithelium.

Longitudinal cross section of the adult intestinal epithelium. The intestinal epithelium is a single cell layer lining the lumen of the intestine, and is structured into proliferative crypts and differentiated villi. Crypts contain both proliferative CBC stem cells and quiescent +4 stem cells. These stem cells give rise to rapidly dividing transit-amplifying cells, which begin differentiation as they migrate out of the crypt. Secretory progenitors differentiated into goblet cells, enteroendocrine cells, Paneth cells. Enterocyte progenitors develop into absorptive enterocytes, which comprise ~90% of the epithelium.

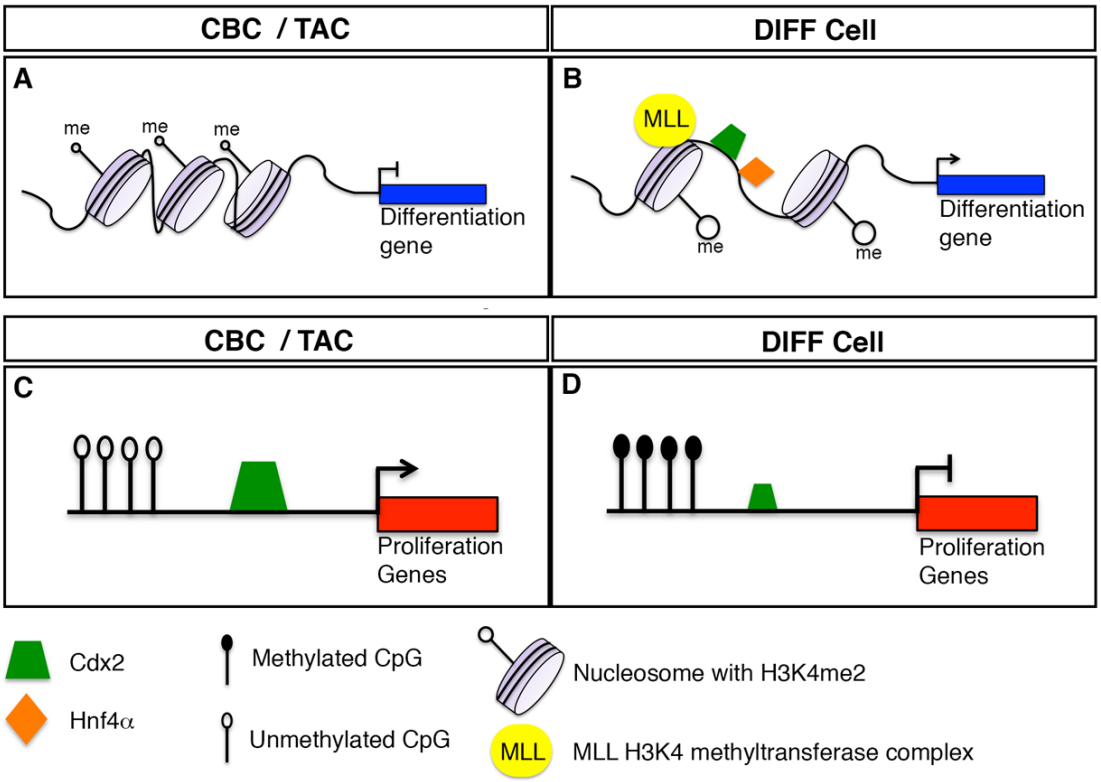

Figure 1.2. Opposing roles for epigenetic modifications in the intestinal epithelium

Figure 1.2. Opposing roles for epigenetic modifications in the intestinal epithelium.

(A,B) Cdx2 maintains the open chromatin state at enhancers during intestinal differentiation. In proliferating cells Cdx2 is not bound at differentiation-enhancers, and these regulatory regions display reduced H3K4me2 (A). As a result, these genes are not highly expressed. In differentiating cells, Cdx2 and Hnf4a bind at enhancer regions marked by increased H3K4me2, which activates expression of enterocyte-lineage genes (B). Cdx2 supports H3K4me2 di-methylation, presumably by MLL methyltransferase complex activity. Loss of Cdx2 binding in these regions leads to reduced H3K4me2 in differentiated villus cells (Verzi, Shin et al. 2013)(Verzi, Shin et al. 2013)(Verzi, Shin et al. 2013)(Verzi, Shin et al. 2013)(Verzi, Shin et al. 2013)(Verzi, Shin et al. 2013).

(C,D) DNA methylation at enhancers upstream of proliferation and/or stem cell genes regulates cell division in crypts. In dividing intestinal cells, enhancers are unmethylated (C), allowing Cdx2 to bind and activate progenitor gene expression. In differentiated cells, enhancers associated with stem cell genes are methylated (D). DNA methylation restricts access by transcription factors, and genes are silenced.

(A,B) adapted from Verzi et al. 2010. (C,D) adapted from Sheaffer et al. 2014.

Chapter 2

Materials and Methods

General Protocols

Animals and genotype analysis *Dnmt1*$^{loxP/loxP}$ and *Dnmt3b*$^{loxP/loxP}$ mice were kindly provided by Rudolf Jaenisch (Jackson-Grusby, Beard et al. 2001, Lin, Yamada et al. 2006), and *VillinCreERT2* mice were received from Sylvia Robine (el Marjou, Janssen et al. 2004). *VillinCre* (Madison, Dunbar et al. 2002) and *Apc*$^{Min/+}$ mice (Moser, Pitot et al. 1990, Su, Kinzler et al. 1992) were obtained from The Jackson Laboratory. Genotyping was performed by PCR analysis. For *VillinCreERT2*-mediated deletion experiments, Cre-recombination was induced by three daily intraperitoneal injections of 1.6 mg tamoxifen (Sigma) in an ethanol/sunflower oil mixture. Littermate controls without the *VillinCreERT2* transgene also received tamoxifen treatment. For 2-hour EdU analysis, I administered EdU by intraperitoneal injection 2 hours prior to dissection. I administered 0.1 mg EdU (Invitrogen) for postnatal day 0 (P0) mice, and 1 mg EdU for 3-month old adult mice. All procedures involving mice were conducted in accordance with approved Institutional Animal Care and Use Committee protocols.

Histology, immunohistochemistry, and immunofluorescence Intestines were fixed O/N in 4% paraformaldehyde and embedded in paraffin. Hematoxylin and eosin (H&E) staining were used to assess global morphology of intestinal epithelial specimens. For all antibody staining, slides were dewaxed and antigen retrieval was performed using the 2100 Antigen-Retriever and R-Buffer A (Electron Microscopy Sciences). Standard immunohistochemistry staining was performed for Dnmt1 (Santa Cruz 20701, 1:200), Ki67 (BD Pharmingen 550609, 1:500), and β-catenin (BD Transduction 610153, 1:200) using the ABC detection system (Vector Laboratories). Briefly, following antigen retrieval all slides were blocked with 3% H_2O_2, avidin, and biotin (Vector Laboratories). Additionally, for staining of Dnmt1 slides were blocked for 30 minutes with CAS Block (Invitrogen), and for staining of Ki67 and β-catenin slides were blocked for 15 minutes with StartingBlock T20 blocking buffer (Thermo Scientific). Sections were incubated with respective primary antibody at 4°C overnight, with the exception of Dnmt1, which was diluted in Antibody Diluent Reagent Solution (Invitrogen). The next day, slides were incubated with biotinylated secondary antibody (Vector Laboratories) followed by treatment with ABC reagent, and

developed with DAB (Vector Laboratories). P21 immunohistochemistry (BD Pharmingen 556430, 1:50) was performed as described previously (van de Wetering, Sancho et al. 2002). Standard immunofluorescence procedures were performed with the following antibodies: Chromogranin A (Immunostar 20085, 1:200), Ki67 (BD Pharmingen 550609, 1:500), Dnmt3a (Santa Cruz 20703, 1:500), Dnmt3b (Imgenex 184A, 1:500), E-cadherin (BD Transduction Lab 610181, 1:500), Epcam (Abcam 71916, 1:500), Lysozyme (Dako A0099, 1:3,000), Mucin2 (Santa Cruz 15334, 1:50), γH2AX (Cell Signaling 2577L, 1:250), and phosphorylated histone H3 (Cell Signaling 3377, 1:500). For E-cadherin, γH2AX, and PH3 staining, tissues were blocked for 15 minutes with CAS Block (Invitrogen). For staining of Ki67, Chromogranin A, Lysozyme, Mucin2, Dnmt3a, and Dnmt3b, tissues were blocked for 2 hours at room temperature with 5% normal donkey serum (EMD Millipore) in 1% BSA in PBS. For Epcam and Ki67, sections were blocked for 15 minutes with StartingBlock T20 blocking buffer (Thermo Scientific). All tissues were incubated with respective primary antibody overnight at 4°C. The following day, slides were incubated with immunofluorescent secondary antibodies (The Jackson Laboratory), counterstained with DAPI, and mounted with fluorescence mounting medium. Co-staining was accomplished by sequential immunohistochemistry and immunofluorescent antibody staining. Alkaline phosphatase staining was performed using NBT and BCIP (Boehringer). Immunofluorescent TUNEL staining was performed using TUNEL Label and Enzyme (Roche) and AlexaFluor 555-aha-dUTP (Life Technologies). For cell replication analysis, we used the Click-iT EdU Alexa Fluor 555 Imaging Kit (Invitrogen). All microscopy was performed on a Nikon Eclipse 80i.

mRNA expression analysis Small intestines and macroscopic tumors were isolated and immediately frozen in Trizol (Invitrogen). RNA was extracted using the Trizol RNA isolation protocol (Invitrogen), followed by RNA cleanup using the RNeasy Mini Kit (Qiagen). mRNA expression was measured using quantitative RT-PCR, as described previously (Gupta, Gao et al. 2007). The SYBR green qPCR master mix (Agilent) was used in all qPCR reactions, and the fold change was calculated relative to the geometric mean of *Tbp* and *β-Actin*, using the ΔCT method. The method of normalizing to the geometric mean of a set of reference genes has been

described previously (Vandesompele, De Preter et al. 2002). Primer sets can be found in Table 2.1.

Protocols specific for Chapter 3: Dnmt1 is essential to maintain progenitors in the perinatal intestinal epithelium.

Cell counting in the* Dnmt1*-deficient neonatal intestine For villi quantification, H&E sections of tissue were scanned at 10X using Metamorph imaging software (Molecular Devices). Per biological replicate, villi were counted for ≥20 mm tissue, measured using ImageJ (Schneider, Rasband et al. 2012). For TUNEL and γH2AX quantification, 500 intervillus cells were counted at 20X for each biological replicate. Intervillus cells were defined as 20 μm from the base of the intestinal epithelium.

EdU quantification in the adult and neonatal intestinal epithelium For EdU quantification, I harvested jejunum from five *Dnmt1*$^{loxP/loxP}$ 3-month old adult mice, and three litters of *Dnmt1*$^{loxP/loxP}$ P0 mice (4 mice per litter). I defined the crypt-villus subunit as the epithelium lying between the peaks of two adjacent villi that share the same crypt. I counted the total number of EdU^{+} nuclei per crypt or intervillus region, and divided this number by the total number of nuclei per crypt villus subunit. Per adult sample, I counted ~8 crypt-villus subunits. Per P0 sample, I counted ~25 crypt-intervillus subunits.

Laser capture microdissection, RNA-Seq, and mRNA expression analysis Laser capture microdissection (LCM) was performed from unstained sections of paraffin-embedded, methacarn-fixed proximal jejunum for 3 controls and 2 mutants, as described previously (Miyoshi, Ajima et al. 2012). For laser-capture microdissection (LCM), proximal jejunum was collected from *Dnmt1*$^{loxP/loxP}$*; VillinCre* neonatal litters. Tissue was fixed for one hour in cold methacarn solution (60% methanol, 30% chloroform, 10% glacial acetic acid), washed 3 times in cold 70% ethanol, and submitted for paraffin embedding and sectioning. Serial sections were cut for mutants (*Dnmt1*$^{loxP/loxP}$*; VillinCre*, n=2) and controls (*Dnmt1*$^{loxP/+}$, n=3). Odd numbered sections were mounted onto charged glass slides, and were used for Ki67 IF staining as described above. Ki67

stained sections were scanned using a 10X objective and Metamorph imaging software; scans served as the map for LCM on unstained sections. Even numbered sections were mounted onto non-charged glass slides for use in LCM.

The PixCell II LCM system (Arcturus, Applied Biosystems; 7.5-μm diameter laser spot) was used to capture $Ki67^-$ intervillus cells from mutants (n=2) and $Ki67^+$ intervillus cells from controls (n=3). Captured cells were collected onto CapSure HS LCM caps (Applied Biosystems), and total cellular RNA was extracted using the PicoPure RNA isolation kit (Applied Biosystems). RNA concentration and quality was assessed on an Agilent 2100 Bioanalyzer (Agilent Technologies). Total RNA isolated by LCM (2.3 ng to 33.3 ng per sample) was amplified using the Ovation RNA-Seq System V2 (NuGEN). 300 ng of each sonicated cDNA sample was used for RNA-Seq library preparation. cDNA sequencing libraries were completed using NEBNext Ultra RNA Library Prep Kit for Illumina (New England Biolabs), Illumina multiplexing adaptors, and the NEBNext ChIP-Seq DNA Sample Prep Reagent Set 1 Kit (New England Biolabs). Single-read sequencing was performed on the Illumina HiSeq 2000 (100 bp reads).

Reads (a minimum of 25 million per sample, ~80% unique mapped reads) were aligned to the mouse reference genome (NCBI build 37, mm9) using TopHat (Trapnell, Roberts et al. 2012). TopHat was run with the University of California at Santa Cruz refFlat annotation file (GTF format) and the "–no-novel-juncs" option to map reads only in the reference annotation. Cutdiff was used to calculate gene expression levels (Trapnell, Roberts et al. 2012). Messenger RNA levels were expressed in reads per kilobase of transcript per million mapped reads (RPKM). Gene Ontology analysis was performed using DAVID (Ashburner, Ball et al. 2000). Cutdiff results were filtered by FDR<0.1, and separated into two categories, upregulated genes and downregulated genes. DAVID functional annotation analysis was performed separately for each gene set.

RNA isolation and qRT-PCR to confirm RNA-Seq For confirmation of RNA-Seq results, proximal jejunal RNA samples were collected by Laser Capture Microdissection using a Leica LMD7000 Laser Microdissection microscope, as described above. Approximately 10,000 cells

were collected per sample. RNA was isolated and cDNA amplified using the protocols described for the RNA-Seq libraries. The SYBR green qPCR master mix (Agilent) was used in all qPCR reactions, and the fold change was calculated relative to the geometric mean of five reference genes: *Tbp*, *b-Actin*, *Rplp0*, *Polr2b*, and *B2m* using the ΔCT method. Primer sets can be found in Table 2.1.

Organoid culture For neonatal *Dnmt1*$^{loxP/loxP}$ (n=3) and *Dnmt1*$^{loxP/loxP}$*; VillinCre* (n=2) organoid culture, duodenum and jejunum were opened longitudinally in cold PBS, cut into 10mm pieces, and incubated in EDTA. Vigorous pipetting released the epithelia from the tissue, and cells were embedded in Matrigel (BD Biosciences) for cell culture, as described previously (Sato, Vries et al. 2009). All organoids were grown at 37°C, 5% CO_2. Cell media (Advanced DMEM/F12, Invitrogen) was supplemented with GlutaMax (Invitrogen), Hepes (Invitrogen), Pen/Strep (Invitrogen), N2 (Invitrogen), B27 (Invitrogen), and N-Acetylcysteine (Sigma). The following growth factors were added to media: mEGF (Invitrogen), mNoggin (Peprotech), hR-Spondin (Peprotech). For the first two days of neonatal organoid growth, cultures were also supplemented with Y-27632 (Sigma) and CHIR-99021 (Biovision). The medium was changed every other day.

Crypts were isolated from jejunum of 3-month-old *Dnmt1*$^{loxP/loxP}$*; VillinCreERT2* (n=4) and *Dnmt1*$^{loxP/loxP}$ (n=2) mice for organoid culture as described previously (Sato, Vries et al. 2009). The following growth factors were added to media: mEGF (Invitrogen), mNoggin (Peprotech), hR-Spondin (Peprotech), and CHIR-99021 (Biovision). The medium was changed every other day. For *VillinCreERT2* induction, 4-hydroxytamoxifen (Sigma H7904) was added to organoid media at a final concentration of 100nm (Sato, Vries et al. 2009). After 48 hours, the 4OHT medium was removed and fresh medium was added to each well. The 100nm concentration was not detrimental to Dnmt1$^{loxP/loxP}$ control organoids at either time point (Fig. S10 and S11).

2 hours prior to organoid harvest, EdU (Invitrogen) was added to each well (10mm). Organoids were harvested using cold PBS, and were fixed in 4% PFA for 1 hour at 4°C. Organoid pellets were suspended in agarose, embedded in paraffin, and sectioned for immunohistochemistry analysis.

Laser capture microdissection and targeted bisulfite sequencing DNA was isolated from paraffin-embedded tissue sections using a Leica LMD7000 Laser Microdissection microscope and the Arcturus PicoPure DNA isolation kit (Applied Biosystems). LCM-isolated DNA was bisulfite-converted and purified using the Epitect Bisulfite Kit (Qiagen). Template DNA was amplified using the KAPA HiFi HotStart Uracil+ ReadyMix PCR Kit (Kapa Biosystems). The LINE1 and H19 PCR assays were described previously (Lane, Dean et al. 2003, Samuel, Suzuki et al. 2009). Additional primer sets were designed using PyroMark software (Qiagen) and are listed in Table 2.2. Adult *Dnmt1*$^{loxP/loxP}$*;VillinCreERT2* mutant and *Dnmt1*$^{loxP/loxP}$ control crypt DNA were kindly provided by K.L.Sheaffer (Sheaffer, Kim et al. 2014).

Sequencing libraries were made using the Ovation SP Ultralow Library system and Mondrian SP+ Workstation (NuGEN). Libraries were pooled at 8 nM, and 150bp paired end sequencing was performed on the Illumina MiSeq (MiSeq v2 Reagent Kit, 300 cycles PE). Converted sequence was aligned to the mouse genome (NCBI build 37, mm9) using BS Seeker (Chen, Cokus et al. 2010).

Data Access All RNA sequencing data generated in this study have been deposited in the NCBI Gene Expression Omnibus (Edgar, Domrachev et al. 2002) under accession number GSE67363.

Protocols specific for Chapter 4: Dnmt1 and Dnmt3b are required for genomic stability in intestinal epithelial homeostasis.

Tumor evaluation procedures Macroscopic tumors were counted immediately after tissue isolation using a stereoscope. Microadenoma counts were performed on sections stained with hematoxilyn and eosin (H&E) for the small intestine and sections stained with β-catenin for the colon. Microadenoma size was calculated by measuring the width of neoplastic lesions on H&E stained small intestine sections using ImageJ (Schneider, Rasband et al. 2012). Histological pathology was performed as described previously (Boivin, Washington et al. 2003).

Loss of heterozygosity at the* Apc *locus Tumor and non-tumor epithelial cell DNA were collected using a Leica LMD7000 Laser Microdissection microscope and the Arcturus PicoPure DNA isolation kit (Applied Biosystems). LOH was performed as done previously (Luongo, Moser et al. 1994).

Phosphorylated-H3 cell cycle quantification *$Apc^{Min/+}$;$Dnmt1^{loxP/loxP}$;VillinCreERT2* mutants and sibling *$Apc^{Min/+}$;$Dnmt1^{loxP/loxP}$* controls were injected with tamoxifen at 1 month of age. Small intestines were collected one month and two months following tamoxifen administration, in separate cohorts of mice. Following fixation, tissue sections were co-stained for phosphorylated histone H3 (PH3) to identify cells in M-phase, and β-catenin to identify hyper-proliferative neoplastic epithelium. I counted the number of $PH3^+$ nuclei, and divided it by the total number of nuclei in the respective region. This calculation was performed for neoplastic intestinal epithelium at both time points, for controls and mutants.

Laser capture microdissection Tumor and non-tumor epithelial cell DNA was collected using a Leica LMD7000 Laser Microdissection microscope and the Arcturus PicoPure DNA isolation kit (Applied Biosystems).

Targeted bisulfite sequencing 100 ng of mouse genomic DNA was bisulfite converted using the Epitect bisulfite kit (Qiagen). Template DNA was amplified using the KAPA HiFi HotStart Uracil+ ReadyMix PCR Kit (Kapa Biosystems) with primers directed to the H19 ICR and LINE1 region and modified with partial Illumina adapter overhangs (PCR#1 F/R). Samples were barcoded by

incorporation of a unique DNA sequencing barcode in a subsequent round of PCR amplification (PCR#2 F/R). Samples were pooled at 2nM, and 150bp paired end sequencing was performed on the Illumina MiSeq (MiSeq v2 Reagent Kit, 300 cycles PE). Converted sequences were aligned to the mouse genome (NCBI build 37, mm9) using BS Seeker (Chen, Cokus et al. 2010). Primer sequences can be found in Table 2.3.

Table 2.1		
qRT-PCR Primer Sequences		
Gene	**Forward 5'-3'**	**Reverse 5'-3'**
Atm	ACCACACAGAGCTCCAGACA	GACATTTTAGCCTGGGTGCT
Atm	CGGCAGTTAGAGCATGACAG	GGCGCTTAAATTTATCCACTTC
B2m	TGGTGCTTGTCTCACTGACC	TATGTTCGGCTTCCCATTCT
Beta-actin	GAAGTGTGACGTTGACATCCG	GTCAGCAATGCCTGGGTACAT
Cdk2	TGTGGCGCTTAAGAAGATCC	TCGGATGGCAGTACTGGGTA
Chek2	AAGAGACGAATACATCATGTCAAAA	TGATCTTTATGGCCACTTTCTG
Dnmt1	CTTCACCTAGTTCCGTGGCTA	CCCTCTTCCGACTCTTCCTT
Dnmt3a	GCACCAGGGAAAGATCATGT	CAATGGAGAGGTCATTGCAG
Dnmt3b	GGATGTTCGAGAATGTTGTGG	GTGAGCAGCAGACACCTTGA
Foxm1	AGCGTTAAGCAGGAACTGGA	CACAGAGTCCTGCCAAGATG
Lyz	ACTGCAGCAGCCATACAATGTGC	GGGACAGATCTCGGTTTTGA
Mcm10	TTAAACAGCCTCCAGGGACA	AAGCACGCTGACTCCTGAAT
Mlh1	CGGCCAATGCTATCAAAGAG	CAGGCCACCTTCCTTAACAA
p21 (Cdkn1a)	ATACCGTGGGTGTCAAAGCAC	AGGGAGGGAGCCACAATACAT
Polr2b	GCCAATGATGCCAAATGAA	GTCAACGTAAAGCGGAGCA
Rplp0	GATTCGGGATATGCTGTTGG	GGAGGTCTTCTCGGGTCCT
TBP	CCCCTTGTACCCTTCACCAAT	GAAGCTGCGGTACAATTCCAG

Table 2.2			
Bisulfite Sequencing Primer Sets			
Gene/element	**Forward 5'-3'**	**Reverse 5'-3'**	**Sequence Analyzed (mm9)**
H19	GTTTGTTGAATTAGTTGTGGGGTTTATA	TAAAAAAAAAAACTCAATCAATTACAATCC	Chr7: 149,767,665-149,767,784
LINE1	GTTAGAGAATTTGATAGTTTTTGGAATAGG	CCAAAACAAAACCTTTCTCAAACACTATAT	Accession# D84391: Position 976-1072
Cdkn1a (p21)	GTTGGGAAGGTGGTTAAGTTTT	ACCAATAATTCATCAAAATTACATAACATC	Chr17: 29,228,756-29,228,867
Cdkn1a (p21)	TTGTTTTAGAGGTAGGATGTTATGTAAT	ATAACAAAACCACCATCTCAACTAA	Chr17: 29,229,016-29,229,196
Mlh1	AGGTGGTATTTTTATTTGATAGTAATTAGA	AATTTTCCCTTTTCAAATCAACTTCTTAA	Chr9: 111,176,163-111,176,288
Atm	GGGATGAAGGAATTTAGTATAGTAGG	TCTTTTTACCCTTAAACCAATTCTTTAT	Chr9: 53,348,223-53,348,411
Chek2	TTTTTTAGGGAGTGATTTTAATTGAGTT	TACCTTTTTCCTCCCCTATCTCA	Chr5: 111,267,185-111,267,229

Table 2.3	
Bisulfite Sequencing Primers with Illumina Adapters	
Primer	**Primer Sequence (5'-3')**
H19 PCR#1 Forward	ACACTCTTTCCCTACACGACGCTCTTCCGATCTGTTTGTTGAATTAGTTGTGGGGTTTATA
H19 PCR#1 Reverse	GTGACTGGAGTTCAGACGTGTGCTCTTCCGATCTTAAAAAAAAAAACTCAATCAATTACAATCC
LINE1 PCR#1 Forward	ACACTCTTTCCCTACACGACGCTCTTCCGATCTGTTAGAGAATTTGATAGTTTTTGGAATAGG
LINE1 PCR#1 Reverse	GTGACTGGAGTTCAGACGTGTGCTCTTCCGATCTCCAAAACAAAACCTTTCTCAAACACTATAT
Unique Barcode PCR#2	AATGATACGGCGACCACCGAGATCTACACTCTTTCCCTACACGAC
Unique Barcode PCR#2	CAAGCAGAAGACGGCATACGAGAT**CGTGAT**GTGACTGGAGTTCAGACGTGT
Color Coding Key	
RED TEXT	Illumina Adapter Sequence
GREEN TEXT	Unique Illumina Sequencing Barcodes, 1-48

Chapter 3

Dnmt1 is essential to maintain progenitors in the perinatal intestinal epithelium

Abstract

The DNA methyltransferase Dnmt1 maintains DNA methylation patterns and genomic stability in several *in vitro* cell systems. Ablation of *Dnmt1* in mouse embryos causes death at the post-gastrulation stage; however, the functions of *Dnmt1* and DNA methylation in organogenesis remain unclear. Here, I report that *Dnmt1* is crucial during perinatal intestinal development. Loss of *Dnmt1* in intervillus progenitor cells causes global hypomethylation, DNA damage, premature differentiation, and apoptosis, and consequently, loss of nascent villi. I further confirm the crucial role for Dnmt1 during crypt development using the *in vitro* organoid culture system, and illustrate a clear differential requirement for Dnmt1 in immature versus mature organoids. These results demonstrate an essential role for Dnmt1 in maintaining genomic stability during intestinal development and the establishment of intestinal crypts.

Introduction

DNA methyltransferase 1 (Dnmt1) maintains DNA methylation following DNA replication, but little is known about its requirement for organ development. Previous studies of mice with global deletion of *Dnmt1* failed to define the contribution of maintenance methylation during organogenesis, because *Dnmt1* null mice die shortly after gastrulation, at approximately embryonic day 9.5 (E9.5) (Li, Bestor et al. 1992). With the advent of Cre-loxP recombination technology and tissue specific gene ablation, the role of Dnmt1 in organ development can now be addressed. For example, Dnmt1 has been ablated during neuronal development and shown to be essential for the survival of fetal mitotic neuroblasts (Fan, Beard et al. 2001). *Dnmt1*-ablated neuroblasts are 95% hypomethylated, and mice die just after birth due to respiratory defects, demonstrating a clear role for *Dnmt1* in organ development and cellular differentiation (Fan, Beard et al. 2001). In the fetal pancreas, deletion of *Dnmt1* causes a decrease in differentiated pancreatic cells with a concomitant increase in p53 levels, cell cycle arrest, and progenitor cell apoptosis. However, this phenotype is dependent on direct binding of the Dnmt1 protein to the *p53* (*Trp53*) locus, and was suggested to be caused by a DNA-methylation independent effect of Dnmt1 (Georgia, Kanji et al. 2013). Thus, it remains unclear whether and how *Dnmt1* and maintenance DNA methylation control different organs during development.

The intestinal epithelium is an especially tractable system for the study of stem cell maintenance and cellular differentiation. Important differences between the neonatal and adult intestinal epithelium led us to investigate the role for *Dnmt1* during fetal gut development. Previous work had shown that *Dnmt1* controls cellular differentiation in the mature intestinal epithelium, but is dispensable for organ maintenance and organismal survival in adult mice (Sheaffer, Kim et al. 2014). However, the intestinal stem cell niche does not develop until approximately one week after birth in mice. During fetal gut development, proliferative progenitor cells become progressively restricted to the intervillus epithelium. Following birth, the proliferative intervillus regions invaginate into the underlying mesenchyme to form intestinal crypts. As a result, there is no defined stem cell population in the late fetal and perinatal intestinal epithelium.

Furthermore, the mitotic index of intestinal epithelial progenitors is highest during the late embryonic and postnatal period, during which time the rate of cell production must dramatically exceed the rate of cell extrusion at the villus tip to allow for rapid villus growth (Al-Nafussi and Wright 1982, Itzkovitz, Blat et al. 2012). This higher rate of cell turnover may indicate a distinct requirement for maintenance DNA methylation, as any delay in cell division would be expected to impair organ development.

Prior studies have failed to provide a clear explanation as to why loss of DNA methylation during organ development, such as in the brain, causes cell death (Fan, Beard et al. 2001). Rescue of the cell death phenotype in *Dnmt1*-deficient cultured fibroblasts via inactivation of *Trp53* strongly suggests that the p53 pathway is partially responsible (Jackson-Grusby, Beard et al. 2001). *In vitro* studies of colorectal cancer (CRC) cell lines demonstrate that loss of DNA methylation results in genomic instability, DNA damage, and mitotic arrest (Chen, Hevi et al. 2007). Indeed, hypomethylation leads to increased mutation rates and reduced genomic stability (Chen, Pettersson et al. 1998), and in human CRC patients aberrant DNA methylation correlates with microsatellite instability (Ahuja, Mohan et al. 1997). Therefore, I set out to determine if loss of *Dnmt1* causes genomic instability and intestinal development failure in the developing gut.

Using cell type-specific gene ablation, I discover that *Dnmt1* is essential for the maintenance of epithelial proliferation and nascent crypt development in the perinatal period. Without maintenance DNA methylation, the rapidly growing epithelium displays increased double-strand breaks, activation of the DNA damage response, and loss of progenitor cells due to both premature differentiation and apoptosis. I validate these results utilizing *in vitro* organoid cultures, demonstrating that Dnmt1 is required to establish organoids from the perinatal intestinal epithelium, but is not essential for the maintenance of mature organoids derived from adult intestinal crypts. These data provide novel evidence for the role of DNA methylation in maintaining genomic stability during the development of highly proliferative tissues.

Results

Dnmt1 is expressed in the proliferative zone of the embryonic and adult intestinal epithelium

To begin my study of the requirement for *Dnmt1* in intestinal epithelial development, I first characterized the localization of Dnmt1 protein at different fetal and postnatal stages in the mouse. At E16.5, E18.5, and on postnatal day 0 (P0), Dnmt1 protein was restricted to the proliferative intervillus regions, while in the adult intestinal epithelium, Dnmt1 was localized to the proliferative crypt zone, as previously reported (Figure 3.1) (Sheaffer, Kim et al. 2014). Furthermore, prior RNA-Seq analysis of isolated cell populations from the adult intestinal epithelium confirms that $Lgr5^{+}$ crypt-based columnar intestinal stem cells (ISCs) express *Dnmt1*, while differentiated villus cells contain little to no *Dnmt1* mRNA (Sheaffer, Kim et al. 2014).

Dnmt1 *ablation causes decreased proliferation and genome hypomethylation in the perinatal intestinal epithelium*

To investigate the function of *Dnmt1* during murine gut development, I employed Cre-*loxP* recombination technology to specifically ablate *Dnmt1* in the intestinal epithelium. The *VillinCre* transgene has been shown to cause activation of a Cre-dependent *lacZ* reporter as early as E12.5 (Madison, Dunbar et al. 2002), but analysis of late gestation $Dnmt1^{loxP/loxP}$*;VillinCre* E18.5 embryos revealed highly mosaic ablation of *Dnmt1* (Figure 3.2 A-C), and no phenotypic effects were observed at this stage (data not shown). The mosaicism can be explained by the fact that the efficacy of Cre-mediated gene ablation varies depending on the design of the *loxP*-flanked target allele and its localization in chromatin (Baubonis and Sauer 1993, Long and Rossi 2009). Because $Dnmt1^{loxP/loxP}$*;VillinCre* mutants were born at the expected Mendelian ratios, I set out to determine the potential requirement for Dnmt1 in the perinatal period.

The majority of $Dnmt1^{loxP/loxP}$;*VillinCre* mutant mice died within the first weeks of life, with only ~35% surviving to weaning (Figure 3.3 A). The variable expressivity of the mutant phenotype

is explained by the mosaicism of gene ablation in *Dnmt1*$^{loxP/loxP}$;*VillinCre* mice. In the first week of life, mutant mice often became runted and failed to compete with healthy littermates for maternal resources. I thus confined my analyses to postnatal day 0 (P0) *Dnmt1*$^{loxP/loxP}$*;VillinCre* mice. Staining of mutant P0 intestine revealed that Dnmt1 protein was absent from 40-60% of progenitor cells (Figures 3.3 C,E and 3.4 A-C). Quantification of the villi present in the mutant neonatal intestinal epithelium showed a 25% decrease in villus number compared to littermate controls (Fig. 3.3 B); the length of the villi, largely reflecting areas in which *Dnmt1* had not been deleted, remained similar across genotypes (data not shown).

To evaluate the possibility that the *de novo* DNA methyltransferases *Dnmt3a* and *Dnmt3b* might compensate for *Dnmt1* deficiency during gut development, I determined mRNA expression and protein localization of these two enzymes in *Dnmt1*$^{loxP/loxP}$;*VillinCre* neonatal mutants and *Dnmt1*$^{loxP/loxP}$ littermate controls. The *Dnmt1*-deficient intestine did not display increased mRNA expression or altered localization of either *de novo* methyltransferase (Figure 3.4 D-I). Thus, there is no compensatory upregulation of expression of Dnmt3a and 3b in the *Dnmt1*-deficient gut epithelium.

The intestinal epithelium of surviving adult *Dnmt1*$^{loxP/loxP}$;*VillinCre* mutants was predominantly Dnmt1^{+}, indicating that “escaper cells” that avoided Cre-mediated excision had repopulated the intestinal epithelium in its entirety (Figure 3.2 D-E). The fact that the epithelium of surviving *Dnmt1*$^{loxP/loxP}$;*VillinCre* mice is made up primarily of Cre-escaper cells, despite the fact that the *Villin* promoter is active throughout adulthood, demonstrates that *Dnmt1*-deficient progenitor cells are at a severe disadvantage compared to *Dnmt1*$^{+}$, Cre-escaper cells.

To investigate the possible causes for the observed postnatal lethality in *Dnmt1*-deficient mice, I first assessed epithelial cell proliferation. In control *Dnmt1*$^{loxP/loxP}$ littermates, all Dnmt1^{+} cells are Ki67^{+}; I defined these proliferative areas in the intervillus regions of the neonatal intestine as the progenitor zone (Figures 3.3 C-D and 3.5 A-B). The *Dnmt1*-ablated epithelium displayed a striking reduction in the number of replicating cells as indicated by Ki67 staining, with many intervillus regions lacking proliferative cells completely (Figures 3.3 E-F and 3.5 C-D).

Regions of the gut that retained *Dnmt1* expression due to inefficient Cre-mediated gene ablation maintained epithelial proliferation, as expected (Figure 3.3 E-F). Furthermore, co-staining of *Dnmt1*$^{loxP/loxP}$*;VillinCre* mutants and littermate controls demonstrated the substantial overlap of Dnmt1 and Ki67 protein localization (Figure 3.5). These results suggest that Dnmt1 is necessary to maintain the proliferation of epithelial progenitors during early postnatal intestinal development.

Next, I determined if ablation of *Dnmt1* resulted in loss of global DNA methylation in progenitor cells. The mosaicism of the *Dnmt1* mutants precluded mechanistic analysis in bulk tissue extracts. To overcome this limitation, I isolated *Dnmt1*$^{loxP/loxP}$;*VillinCre* mutant and *Dnmt1*$^{loxP/+}$ control jejunal progenitor cells by laser-capture microdissection (LCM). I stained serial sections for Ki67 to identify *Dnmt1*-ablated and *Dnmt1*-positive areas corresponding to non-proliferative and proliferative progenitor zones, respectively, and used the adjacent serial sections for LCM. I isolated approximately 10,000 cells per biological replicate for DNA methylation analysis (n=4 per group). LINE1 repetitive elements comprise 18% of the mouse genome (Waterston, Lindblad-Toh et al. 2002) and are a representative measure of genome-wide DNA methylation (Lane, Dean et al. 2003, Yang, Estécio et al. 2004). Bisulfite-sequencing of LINE1 elements demonstrated global demethylation of the mutant genome, exceeding 50% for several CpGs, confirming a dramatic loss of maintenance methylation (Figure 3.3 G). To further probe the DNA methylation status of mutant cells, I also bisulfite-sequenced the imprinting control region (ICR) of the *H19* locus. The *H19* ICR is methylated on the paternal allele, meaning that *H19* is only expressed from the maternally inherited copy (Tremblay, Saam et al. 1995). Targeted bisulfite-sequencing demonstrated a consistent reduction of DNA methylation at the *H19*-ICR locus in mutants compared to controls (Figure 3.3 H). These data likely still underestimate the degree of methylation loss, as even the most careful LCM resulted in the capture of 10% *Dnmt1*$^{+}$ cells from mutant tissues, as indicated by my RNA-Seq analysis (see below, Figure 3.6 B). Overall, these bisulfite-sequencing results indicate a genome-wide reduction in DNA methylation.

To determine the changes *Dnmt1* ablation causes in gene expression, I isolated *Dnmt1*$^{loxP/loxP}$;*VillinCre* mutant and *Dnmt1*$^{loxP/+}$ control progenitor cells using infrared (IR) laser

capture on the Arcturus PixCell IIe (Figure 3.7 A-B). I isolated approximately 10,000 cells from the proximal jejunum of each biological replicate and performed RNA-Seq to investigate the global transcriptome of intervillus progenitor cells. By combining the transcriptome data with my immunostaining analysis, I was able to correlate gene expression changes with protein expression and localization alterations in the *Dnmt1*-ablated intestinal epithelium.

I found that *Dnmt1* expression was reduced by ~90% in our mutant samples, with the remaining *Dnmt1* transcripts stemming from contaminating mesenchymal or Cre-escaper cells, as indicated by RNA-Seq analysis of *Dnmt1* exon 5, which is excised upon Cre-activation (Jackson-Grusby, Beard et al. 2001) (Figure 3.6 B). By contrast, *Dnmt3a* and *Dnmt3b* mRNA levels were unaffected, in agreement with my previous observations (Figure 3.6 A). Several imprinted genes, including *H19*, were misregulated in mutant cells (Table 3.1), as expected. DAVID gene ontology (GO) analysis (Ashburner, Ball et al. 2000) did not define any specific terms for upregulated genes in *Dnmt1*-mutants, although I found increased expression of several differentiation-related genes (Table 3.1 and Figure 3.7 C).

Partial induction of differentiation markers in* Dnmt1*-deficient progenitor zones

To test the possibility of premature differentiation of progenitor cells, I combined my RNA-Seq results with immunostaining for markers of differentiated cells present in the neonatal intestine, including enterocytes, Goblet cells, and enteroendocrine cells. These experiments did not reveal consistent differences in Goblet cell differentiation and localization compared to age-matched controls (Figure 3.8 M-P). There were small but statistically significant increases in alkaline phosphatase (*Alpi*) and chromogranin A (*Chga*) expression in mutant progenitors as determined by RNA-Seq (Table 3.1). However, the vast majority of mutant intervillus progenitor cells were neither Alpi^{+} nor Chga^{+} (Figure 3.8 A-H), suggesting that premature differentiation is not the predominant cause of the *Dnmt1*-mutant phenotype.

Lysozyme^{+} Paneth cells do not appear in the normal mouse intestinal epithelium until crypt maturation begins at ~P10, and drastically increase in number from P14 to P24 during crypt

fission (Bry, Falk et al. 1994). Interestingly, lysozyme (*Lyz*) expression was markedly increased in *Dnmt1*-ablated intestinal progenitors relative to controls by RNA-Seq, immunofluorescent staining, and qRT-PCR (Table 3.1, Figures 3.7 D-E, 3.8 I-L, and 3.6 C, respectively). Further analysis of RNA-Seq data showed that mutant progenitors exhibit increased expression of several Paneth-cell related genes, including *Ang4*, *Defa20*, and *Pla2g2a* (Table 3.1) (Bevins and Salzman 2011). Thus, it appears that a fraction of mutant progenitors halt the cell cycle and prematurely differentiate into Paneth cells. However, my staining clearly indicates that only a small fraction of mutant progenitors are differentiated (Figures 3.7 D-E and 3.8 I-L), suggesting that other pathways, such as apoptosis, may also be activated. It is important to note that the perinatal progenitor zone is not a homogeneous stem cell population; indeed, there may be subpopulations of different progenitor cell types that are leading to the variable phenotypes we observe.

Dnmt1-*ablated progenitor cells exhibit altered mRNA expression and DNA methylation of cell cycle and DNA damage response genes*

GO analysis of downregulated genes indicated significant enrichment for the GO terms 'cell division', 'DNA replication', and 'DNA damage response' (Figure 3.7 C). A subset of these misexpressed genes, including *Atm*, *Chek2*, *p21* (*$p21^{CIP1/WAF1}$* or *Cdkn1a*), and *Mlh1* were confirmed in three independent LCM samples by qRT-PCR (Figure 3.6 C-D). These results demonstrate that loss of *Dnmt1* caused decreased expression of DNA damage response and cell- cycle related genes. Dnmt1 is known to play a crucial role in genomic stability, as ablation of *Dnmt1* in cell lines can result in mitotic defects and G2/M arrest (Chen, Hevi et al. 2007), or DNA replication errors and activation of the G1/S checkpoint (Knox, Araujo et al. 2000, Unterberger, Andrews et al. 2006). Additionally, loss of *Dnmt1* in murine embryonic stem cells increases mitotic mutation rates (Chen, Pettersson et al. 1998), further pointing to the necessity of Dnmt1 in maintaining genomic integrity.

My RNA-Seq data showed increased expression of the p53 target *p21*, which has an established role in activating the G1/S and G2/M phase checkpoints and inducing cellular senescence (Table 3.1 and Figure 3.6 D) (Deng, Zhang et al. 1995, Bunz, Dutriaux et al. 1998). p21 is often increased in response to DNA damage, and inhibits the transcription of many genes involved in cell cycle progression, leading to cell cycle arrest (Chang, Watanabe et al. 2000). Furthermore, *p21* has been shown to be upregulated in response to loss of *Dnmt1* in CRC cell lines (Chen, Hevi et al. 2007), and several studies suggest that *p21* expression is controlled by DNA methylation (Allan, Duhig et al. 2000, Zhu, Srinivasan et al. 2003, Brenner, Deplus et al. 2005). Immunostaining confirmed an increase in p21 protein levels in the *Dnmt1*-ablated intervillus epithelium compared to control progenitor cells, while p21 levels in postmitotic villus cells were comparable between the two genotypes (Figure 3.7 F-I). Taken together, my transcriptome and immunostaining analyses suggest that *Dnmt1*-deficient cells undergo cell cycle arrest.

To further interrogate the extent of hypomethylation and the mechanism underlying the *Dnmt1*$^{loxP/loxP}$;*VillinCre* mutant phenotype, I performed laser capture microdissection (LCM) and targeted bisulfite sequencing near the promoter regions of *Atm*, *Chek2*, *p21*, and *Mlh1*. I examined the methylation near the transcription start site (TSS) of these genes, but due to the presence of CpG islands in the proximal promoters of all four genes, the baseline methylation levels in controls were only 0-5% (data not shown). Next, I analyzed low-density CpGs clusters in putative regulatory regions 2 to 4 kb upstream of the respective transcription start site, and found that in all four cases the regions analyzed were significantly demethylated in the *Dnmt1*-deficient gut epithelium compared to control (Figure 3.9). The drastic loss of DNA methylation correlated with either increased or decreased mRNA levels, depending on the specific gene (Table 3.1 and Figure 3.6 C-D), suggesting that the upstream regulatory elements analyzed might function as enhancer (*p21*) or silencer (*Chek2*, *Atm*, *Mlh1*) regions (Jones and Takai 2001).

Dnmt1 ***ablation results in increased DNA damage and apoptosis in the progenitor zone***

Given the activation of apoptosis reported in other models following loss of *Dnmt1* (Li, Bestor et al. 1992, Jackson-Grusby, Beard et al. 2001, Chen, Hevi et al. 2007), I investigated the levels of apoptosis and DNA damage in mutant intestinal progenitors. In control progenitor regions, as expected, there were no apoptotic cells, as dying epithelial cells are normally confined to the villus tip (Figure 3.10 A) (Hall, Coates et al. 1994). Surprisingly, I found a significant number of apoptotic progenitor cells in mutant tissue (Figure 3.10 B), increased more than fifty-fold relative to littermate controls (Figure 3.10 C). To evaluate if increased apoptosis was confined to *Dnmt1*-deficient, non-replicating intervillus cells, I co-stained to confirm loss of Ki67 in TUNEL-positive areas (Figure 3.11 A-F). These data demonstrate that ablation of *Dnmt1* not only blocks proliferation, but also induces cell death in the progenitor compartment of the perinatal intestine. The variability in the amount of cells undergoing apoptosis at any one point in time reflects the stochastic cell death observed in the global *Dnmt1*-mutant embyros (Li, Bestor et al. 1992, Jackson-Grusby, Beard et al. 2001), but may also be due to the action of Cre in progenitor cells at different points during development.

I considered the possibility that apoptosis of *Dnmt1*-deficient progenitors might be the result of activation of the DNA damage response. Hypomethylation causes genomic instability and increased mutation rates, which can lead to activation of cell cycle checkpoints and the DNA damage response (Chen, Pettersson et al. 1998, Chen, Hevi et al. 2007, Loughery, Dunne et al. 2011). In addition, my own data demonstrate increased p21 levels in *Dnmt1*-mutant intervillus cells (Figure 3.7 G-H), which indicates cell cycle arrest. To assess DNA damage response activation in our mutants directly, I stained for γH2AX foci, which accumulate at double-stranded DNA breaks (Figures 3.10 D-E and 3.11 G-L). I found a more than 1,000-fold increase in γH2AX foci ($p<0.001$) in the mutant intervillus intestinal epithelium relative to littermate controls (Figure 3.10 F, compare red brackets in 3.10 D&E). These results indicate loss of *Dnmt1* causes increased DNA damage, cell cycle arrest, and subsequent cell death.

Adult Dnmt1*-ablated crypt cells maintain methylation of DNA damage response genes*

Given the opposing phenotypes we describe above for the neonatal intestine versus that observed in mice with *Dnmt1* ablation in the adult gut epithelium (Sheaffer, Kim et al. 2014), I also analyzed DNA methylation in the adult crypt epithelium. Global methylation of repetitive LINE1 elements and the imprinted *H19* locus is reduced in adult mice with intestinal epithelial-specific *Dnmt1* ablation to about the same extent as that seen in the perinatal ablation model described here (compare Figure 3.12 A-B to 3.3 G-H). Strikingly, however, *p21* and *Chek2* are not demethylated in the adult *Dnmt1* ablation model (Figure 3.12 C-D), and *Atm* is only significantly demethylated when comparing the entire sequenced region relative to control crypt epithelium (Figure 3.12 E). *Mlh1* is demethylated to a greater extent than the other genes analyzed (Figure 3.12 F), indicating that *Mlh1* is particularly sensitive to loss of *Dnmt1*. These results demonstrate that loss of *Dnmt1* in the adult epithelium is not equivalent to the loss of *Dnmt1* in the neonatal epithelium. I postulate that the differing requirement for Dnmt1 maintenance DNA methylation between the adult crypt compartment and the intervillus regions of the neonatal gut might be related to the more than 2-fold higher fractional proliferation rate of the latter compared to the former (Figure 3.13; (Itzkovitz, Blat et al. 2012)). I next sought to determine the differential requirement for Dnmt1 in developing versus mature intestinal epithelial crypts in an *in vitro* organoid culture system.

Dnmt1 *is required for establishing organoids* in vitro

To demonstrate that *Dnmt1* is required for organoid crypt culture from perinatal intestine, I employed EDTA-disassociation to isolate intestinal epithelia from postnatal day 1 (P1) *Dnmt1*$^{loxP/loxP}$*;VillinCre* mutants and *Dnmt1*$^{loxP/loxP}$ littermate controls (Figure 3.10 G). I grew these perinatal organoid cultures in Matrigel with the 'ENR' (EGF, Noggin, R-Spondin) growth factor cocktail, allowing me to observe the development and maintenance of the perinatal intestinal epithelium in real time (Sato, Vries et al. 2009). I counted the number of organoids per well on days 3-5 of culture, and observed very few organoids (<10 per well) established from the

Dnmt1$^{loxP/loxP}$*;VillinCre* mutant intestinal epithelium compared to the robust establishment of organoids (>150 per well) from control gut (Figure 3.10 H). On day 4, I observed nascent buds in the control *Dnmt1*$^{loxP/loxP}$organoids (Figure 3.10 K), but little sustained growth from the *Dnmt1*$^{loxP/loxP}$*;VillinCre* mutant organoids (Figure 3.10 L). By day 5, it was apparent that no healthy, budding organoids were produced from the *Dnmt1*-mutant intestine relative to littermate controls (Figure 3.10 H,M,N). These results strongly support my *in vivo* data showing that *Dnmt1* is essential to maintain perinatal intestinal progenitor cells.

To further probe the mechanism underlying the difference between the neonatal and adult *Dnmt1*-ablation phenotypes, I employed *Dnmt1*$^{loxP/loxP}$*;VillinCreERT2* (Sheaffer, Kim et al. 2014) mice for *in vitro* organoid experiments. The *VillinCreERT2* transgene allows temporal control of *Dnmt1* ablation via addition of 4-hydroxytamoxifen (4OHT) to cells in culture. I hypothesized that *Dnmt1* might be necessary for establishing the crypt compartment in neonatal mice, but not be required for the maintenance and survival of mature crypts in adult mice. To test this hypothesis, I isolated crypts from adult *Dnmt1*$^{loxP/loxP}$ and *Dnmt1*$^{loxP/loxP}$*;VillinCreERT2* mice, and ablated *Dnmt1* at two different time points during organoid growth. In one set of experiments, I added 4OHT during the first two days of culture, when organoids are growing but have not yet established buds and crypt structures (Sato, Vries et al. 2009) (Figure 3.14 A). For the second set of experiments, I added 4OHT on days 5-7 of culture, after organoids had established proper crypt hierarchy in budding outgrowths (Sato, Vries et al. 2009) (Figure 3.15 A).

In the "early" experiments, in which *Dnmt1* had been acutely ablated by addition of 4OHT, *Dnmt1*-deficient organoids failed to grow beyond small cyst-like structures, while control organoids began to exhibit buds by day 4 (Figure 3.14 B-E). Dnmt1 immunostaining confirmed loss of the enzyme in 4OHT-treated *VillinCreERT2*$^{+}$ organoids (Figure 3.14 I). Addition of EdU to media 2 hours prior to cell harvest allowed analysis of replication rate. There were almost no EdU^{+} cells in the 4OHT-treated, *Dnmt1*-ablated organoids, in contrast to controls in which replicating cells were abundant (Figure 3.14 J-M). TUNEL staining demonstrated an increase in the frequency of TUNEL^{+} apoptotic nuclei in surviving *Dnmt1*-ablated organoids compared to

controls (Figure 3.14 N-Q). Overall, the loss of *Dnmt1* during the establishment of organoid cultures parallels the phenotype seen in the perinatal *Dnmt1*$^{loxp/lxop}$*; VillinCre* mutant intestine, strongly suggesting a unique role for *Dnmt1* in crypt development.

In stark contrast, the addition of 4OHT on days 5-7 of organoid culture, after large, multi-crypt organoids had formed, had little effect on the growth and replication of mature organoids (Figure 3-15 B-E and J-M). I confirmed loss of Dnmt1 in 4OHT-treated, *VillinCreERT2*$^{+}$ organoids by immunohistochemistry (Figure 3.15 F-I). Additionally, TUNEL staining demonstrated no increase in apoptosis rate in the 4OHT-treated, *Dnmt1*-ablated mature organoids (Figure 3.15 N-Q). These results support my hypothesis that Dnmt1 performs unique functions in the developing intestinal epithelium, and plays a role in the establishment but not maintenance of crypts postnatally.

Discussion

Taken together, my RNA-Seq, immunostaining, and organoid data reveal a crucial role for Dnmt1 in maintaining DNA methylation patterns, genomic stability, and progenitor cell status during intestinal development *in vivo*. I observed significant genome-wide DNA demethylation by targeted bisulfite sequencing of the LINE1 locus and the *H19* ICR (Figure 3.3 G-H). My RNA-Seq and immunostaining data demonstrate that *Dnmt1*-deficient progenitors express decreased levels of genes essential for mitosis and chromosome segregation (Table 3.1 and Figure 3.7 C), and have increased rates of double-strand breaks (Figure 3.10 D-F). An increased rate of double-strand breaks during the S-Phase of the cell cycle activates the G1/S checkpoint, mediated by p53 and p21. Indeed, increased *p21* expression in the *Dnmt1*-deficient epithelium indicates that this checkpoint is active in mutant cells (Figures 3.10 G-H and 3.6 D). However, downstream targets of the DNA damage response pathway, including *Atm*, *Chek2*, and *Mlh1*, exhibit decreased expression by RNA-Seq (Table 3-1 and Figure 3.6 C), suggesting that *Dnmt1*-deficient intestinal progenitor cells are unable to activate the normal response to accumulated DNA damage. As a result, these *Dnmt1*-deficient progenitors undergo apoptosis, which leads to global loss of the intestinal epithelium (Figure 3.10 A-C). These findings are supported by previous studies implicating a requirement for Dnmt1 in DNA replication (Knox, Araujo et al. 2000), the DNA damage response (Mortusewicz, Schermelleh et al. 2005, Unterberger, Andrews et al. 2006, Loughery, Dunne et al. 2011), and cell cycle arrest (Chen, Hevi et al. 2007).

My results demonstrate an essential role for Dnmt1 in maintaining epithelial genomic integrity during perinatal intestinal development. Interestingly, when I ablated *Dnmt1* in the adult intestinal epithelium using a tamoxifen-inducible *VillinCreERT2* transgene, I did not see a requirement for Dnmt1 in crypt cell survival, despite demethylation at the LINE1 locus (Figure 3.12 A) (Sheaffer, Kim et al. 2014). These opposing phenotypes raise several questions. It is possible that in the adult intestinal epithelium, loss of Dnmt1 protein is compensated for by the *de novo* methyltransferases Dnmt3a and Dnmt3b. Alternatively, the unique requirement for Dnmt1 in newborn mice may be due to the significantly increased replication rate of neonatal progenitors

compared to adult crypt cells (Itzkovitz, Blat et al. 2012). As shown in Figure 3.13, the neonatal intestinal epithelium displays twice the fractional proliferation rate than that of adult mice. Thus, I hypothesize that as the neonatal *Dnmt1*-ablated cells divide their DNA methylation levels are rapidly reduced, and Dnmt3a and Dnmt3b do not compensate this loss. The high rate of proliferation in the neonatal intestine also distinguishes these findings concerning the developing intestine from studies of neuroblasts (Fan, Beard et al. 2001) or embryonic pancreas (Georgia, Kanji et al. 2013).

Another possibility to explain the diverging phenotypes of adult and neonatal intestinal *Dnmt1*-ablation is that DNA methylation might not be crucial for cell survival and function in the mature crypt architecture. This explanation is supported by our organoid culture experiments (Figures 3.10 G-N, 3.14, and 3.15). The perinatal *Dnmt1*-deficient intestine fails to successfully produce organoids, in contrast to littermate controls (Figure 3.10 G-N). To test the differing requirements for Dnmt1 during organoid crypt development and maintenance, I used the inducible *Dnmt1*$^{loxP/loxP}$*;VillinCreERT2* system (Sheaffer, Kim et al. 2014). When *Dnmt1* was ablated before budding structures appear, organoids failed to thrive and eventually died (Figure 3.14). However, ablation of *Dnmt1* after organoid buds and the ISC niche are established had little effect on the maintenance of replicating progenitors (Figure 3.15).

Several recently published studies analyze the differences between fetal progenitors and adult ISCs (Fordham, Yui et al. 2013, Mustata, Vasile et al. 2013). Fordham and colleagues report that intestinal progenitor cell maturation correlates with increased Wnt signaling. In their study, Lgr5^{+} cells isolated from neonatal intestine produced budding organoids, with high expression of adult stem cell markers. Lgr5^{-} cells isolated from the same neonatal tissue formed fetal enterospheres (FENs), which expressed low levels of Wnt factors and ISC markers, and did not display budding activity. My results strongly support the notion that adult and perinatal intestinal progenitors are not equivalent populations, and have differential requirements for cell maintenance.

In conclusion, I have demonstrated an important role for *Dnmt1* in establishing intestinal epithelial crypts following birth. I suggest that *Dnmt1* is essential during the first few weeks of life to maintain genomic methylation patterns during this period of intense cellular proliferation and villus growth, and to prevent genome alterations that lead to progenitor cell death. Future research in this field should focus on the varying requirements for DNA methylation during development, particularly in supporting genomic stability and proliferation during organ development, in contrast to those necessary in adulthood.

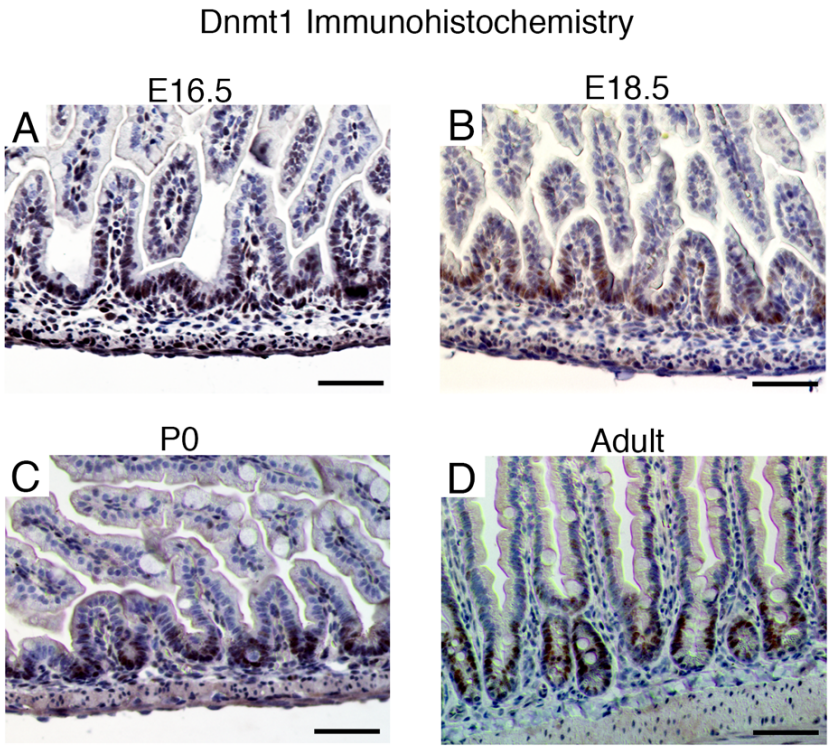

Figure 3.1. Time course of Dnmt1 localization during intestinal epithelial development

Figure 3.1. Time course of Dnmt1 localization during intestinal epithelial development.

(A-D) Dnmt1 is expressed in the intervillus regions during late fetal development, and becomes restricted to crypts in the adult intestine. Dnmt1 protein stain is brown; hematoxylin nuclear counterstain is blue. Scale bars are 50 μm.

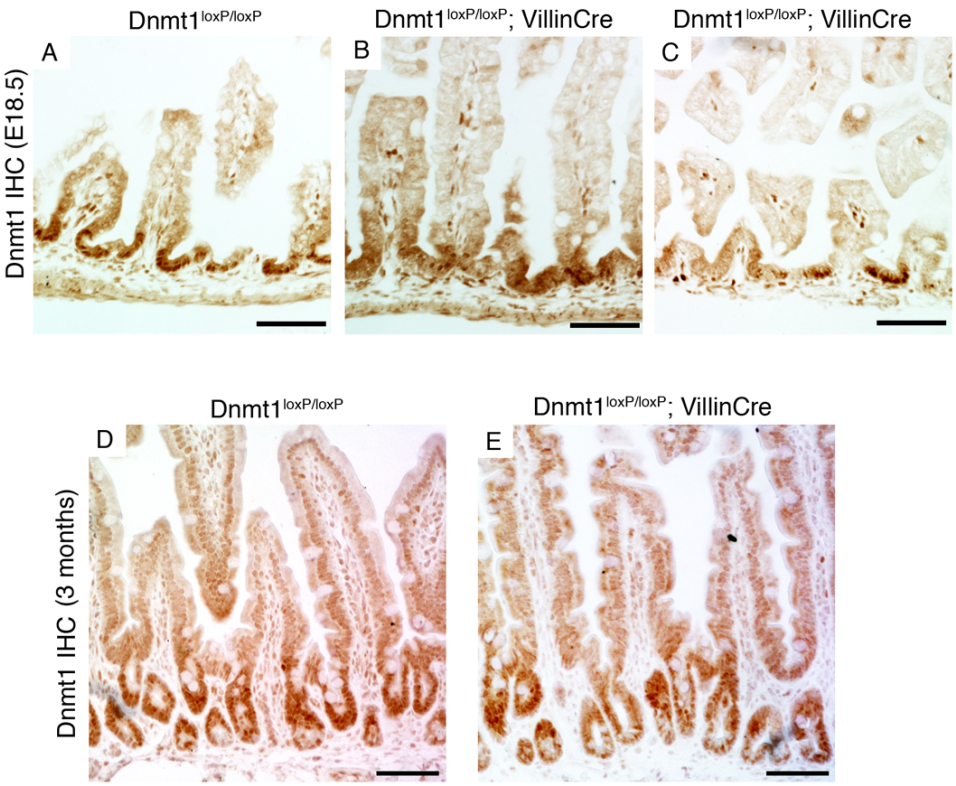

Figure 3.2. Embryonic *Dnmt1$^{loxP/loxP}$;VillinCre* intestine is highly mosaic for *Dnmt1* ablation, while the adult *Dnmt1$^{loxP/loxP}$;VillinCre* is repopulated by cells that have escaped Cre-mediated Dnmt1 ablation

Figure 3.2. Embryonic *Dnmt1$^{loxP/loxP}$;VillinCre* intestine is highly mosaic for Dnmt1 ablation, while the adult *Dnmt1$^{loxP/loxP}$;VillinCre* is repopulated by cells that have escaped Cre-mediated *Dnmt1* ablation.

(A-C) E18.5 mutants showed variable levels of *Dnmt1*-ablation, with the majority of intervillus regions retaining expression of Dnmt1 protein (B,C). (D,E) Dnmt1 immunohistochemistry in controls and mutants at 3 months of age revealed that mutant intestines are predominantly Dnmt1^{+}. Scale bars are 50 μm.

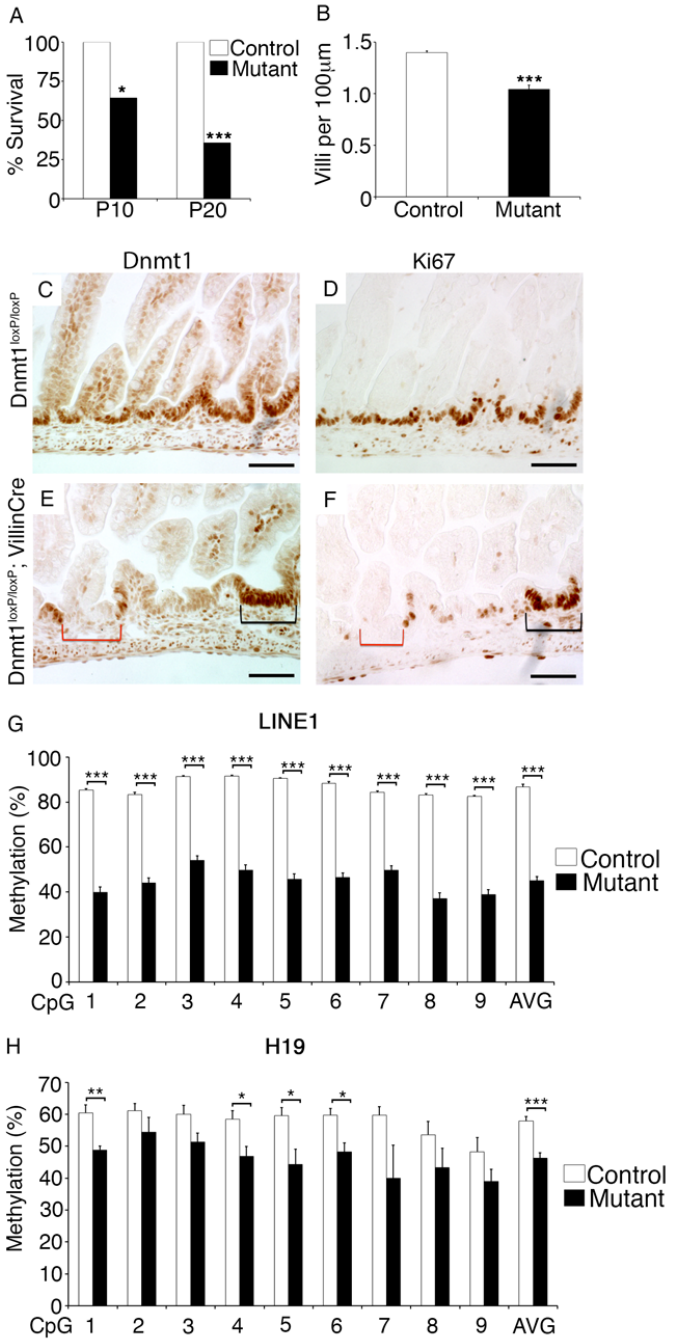

Figure 3.3. Ablation of *Dnmt1* in the developing intestinal epithelium causes reduced proliferation and DNA hypomethylation

Figure 3.3. Ablation of *Dnmt1* in the developing intestinal epithelium causes reduced proliferation and DNA hypomethylation.

(A) Only 35% of *Dnmt1*$^{loxP/loxP}$*;VillinCre* mutants survived to postnatal day 20 (P20) (n=14). (B) P0 mutants have significantly fewer villi relative to littermate controls (n=4). (C,E) Dnmt1 protein immunohistochemistry, (D,F) Ki67 protein immunohistochemistry. P0 mutants display mosaic *Dnmt1* ablation compared to controls (C,E). Absence of Dnmt1 (E, red brackets) corresponds to loss of proliferation in mutant progenitors as assessed by Ki67 staining of adjacent section (F, red brackets). Dnmt1^{+} progenitors show similar proliferation in mutants (black bars E,F) compared to controls (D). (G) LINE1 repeat DNA methylation levels as assessed by bisulfite-sequencing (n=4). Decreased LINE1 methylation indicates global demethylation in *Dnmt1* mutant progenitor cells compared to controls. (*H*) H19 imprinting control region (ICR) DNA methylation levels are decreased in mutant progenitor cells relative to controls (n=4). For all graphs, data are represented as mean ± SEM. **P*<0.05; ***P*<0.01; ****P*<0.001, two-tailed Student's *t*-test. Scale bars are 50 μm.

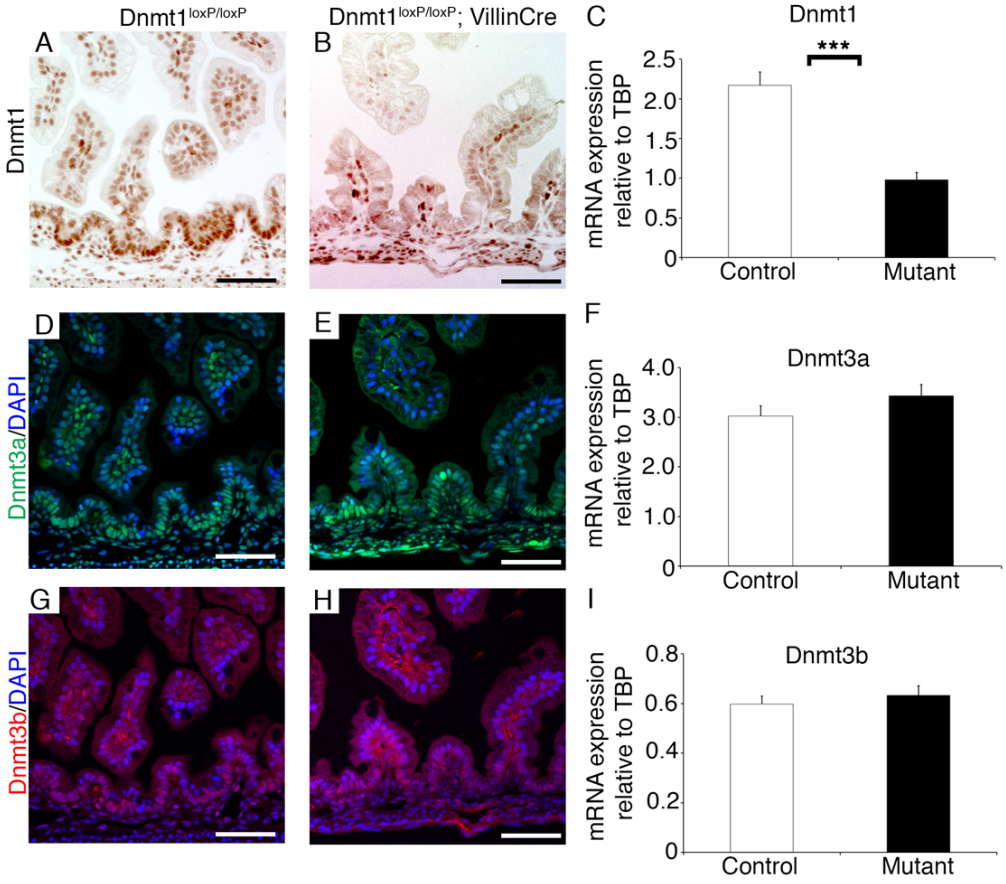

Figure 3.4. Dnmt3a and Dnmt3b are not upregulated in the *Dnmt1$^{loxP/loxP}$;VillinCre* neonatal intestine

Figure 3.4. Dnmt3a and Dnmt3b are not upregulated in *Dnmt1$^{loxP/loxP}$;VillinCre* neonatal mutants.

(A,B) Immunohistochemistry for Dnmt1 in *Dnmt1$^{loxP/loxP}$* controls and *Dnmt1$^{loxP/loxP}$*;*VillinCre* mutants. (C) qRT-PCR of whole neonatal proximal jejunum showed a significant decrease in *Dnmt1* transcript in mutants compared to littermate controls. (D-E,G-H) Immunostaining on serial sections demonstrated no change in Dnmt3a (green, second row) and Dnmt3b (red, third row) localization. (F,I) qRT-PCR does not reveal a significant difference in *Dnmt3a* or *Dnmt3b* gene expression. In all images, scale bars are 50 μm. For all qRT-PCR, control n=10, mutant n=12. Data are represented as mean ± SEM. ****P*<0.001, two-tailed Student's *t*-test.

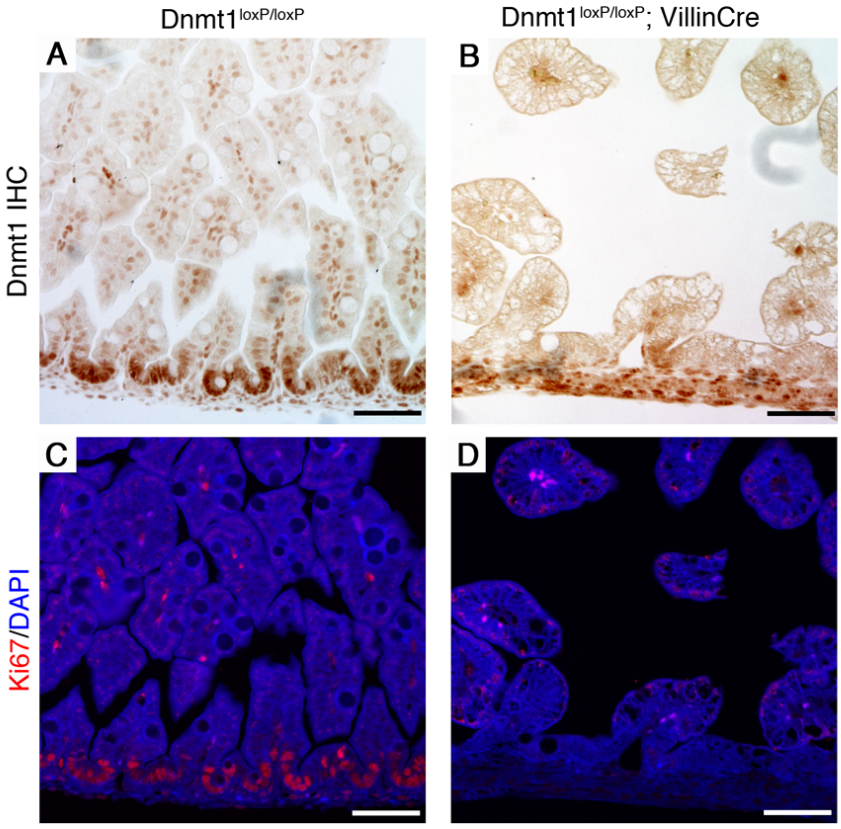

Figure 3.5. Dnmt1 and Ki67 protein are co-localized in the intervillus progenitor zone

Figure 3.5. Dnmt1 and Ki67 protein are co-localized in the intervillus progenitor zone.

(A-D) Co-staining for Dnmt1 (A,B) and Ki67 (C,D) using separate imaging of each protein on the same section revealed strong overlap of Dnmt1 and Ki67 proteins in controls (A,C). *Dnmt1*$^{loxP/loxP}$*;VillinCre* epithelial cells with *Dnmt1* ablation (B), do not express Ki67 (D). In all images, scale bars are 50 μm.

A

RNA-Seq Gene Expression Data			
Gene ID	**Transcript**	**Fold Change**	**p-Value**
Mki67	NM_001081117	0.53	8.74E-08
Dnmt3a	NM_007872	0.96	0.72
Dnmt3b	NM_001003961	1.00	0.99

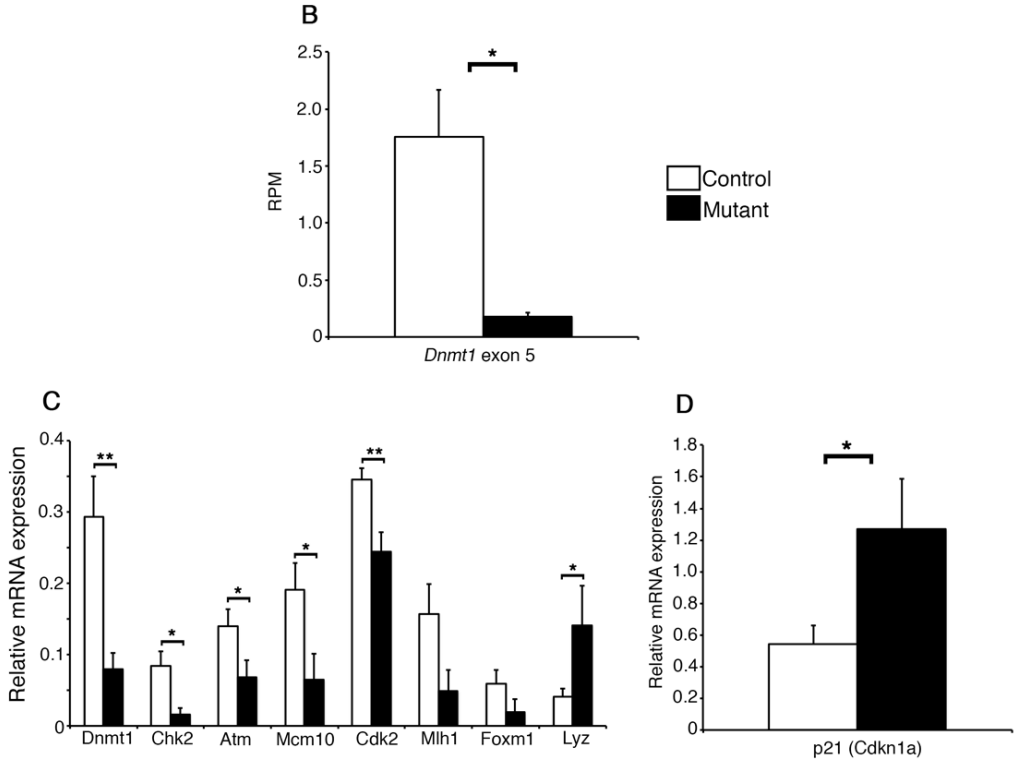

Figure 3.6. Collection of *Dnmt1*-ablated progenitors cells by Laser Capture Microdissection (LCM)

Figure 3.6. Collection of *Dnmt1*-ablated progenitors cells by Laser Capture Microdissection (LCM).

(A) Gene expression levels of *Dnmt3a*, *Dnmt3b*, and *mKi67* from RNA-Seq data. Fold change is relative to control. (B) RNA-Seq expression of *Dnmt1* exon 5, which is excised upon Cre activation, indicates a nearly 90% reduction in *Dnmt1* mRNA levels in the LCM tissue of *Dnmt1*$^{loxP/loxP}$*;VillinCre* compared to controls (RPM, Reads per Million). (C,D) We performed additional LCM to confirm RNA-Seq data in independent biological replicates (*Dnmt1*$^{loxP/loxP}$ controls, n=4; *Dnmt1*$^{loxP/loxP}$*;VillinCre* mutants, n=3). (C) qRT-PCR confirmation of genes that are misregulated in RNA-Seq data: *Dnmt1*, *Chek2*, *Atm*, *Mcm10*, *Cdk2*, *Mlh1*, *Foxm1*, and *Lyz*. (D) Validation of *p21* expression levels, which is upregulated in our RNA-Seq data. qRT-PCR data are presented normalized to the geometric mean of 5 reference genes: *Tbp*, *B2m*, *β-actin*, *Polr2b*, and *Rplp0*. (B-D) Data are represented as mean ± SEM. **P*<0.05, ***P*<0.01, one-tailed Student's *t*-test.

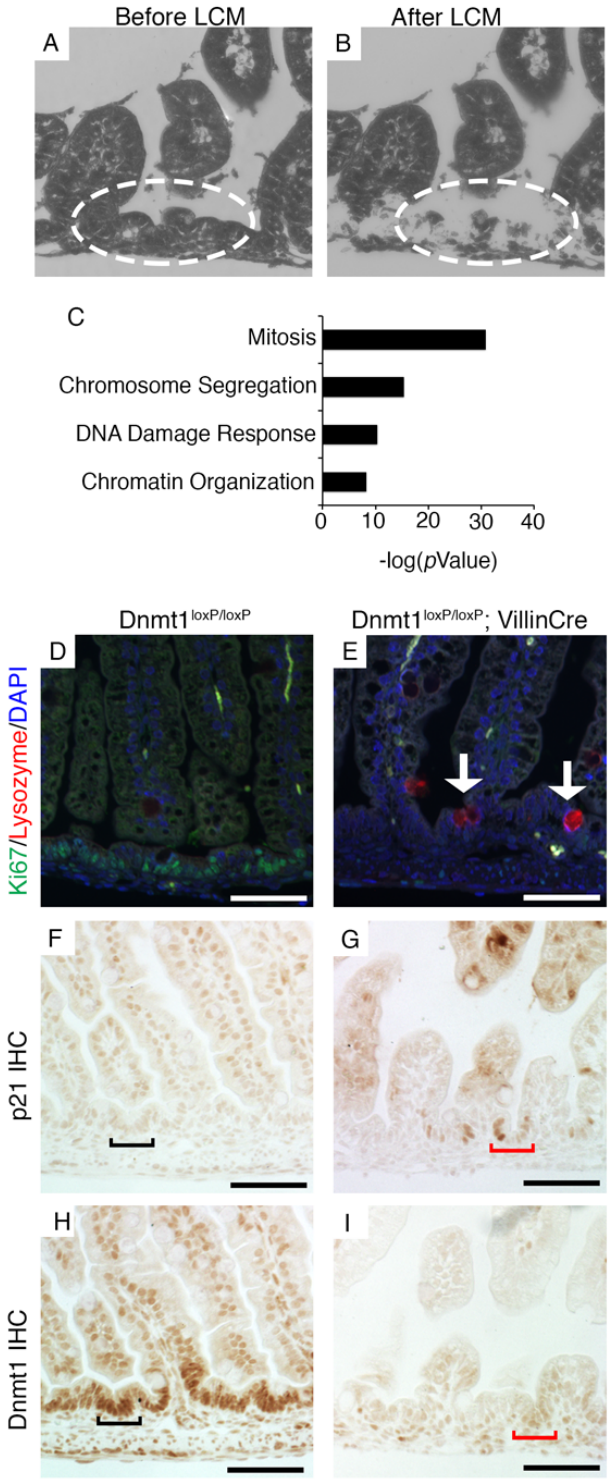

Figure 3.7. RNA-Seq analysis reveals decreased expression of crucial cell-cycle regulators in *Dnmt1*-deficient progenitor cells

Figure 3.7. RNA-Seq analysis reveals decreased expression of crucial cell-cycle regulators in *Dnmt1*-deficient progenitor cells.

(A, B) Collection of intervillus regions (encircled) before (A) and after (B) laser capture microdissection (LCM). (C) DAVID gene ontology analysis of genes with transcripts are downregulated in *Dnmt1*-deficient epithelial cells as determined by RNA-Seq. (D,E) Co-staining for Ki67 (green) and lysozyme (red) in control and *Dnmt1* mutant intestine. A fraction of non-replicating *Dnmt1*-negative cells exhibit increased lysozyme protein levels (E, arrows), a marker for Paneth cell differentiation, relative to controls (D). (F,G) Immunohistochemistry (IHC) showing that in controls p21 protein is confined to differentiated cells in the villus; in *Dnmt1* mutants, expression is strikingly increased in intervillus regions (black bracket in F versus red bracket in G). (H,I) Dnmt1 immunohistochemistry on serial sections confirms *Dnmt1* ablation in cells indicated by red brackets in G,I. In all images, scale bars are 50 μm.

Table 3.1		
Differentially expressed genes between *Dnmt1$^{loxP/loxP}$;VillinCre* and *Dnmt1$^{loxP/+}$* intestine identified by RNA-Seq		
Differentiation Genes		
Gene ID	**Fold Change**	**p Value**
Lyz	7.10	3.50E-30
Defa20	4.19	2.31E-03
Ang4	2.61	6.94E-09
Chga	1.56	8.95E-04
Alpi	1.31	1.02E-02
DNA Replication Genes		
Gene ID	**Fold Change**	**p Value**
Foxm1	0.53	4.07E-07
Mcm10	0.53	4.84E-06
Top2a	0.57	2.22E-05
Ccnb1	0.59	1.34E-04
Mcm6	0.60	6.45E-05
Dna2	0.61	4.08E-04
Cdk2	0.61	6.73E-04
Cdk1	0.64	9.93E-04
DNA Damage Response Genes		
Gene ID	**Fold Change**	**p Value**
Cdkn1a	2.28	5.16E-11
Mlh1	0.54	1.61E-04
Msh3	0.59	2.04E-04
Pms2	0.63	5.01E-03
Brca2	0.64	2.07E-03
Chek2	0.64	8.10E-03
Atm	0.69	3.64E-03
Imprinted Genes		
Gene ID	**Fold Change**	**p Value**
H19	3.07	1.53E-15
Plagl1	1.95	6.16E-08
Nespas	0.38	4.16E-03
Slc22a3	0.12	1.47E-05

Table 3.1. Genes differentially expressed between *Dnmt1*$^{loxP/loxP}$*;VillinCre* and *Dnmt1*$^{loxP/+}$ intestine.

RNA-Seq data from LCM tissue for genes of interest. Fold change indicates expression levels relative to control. FDR<0.1.

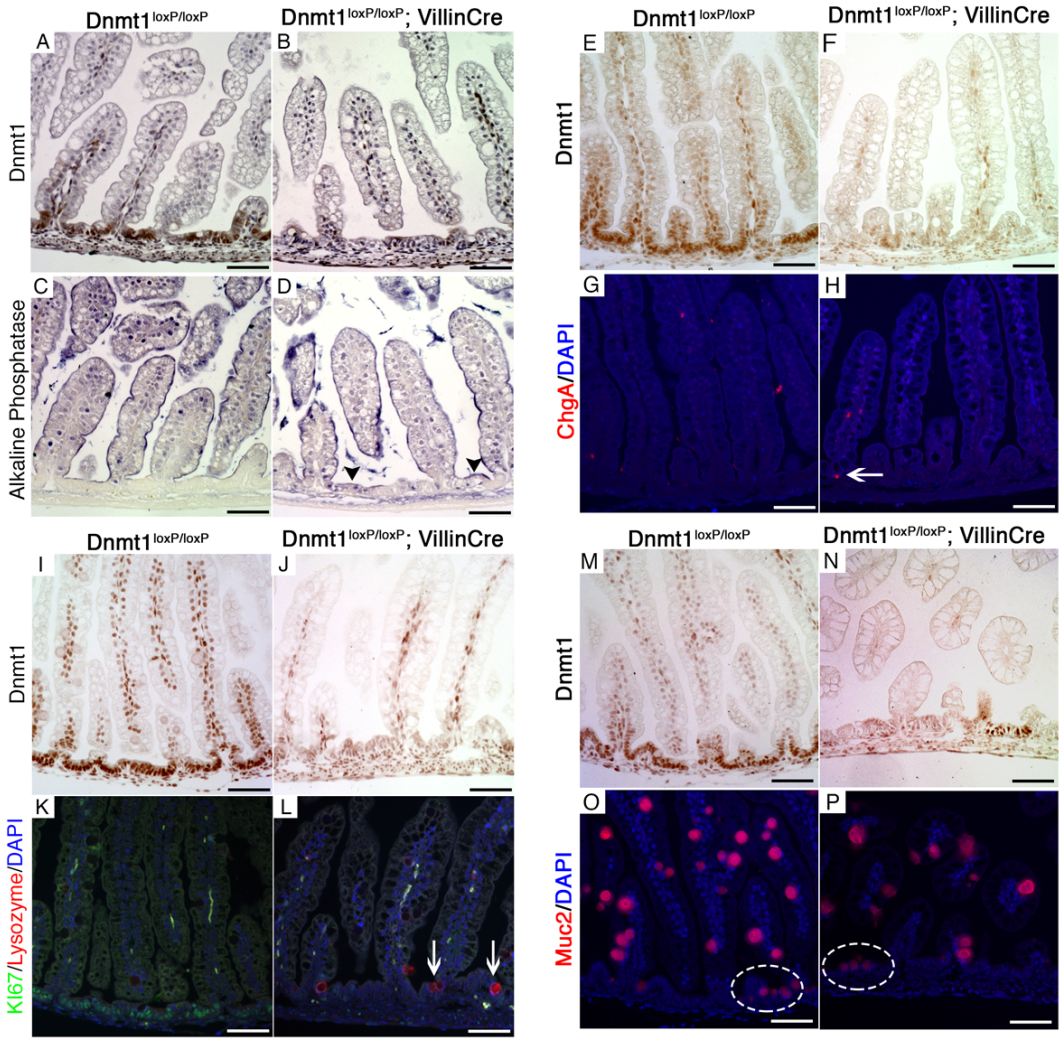

Figure 3.8. Enterocyte, enteroendocrine, Paneth, and goblet cell populations in *Dnmt1$^{loxP/loxP}$;VillinCre* mutants

Figure 3.8. Enterocyte, enteroendocrine, Paneth, and goblet cell populations in *Dnmt1$^{loxP/loxP}$;VillinCre* mutants.

(A-B, E-F, I-J, M-N) Dnmt1 immunohistochemistry on serial sections confirms loss of Dnmt1 in the mutant regions analyzed. (A-D) Alkaline phosphatase (AP) staining for absorptive enterocytes revealed a small increase in AP+ mutant progenitor cells (black arrowheads in D) relative to controls (C). (E-H) Chromogranin A (ChgA) staining for enteroendocrine cells revealed a small increase in ChgA+ progenitor cells in mutants (H, white arrow) compared to controls (G). (I-L) Co-staining for Ki67 (green) and lysozyme (red) in control and Dnmt1 mutant intestine. Non-replicating Dnmt1-mutant progenitors had increased lysozyme protein (L, white arrows), a marker for Paneth cell differentiation, relative to controls (K). (M-P) Mucin2 staining showed similar staining patterns of goblet cells in control (O, circled cells) and Dnmt1 mutant (P, circled cells) progenitor zones. In all images, scale bars are 50 μm.

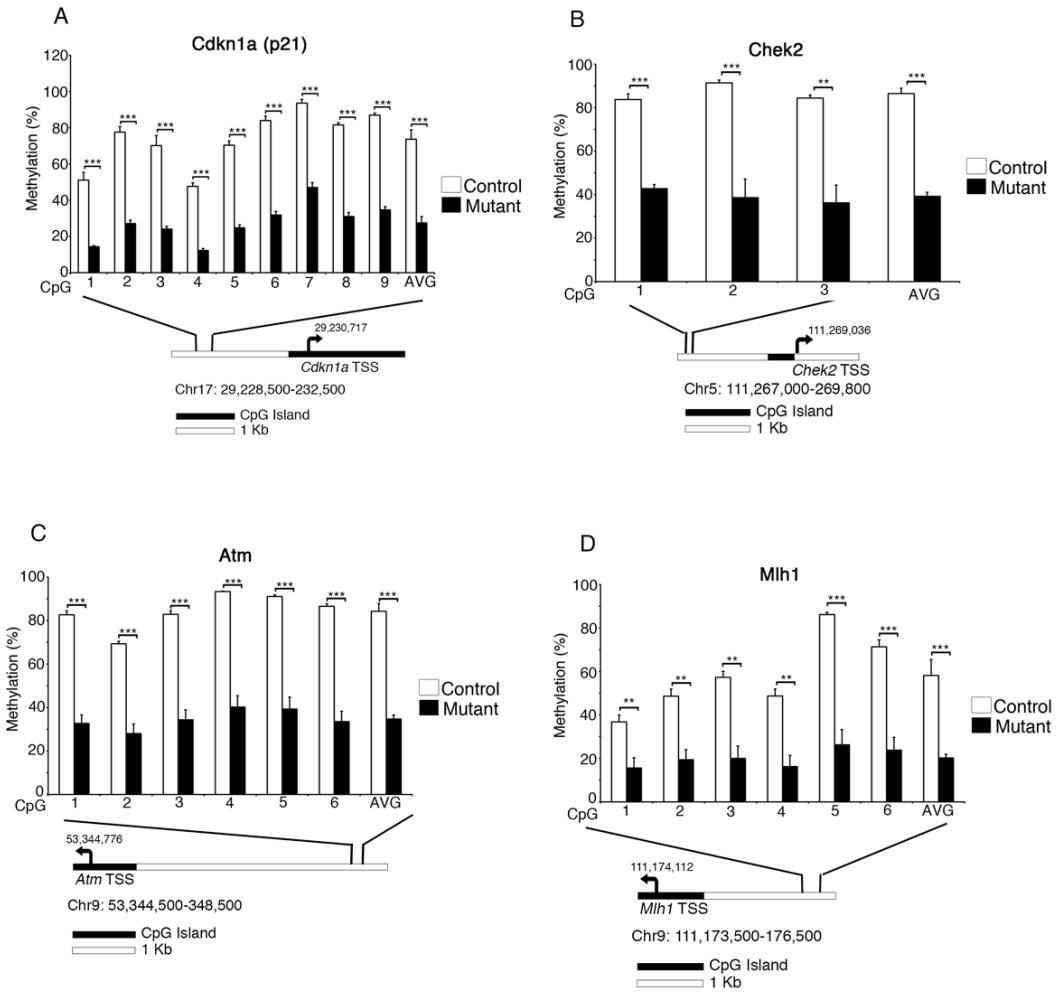

Figure 3.9. Key DNA damage response genes are significantly demethylated in *Dnmt1*-ablated perinatal intestinal epithelial progenitors

Figure 3.9. **Key DNA damage response genes are significantly demethylated in *Dnmt1*-ablated perinatal intestinal epithelial progenitors.**

(A-D) Targeted bisulfite-sequencing analysis of DNA damage response genes demonstrates significant demethylation upstream of *p21* (A), *Chek2* (B), *Atm* (C), and *Mlh1* (D) in *Dnmt1*$^{loxP/loxP}$*;VillinCre* mutants compared to littermate controls. Beneath each bar chart is a diagram indicating the position of the transcription start site (TSS, arrow) and CpG islands relative to the regions sequenced. Each region is ~2-4 kb upstream of the TSS. For all graphs, error bars are ± SEM, ***P*<0.01, ****P*<0.001, two-tailed Student's *t*-test.

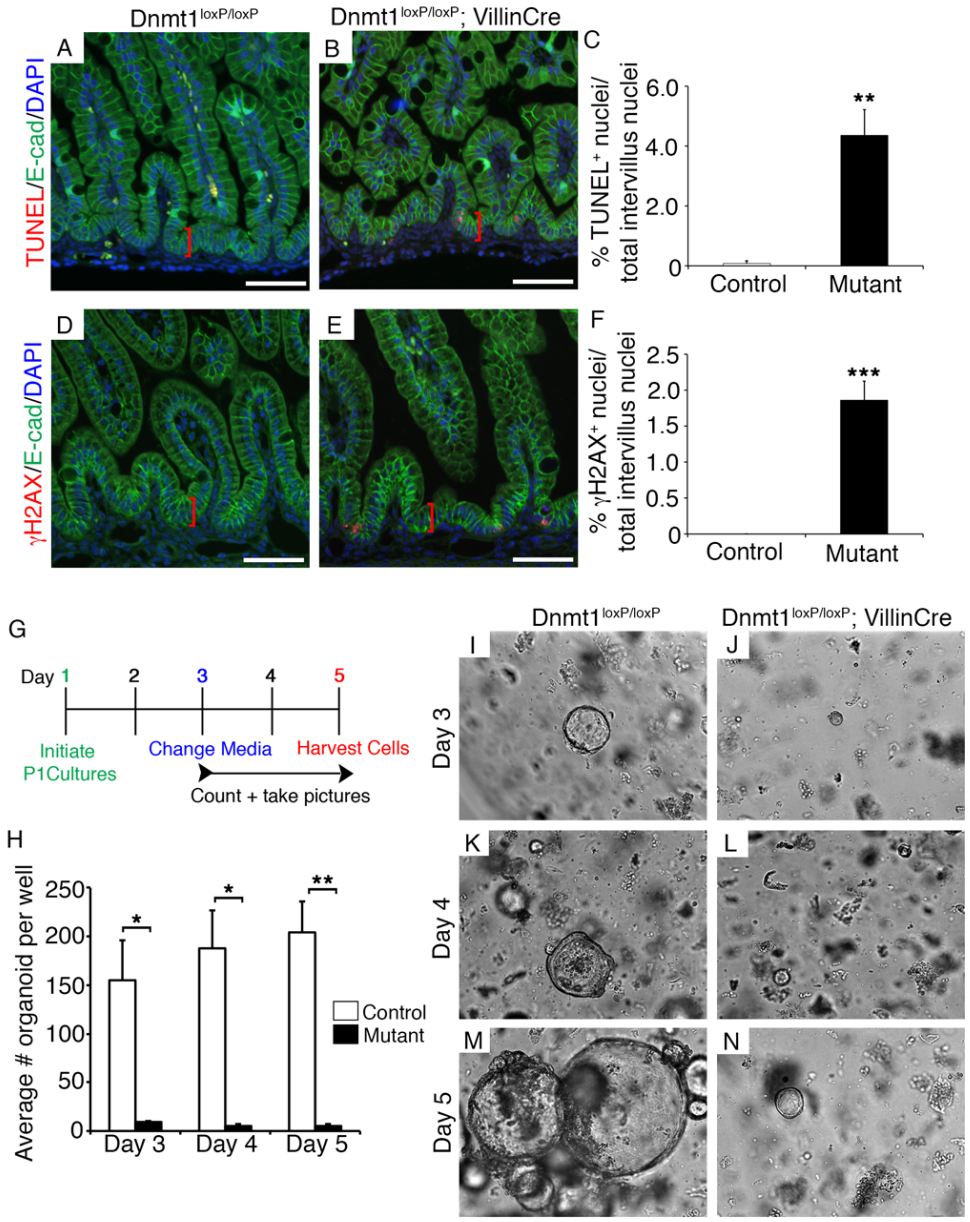

Figure 3.10. Ablation of *Dnmt1* in the immature intestine results in loss of progenitor cells via apoptosis *in vivo* and *in vitro*

Figure 3.10. Ablation of *Dnmt1* in the immature intestine results in loss of progenitor cells via apoptosis both *in vivo* and *in vitro*.

(A,B) TUNEL staining in red, E-cadherin in green, DAPI in blue. TUNEL staining demonstrates increased levels of apoptosis in *Dnmt1* mutant progenitor cells (A) compared to control (B). (C) TUNEL-positive intervillus nuclei within 20 μm from the epithelial base (red vertical bars in A,B) were quantified in *Dnmt1* mutants and littermate controls (n≥5). (D-F) *Dnmt1* mutant progenitors (E) have increased DNA double strand breaks compared to controls (D), as determined by γH2AX staining. (F) Quantification of $\gamma H2AX^+$ cell number as performed for $TUNEL^+$ cells (n=4); 20 μm vertical bar shown in (D,E). (G) Experimental outline for postnatal day 1 (P1) $Dnmt1^{loxP/loxP}$ (n=3) and $Dnmt1^{loxP/loxP}$*;VillinCre* (n=2) intestinal organoid cultures. (H) Average number of organoids per well during timecourse experiment. Organoids were grown in triplicate for each biological replicate. (I-N) Live phase contrast imaging of $Dnmt1^{loxP/loxP}$ control and $Dnmt1^{loxP/loxP}$*;VillinCre* mutant organoids on each day of culture. Surviving mutant organoids on day 5 persisted as very small cysts (N), while controls were considerably larger and exhibited budding activity (M). Phase contrast images were all captured at 10X. For all graphs, error bars are ± SEM. **P*<0.05, ***P*<0.01, ****P*<0.001, two-tailed (C,F) or one-tailed (H) Student's *t*-test. Scale bars are 50 μm.

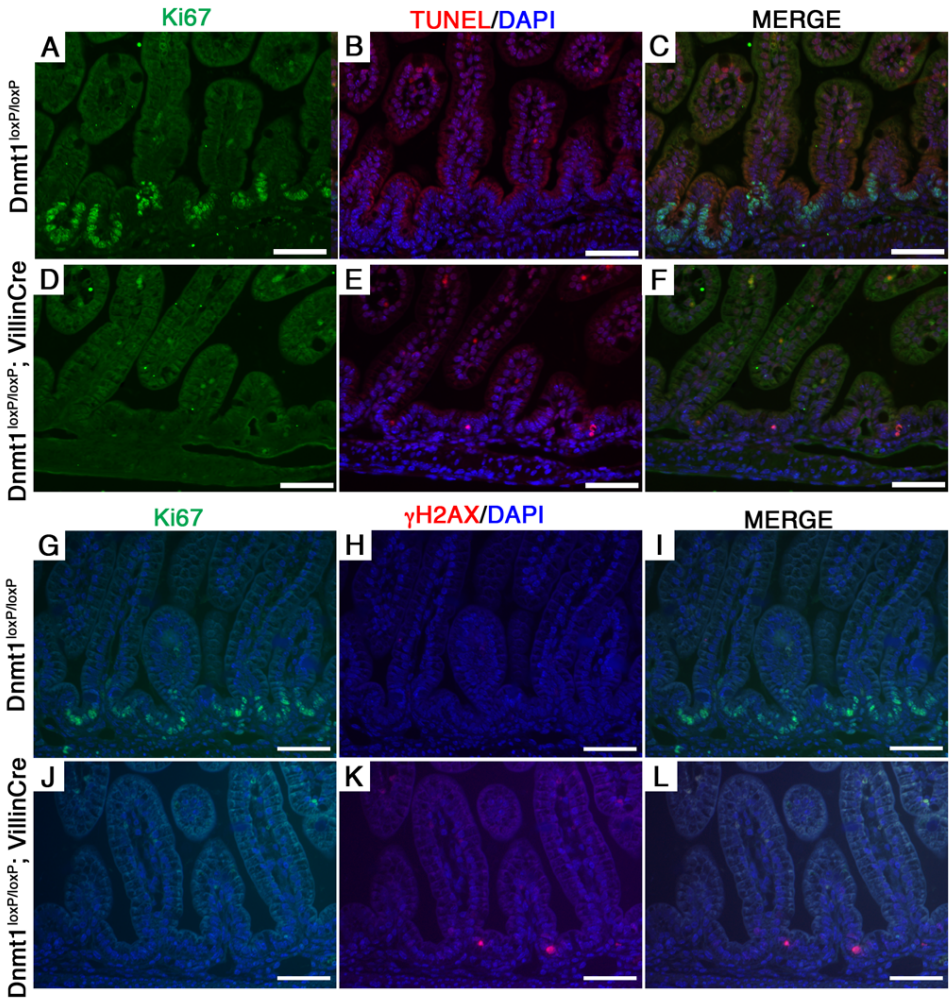

Figure 3.11. Apoptosis and DNA damage in *Dnmt1*$^{loxP/loxP}$*;VillinCre* mutant mice are confined to the non-replicating intervillus epithelium

Figure 3.11. Apoptosis and DNA damage in *Dnmt1$^{loxP/loxP}$;VillinCre* mutant mice are confined to the non-replicating intervillus epithelium.

(A-F) Co-staining for Ki67 (green, A,D) with TUNEL (red, B,E) in control (A-C) and *Dnmt1*-mutants (D-F). Mutant progenitor zones harbor TUNEL+ apoptotic cells that correspond with Ki67-negative non-proliferative regions (D-F). (G-M) γH2AX co-stained with Ki67 revealed that control epithelium does not contain DNA-damaged cells in the progenitor zone (G-I). Ki67-negative, mutant progenitors cells have increased levels of DNA damage (J-L). Scale bars are 50 μm.

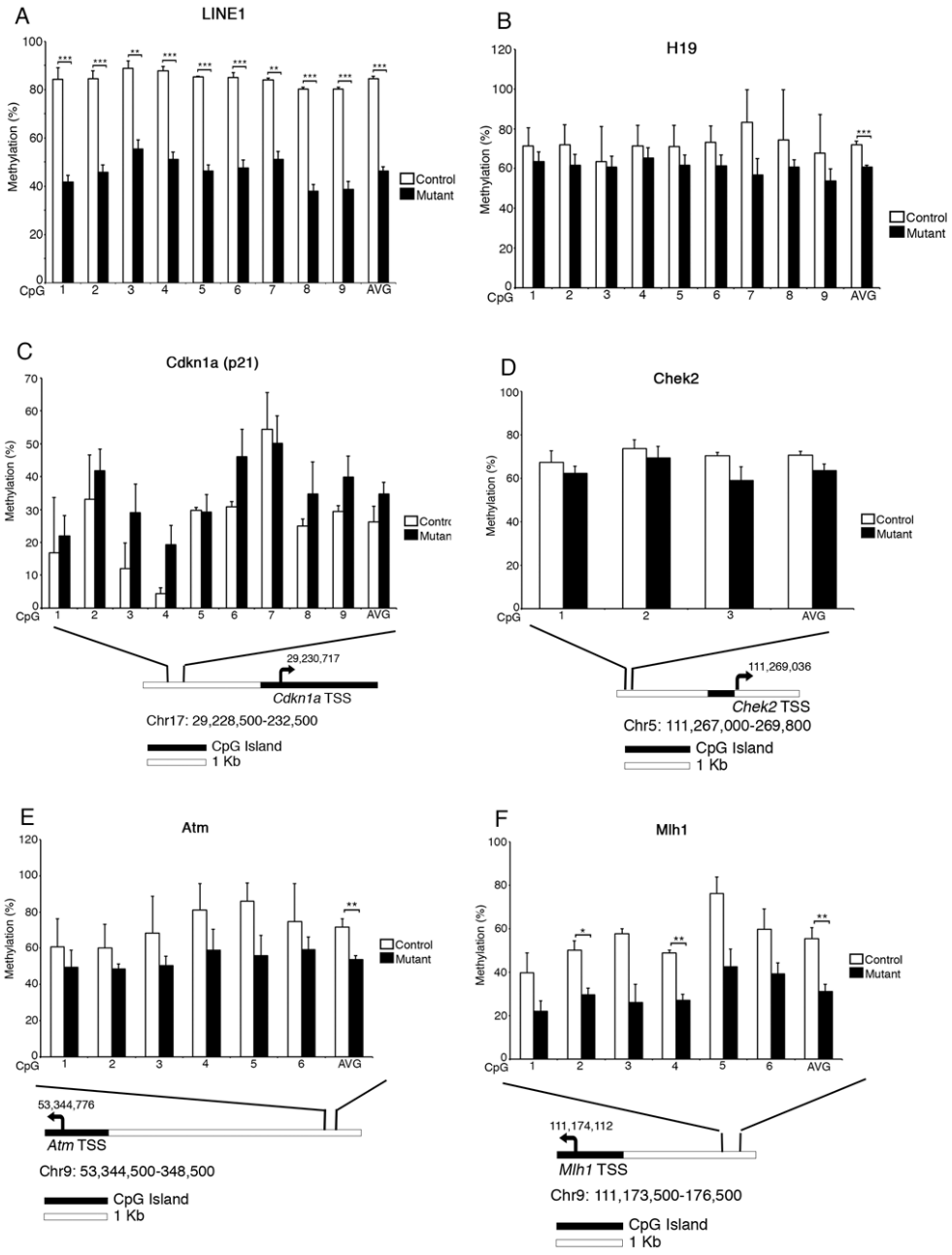

Figure 3.12. *Dnmt1*$^{loxP/loxP}$*;VillinCreERT2* adult crypt epithelial cells are demethylated at the LINE1 locus, but not at DNA damage response genes

Figure 3.12. *Dnmt1*$^{loxP/loxP}$*;VillinCreERT2* adult crypt epithelial cells are demethylated at the LINE1 locus, but not at DNA damage response genes.

(A) LINE1 repeat DNA methylation levels as assessed by bisulfite-sequencing. Decreased LINE1 methylation suggests global demethylation in *Dnmt1*-ablated adult crypt cells relative to controls. (B) In the *H19* imprinting control region (ICR), DNA methylation levels are slightly decreased in adult *Dnmt1*-mutant crypt cells relative to controls. (C-F) Targeted bisulfite-sequencing analysis of DNA damage response genes revealed similar levels of DNA methylation in adult *Dnmt1*-ablated crypt cells compared to controls. (C,D) *p21* (*Cdkn1a*) and *Chek2* are not differentially methylated in adult *Dnmt1*-mutant crypts. *Atm* (E) and *Mlh1* (F) show an overall decrease in DNA methylation relative to control, but are not significantly altered at each CpG analyzed. Beneath bar charts (C-F) is a diagram indicating the position of the transcription start site (TSS, arrow) and CpG islands relative to the regions sequenced. Each region is ~2-4 kb upstream of the TSS. Mutant n=5; Control n=2. Data are represented as mean ± SEM, ***P*<0.01, ****P*<0.001, two-tailed Student's *t*-test.

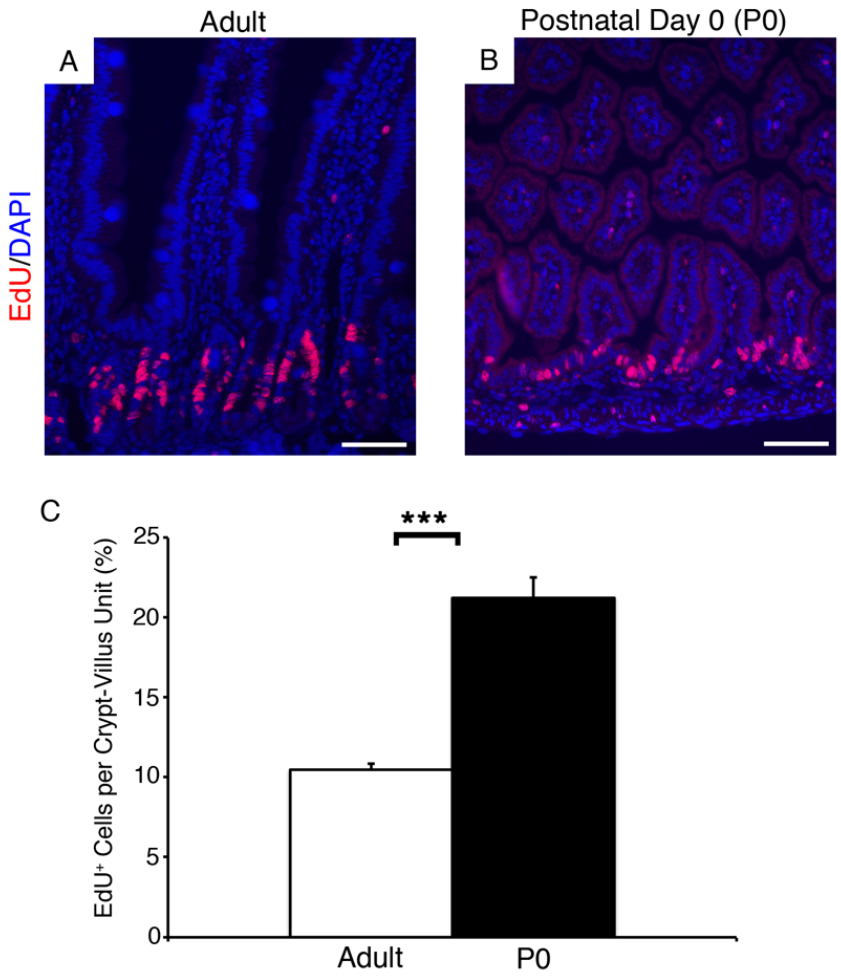

Figure 3.13. Neonatal intervillus regions display increased rate of replication compared to adult crypts

Figure 3.13. Neonatal intervillus regions display increased rate of replication compared to adult crypts.

(A,B) Representative images of adult (A, n=5) and postnatal day 0 (B, n=12) jejunum stain for EdU following a 2-hour EdU pulse (red). (C) Percent of EdU^+ cells per crypt-villus subunit is approximately two-fold higher in the neonatal compared to the adult jejunum. Rates calculated as percent EdU^+ nuclei of total nuclei between two adjacent villi peaks. Scale bars are 50 μm. Data are represented as mean ± SEM. ****P*<0.001, two-tailed Student's *t*-test.

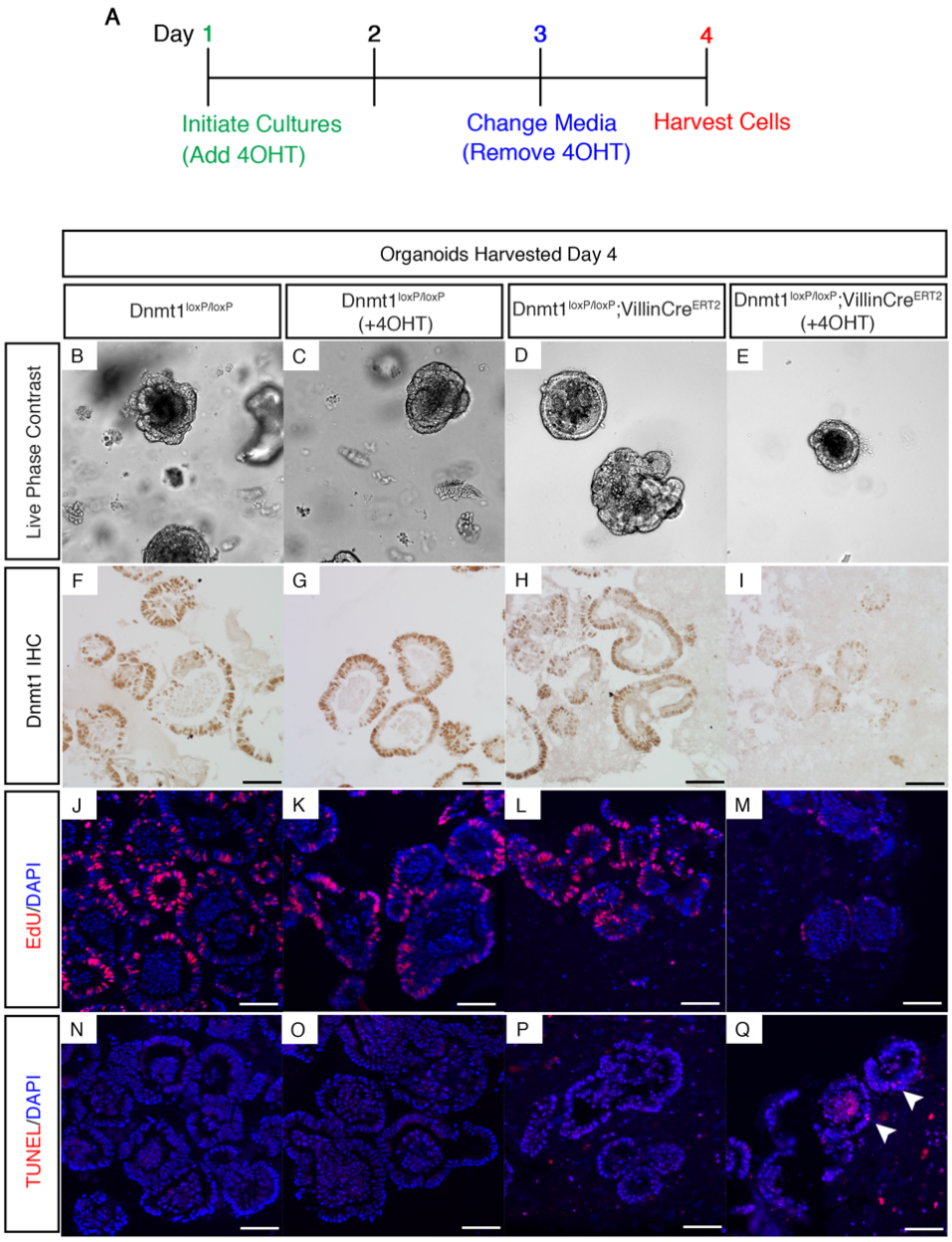

Figure 3.14. *Dnmt1* is required to establish intestinal organoid cultures

Figure 3.14. Dnmt1 is required to establish intestinal organoid cultures.

(A) Time course of 4OHT treatment in organoids from *Dnmt1*$^{loxP/loxP}$ and *Dnmt1*$^{loxP/loxP}$*;VillinCreERT2* adult intestine to test the requirement for Dnmt1 in establishment of intestinal crypts *in vitro*. (B-Q) Immunohistochemical analysis of organoids described in (A). (B-E) Live phase contrast imaging demonstrates reduced size and budding activity of *Dnmt1*-ablated organoids (E) compared to controls (B-D). All phase contrast images were captured at 10X. (F-I) Dnmt1 protein is reduced in *Dnmt1*$^{loxP/loxP}$;*VillinCreERT2* organoids upon treatment with 4OHT (I), relative to control organoids (F-G). (J-M) 2 hour EdU treatment shows reduced replication rate of Dnmt1-mutant organoids (M) compared to controls (J-L). (N-Q) Dnmt1-ablated organoids (Q) display increased apoptosis (white arrowheads) relative to non-treated controls (N,P). Additionally, apoptosis is not increased in control *Dnmt1*$^{loxP/loxP}$ organoids treated with 4OHT (O). All scale bars are 50 μm.

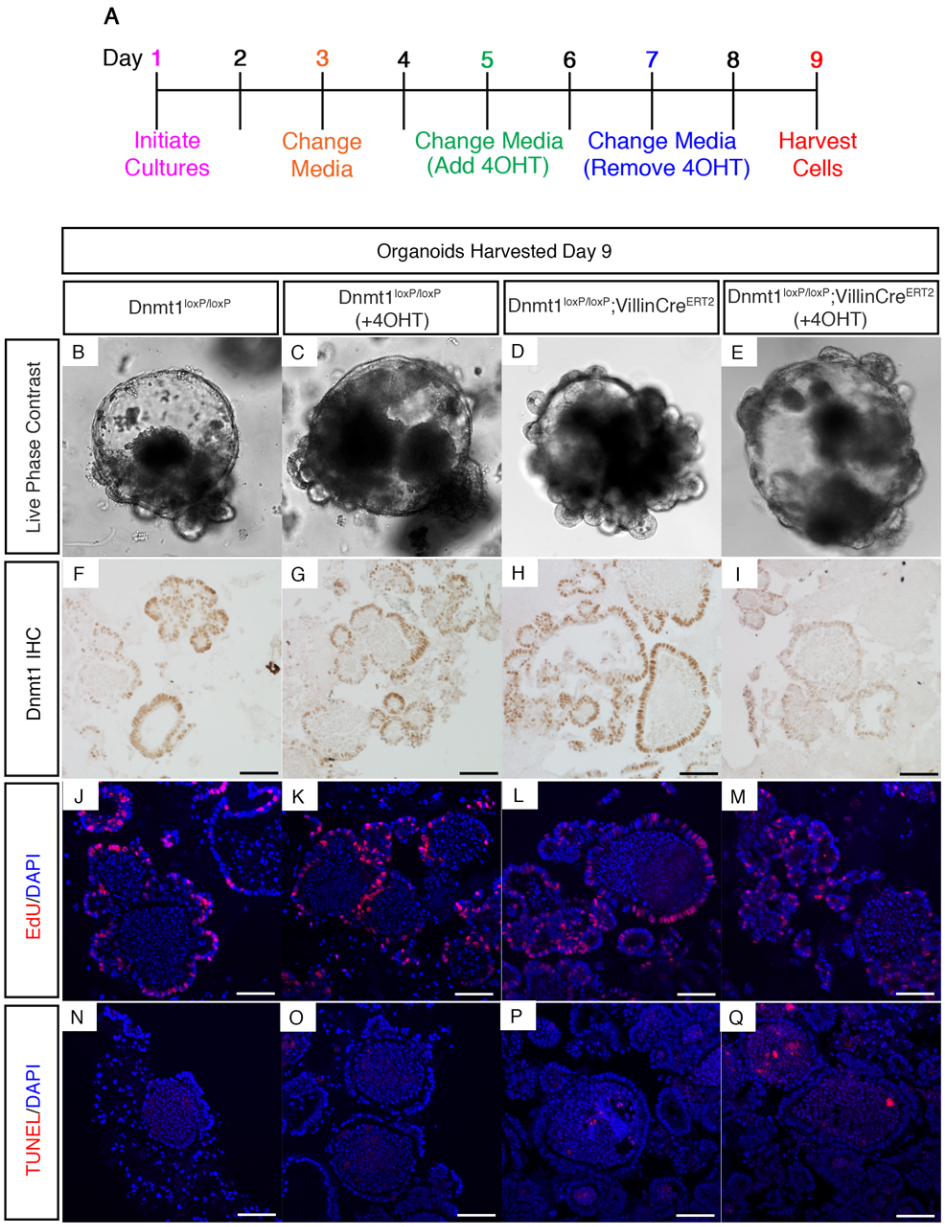

Figure 3.15. *Dnmt1* is not necessary to maintain established intestinal organoid cultures

Figure 3.15. Dnmt1 is not necessary to maintain established intestinal organoid cultures. (A) Time course of 4OHT treatment to test requirement for Dnmt1 in maintenance of intestinal crypts in vitro. (B-Q) Immunohistochemical analysis of organoids described in (A). (B-E) Live phase contrast imaging demonstrates similar size of *Dnmt1*-ablated organoids (E) at day 9 of culture relative to 4OHT-treated (C) and non-treated (B,D) controls. All phase contrast images were captured at 10X. (F-I) Confirmation of Dnmt1 protein depletion in 4OHT-treated *Dnmt1*$^{loxP/loxP}$*;VillinCreERT2* organoids (I) compared to controls (F-H). (J-M) A 2-hour pulse of EdU reveals preserved replication of *Dnmt1*-mutant organoids (M), similar to that observed in control organoids (J-L). (E,I) *Dnmt1*-ablated organoids do not display any changes in apoptosis (Q) compared to treated (O) or non-treated (N,P) control organoids. TUNEL positive material in (P,Q) is typical debris accumulation within organoids. All scale bars are 50 μm.

Chapter 4

Dnmt1 and Dnmt3b are required for genomic stability in intestinal epithelial homeostasis

Abstract

Colorectal cancer (CRC) is a heterogeneous disease accompanied by a sequence of genetic mutations and epigenetic changes. DNA methylation is thought to drive CRC progression by the repression of tumor suppressor genes via promoter methylation. The DNA methyltransferase *Dnmt1* is required for appropriate expression of stem cell genes and differentiation of the intestinal epithelium. Using temporally controlled intestinal epithelial-specific gene ablation, I show that loss of *Dnmt1* in the $Apc^{Min/+}$ mouse model of intestinal cancer surprisingly causes accelerated, not delayed, adenoma formation. Loss of Dnmt1 precipitates an acute response characterized by hypomethylation of repetitive elements, genomic instability, and apoptosis, which is followed by remethylation with time. This recovery is entirely dependent on the activity of the *de novo* methyltransferase Dnmt3b. In light of these data, the current dogma regarding the role of DNA methylation in colon cancer needs to be revisited.

Introduction

Colorectal cancer (CRC) is a multifactorial disease with various inputs including diet, environment, genetic mutations, and epigenetic abnormalities. The disease first manifests as an over-proliferation defect in the form of polyps that, if not removed, can progress to precancerous adenomas. Further transition to invasive and metastatic cancer is due to the accumulation of multiple genetic mutations and epigenetic changes that alter gene expression patterns, driving neoplastic transformation and growth (Fearon 2011). However, the extent to which epigenetic modifications, and specifically DNA methylation, contribute to the initiation and progression of CRC is unclear.

DNA methylation patterns are established by DNA methyltransferase enzymes (Dnmts), of which there are two categories. The 'maintenance' methyltransferase, Dnmt1, has a high affinity for hemi-methylated DNA *in vitro*, and preserves DNA methylation in replicating cells. The '*de novo'* methyltransferases, Dnmt3a and Dnm3b, establish novel patterns of DNA methylation, and prefer to bind unmethylated DNA *in vitro*. DNA methylation is generally found in the context of CpG dinucleotides in mammals, and while most of the genome is highly methylated, promoter and distal regulatory regions display low levels of DNA methylation (Stadler, Murr et al. 2011, Ziller, Gu et al. 2013, Sheaffer, Kim et al. 2014). Regulatory regions also exhibit the most dynamic DNA methylation among distinct tissue types, and are commonly hypomethylated in cancer (Irizarry, Ladd-Acosta et al. 2009, Stadler, Murr et al. 2011, Ziller, Gu et al. 2013). Comparison of human colon adenomas to control tissue revealed that although proximal promoter CpG islands are generally hypermethylated in tumors, DNA hypomethylation is found genome-wide, including at neighboring CpG island shores, intergenic regions, and repetitive elements (Berman, Weisenberger et al. 2012, Luo, Wong et al. 2014).

DNA methylation is critical for intestinal epithelial homeostasis (Sheaffer, Kim et al. 2014, Elliott, Sheaffer et al. 2015). Intestinal stem cells are located in the crypt and respond to multiple signaling pathways that control proliferation and differentiation (Sheaffer and Kaestner 2012). Loss of *Dnmt1* in the mouse intestine causes hypomethylation of regulatory regions associated

with several intestinal stem cell genes, resulting in inappropriate activation during differentiation, and expansion of the crypt zone (Sheaffer, Kim et al. 2014). Many intestinal stem cell factor genes, such as *LGR5*, *OLFM4*, and *HES1*, are also highly expressed in human colon cancer (van der Flier, Haegebarth et al. 2009, Chen, Zhang et al. 2014, Gao, Zhang et al. 2014). These data suggest that DNA hypomethylation may play an important role in intestinal cancer progression.

Previously, the role of Dnmt1 in intestinal tumorigenesis was studied in the $Apc^{Min/+}$ mouse model. This paradigm mimics the hereditary human colon cancer syndrome Familial Adenomatous Polyposis (FAP), which is caused by germline mutations of the *APC* gene (Su, Kinzler et al. 1992). Loss of heterozygosity (LOH) at the *APC* locus causes β-catenin stabilization and unrestricted Wnt activity, resulting in the formation of microadenomas, which progress to large adenomas over time. Multiple hypomorphic *Dnmt1* paradigms show complete block of macroscopic tumor formation (Laird, Jackson-Grusby et al. 1995, Cormier and Dove 2000, Eads, Nickel et al. 2002, Trasler, Deng et al. 2003, Yamada, Jackson-Grusby et al. 2005). The authors concluded that Dnmt1 and DNA methylation are required for adenoma development in the $Apc^{Min/+}$ model. These studies employed hypomorphic *Dnmt1* mice, which express constitutively reduced Dnmt1 levels from earliest development onward in all tissues (Laird, Jackson-Grusby et al. 1995), including non-epithelial cells, such as myofibroblasts. Mesenchymally expressed genes have been shown to be strong modifiers of the $Apc^{Min/+}$ tumor load (Perreault, Sackett et al. 2005), and could thus contribute to the observed phenotype in the *Dnmt1*-hypomorphic $Apc^{Min/+}$ intestine. Due to these limitations, the precise mechanism of how DNA methylation acts within the intestinal epithelium during adenoma initiation and progression remains to be determined.

To address this important knowledge gap, I employed a temporally controlled, intestinal epithelial-specific gene ablation model to delete *Dnmt1* and decrease maintenance DNA methylation. I find that deletion of *Dnmt1* causes accelerated loss of heterozygosity at the *Apc* locus, with a dramatic increase in adenoma initiation and progression. Ablation of Dnmt1 causes a severe acute phenotype characterized by global DNA hypomethylation, genome instability, and apoptosis. Contrary to the current dogma, I demonstrate that the *de novo* methyltransferase

Dnmt3b is essential for epithelial recovery following *Dnmt1* ablation, and provide evidence that Dnmt3b compensates for the maintenance methyltransferase *in vivo*.

Results

Deletion of Dnmt1 *in the intestinal epithelium of adult* $Apc^{Min/+}$ *mice accelerates adenoma initiation.*

To determine the role of *Dnmt1* in intestinal adenoma formation, I employed $Apc^{Min/+}$;$Dnmt1^{loxP/loxP}$;*VillinCreERT2* mice to inducibly delete *Dnmt1* throughout the intestinal and colonic epithelia. $Apc^{Min/+}$;$Dnmt1^{loxP/loxP}$;*VillinCreERT2* mice and their $Apc^{Min/+}$;$Dnmt1^{loxP/loxP}$ siblings were injected with tamoxifen to induce *Dnmt1* deletion at four weeks of age (see experimental schema in Figure 4.1). At three months of age, the small intestine and colon were examined for neoplastic transformation. *Dnmt1* deletion was effective throughout the mutant epithelia of small intestine and colon (Figures 4.2 A,B and 4.3 A,B). Surprisingly, hematoxylin and eosin staining revealed a dramatic increase in the number of neoplastic lesions throughout the entire *Dnmt1*-deficient small intestine, where mutants displayed >6-fold more macroscopic adenomas (Figure 4.2 C-E).

Previously, it had been reported that partial loss of *Dnmt1* produces a block in the progression of adenomas in the $Apc^{Min/+}$ mouse paradigm (Laird, Jackson-Grusby et al. 1995, Cormier and Dove 2000, Eads, Nickel et al. 2002, Trasler, Deng et al. 2003, Yamada, Jackson-Grusby et al. 2005), which is in sharp contrast to our finding of an increased number of macroscopic lesions in the $Apc^{Min/+}$;$Dnmt1^{loxP/loxP}$;*VillinCreERT2* deletion model. To confirm that these lesions are bona fide adenomas, I performed histopathologic assessment on the intestines of three-month old $Apc^{Min/+}$;$Dnmt1^{loxP/loxP}$;*VillinCreERT2* and $Apc^{Min/+}$;$Dnmt1^{loxP/loxP}$ mice which had been tamoxifen treated at 4 weeks of age. Using criteria described by Biovin *et al.* (2003), I found 15-fold more lesions that had progressed to adenomas in *Dnmt1*-deficient mice as compared to $Apc^{Min/+}$ animals (Figure 4.2 F). In addition, *Dnmt1*-deficient small intestinal tumors were on average twice as large as those of controls (Figure 4.2 G).

Adenoma formation in the $Apc^{Min/+}$ mouse model is driven by loss of heterozygosity (LOH) at the *Apc* locus, which causes nuclear accumulation of β-catenin and activation of Wnt signaling. LOH is observed in virtually all $Apc^{Min/+}$ intestinal tumors (Levy, Smith et al. 1994, Luongo, Moser

et al. 1994). Thus, increased tumor load likely reflects accelerated LOH at earlier time points. To establish if increased macroadenoma formation in three-month old *Dnmt1*-mutants correlated with earlier tumor initiation, I injected four-week old *Apc*$^{Min/+}$*;Dnmt1*$^{loxP/loxP}$*;VillinCreERT2* mice (mutant) and their *Apc*$^{Min/+}$*;Dnmt1*$^{loxP/loxP}$ (control) siblings with tamoxifen, and examined the small intestine at two months of age for microadenomas (see schema in Figure 4.1). Mutant animals displayed an increase in microadenoma number in the small intestine compared to controls (Figure 4.2 H), even though lesions were still comparable in size (Figure 4.2 G). All lesions observed in two-month old animals showed similar histopathology and were characterized as gastrointestinal intraepithelial neoplasias (data not shown).

Previous studies also reported increased colonic microadenomas in *Dnmt1*-hypomorphic *Apc*$^{Min/+}$ mice (Yamada, Jackson-Grusby et al. 2005). To investigate microadenoma formation in the colon, I employed nuclear β-catenin staining to identify neoplastic lesions in three-month old mice. Only 14% of control mice displayed neoplastic transformation in the colon (n=7). However, 58% of *Dnmt1*-deficient *Apc*$^{Min/+}$ colons (n=12) showed at least one incidence of microadenoma, including several mice with multiple lesions (Figure 4.3 D). Since *Apc*$^{Min/+}$ mice exhibit tumors predominantly in the small intestine (Moser, Pitot et al. 1990, Moser, Dove et al. 1992), I focused my studies on adenoma development and progression in the small intestinal epithelium.

To characterize adenoma initiation by LOH in detail, I employed laser capture microdissection to isolate neoplastic and normal intestinal epithelial cells in tamoxifen-treated two- and three-month old *Apc*$^{Min/+}$*;Dnmt1*$^{loxP/loxP}$*;VillinCreERT2* mutant mice and their *Apc*$^{Min/+}$*;Dnmt1*$^{loxP/loxP}$ control siblings. DNA was isolated from these samples (approximately 1,000 cells per sample) and the status of the *Apc* alleles was examined as performed previously (Luongo, Moser et al. 1994). Analysis of control and mutant mice produced bands for both the wildtype *Apc* and the *Apc*^{Min} alleles in the normal epithelium, as expected, while neoplastic lesions showed only the *Apc*^{Min} allele band (data not shown).

Several lines of evidence confirm that the numerous adenomas that develop in the *Dnmt1*-deficient *Apc*$^{Min/+}$ mice are the result of Wnt pathway activation. Thus,

Apc$^{Min/+}$*;Dnmt1*$^{loxP/loxP}$*;VillinCreERT2* (mutant) adenomas showed increased nuclear β-catenin protein (Figure 4.4 B,C), and multiple Wnt signaling targets, such as *CycD1* (Figure 4.4 E,F) and *Sox9* (Figure 4.4 H,I) were also strongly activated. These data demonstrate that total loss of *Dnmt1* in the mature small intestinal epithelium promotes neoplastic progression, in stark contrast to what had been reported previously (Laird, Jackson-Grusby et al. 1995, Cormier and Dove 2000, Eads, Nickel et al. 2002, Trasler, Deng et al. 2003, Yamada, Jackson-Grusby et al. 2005).

Dnmt1-*null adenomas display increased chromosome instability*

Due to the dramatic difference in lesion size and grade observed in three-month old animals, I investigated whether *Dnmt1*-deficiency had any impact on cell proliferation or death in *Apc*$^{Min/+}$ adenomas. I analyzed *Apc*$^{Min/+}$*;Dnmt1*$^{loxP/loxP}$ (control) and *Apc*$^{Min/+}$*;Dnmt1*$^{loxP/loxP}$*;VillinCreERT2* (mutant) tumor proliferation using the cell cycle marker, Ki67 (Figure 4.5 B-D). Non-tumor *Dnmt1*-deficient intestinal epithelium displayed a slight expansion of the crypt zone, as reported previously (Sheaffer, Kim et al. 2014). I also determined the percentages of control and mutant epithelial cells in M-phase by staining for phosphorylated-H3 (PH3) (Figure 4.5 A). These data show that the proliferation rate was equivalent in Dnmt1-positive or -negative tumors, at both two months and three months of age. Furthermore, comparison of three-month old control and two-month old mutant adenomas revealed that similarly sized tumors had comparable rates of cellular proliferation (Figure 4.5 B,C). I also examined neoplastic cells for signs of cell death using terminal deoxynucleotidyl transferase dUTP nick end labeling (TUNEL), which detects DNA fragmentation in apoptotic cells. Both control and mutant adenomas exhibited only rare epithelial cells positive for TUNEL, and I found no difference in cell death between *Dnmt1*-mutant and control neoplastic epithelia. However, many subepithelial cells were TUNEL positive (Figure 4.5 E-G). These data demonstrate that loss of *Dnmt1 in vivo* has no effect on *Apc*$^{Min/+}$ adenoma proliferation or cell death, and indicates that the increase in adenoma number and size found in three-month old *Dnmt1*-mutant mice is driven by accelerated tumor initiation through loss of heterozygosity.

I next investigated the requirement of *Dnmt1* for chromosome stability in our intestinal cancer model. Global DNA hypomethylation correlates with chromosomal instability in CRC (Lengauer, Kinzler et al. 1997, Rodriguez, Frigola et al. 2006). I employed γH2AX staining to visualize DNA double-strand breaks as a marker of chromosomal instability, and found many more epithelial cells within *Dnmt1*-deficient adenomas to be $\gamma H2AX^{+}$ compared to control adenomas (Figure 4.5 H-J). Notably, γH2AX foci had already appeared in two-month old mutant adenomas that are of similar size to control three-month old adenomas (Figure 4.5 H,I). These data indicate that increased double strand breaks are not simply the consequence of rapid tumor growth, but an early event in tumorigenesis in the *Dnmt1*-deficient $Apc^{Min/+}$ mouse.

Dnmt1 *deletion in* $Apc^{Min/+}$ *mice causes massive epithelial remodeling within one week*

To determine the underlying causes of accelerated loss of heterozygosity and increased tumorigenesis in the $Apc^{Min/+};Dnmt1^{loxP/loxP};VillinCreERT2$ mutant intestine, I next focused on the earliest events following *Dnmt1* ablation. To this end, I injected tamoxifen in four-week old $Apc^{Min/+};Dnmt1^{loxP/loxP};VillinCreERT2$ mice (mutant) and their $Apc^{Min/+};Dnmt1^{loxP/loxP}$, $Dnmt1^{loxP/loxP};VillinCreERT2$, and $Dnmt1^{loxP/loxP}$ siblings (controls), and examined the small intestine one week later (see Figure 4.1 for experimental schema). I confirmed loss of Dnmt1 protein (Figure 4.6 E-H), and proceeded to gross histological analysis. Acute loss of *Dnmt1* in $Dnmt1^{loxP/loxP};VillinCreERT2$ mice caused crypt expansion compared to controls (Figure 4.6 A-B), as described previously (Sheaffer, Kim et al. 2014). Although the $Apc^{Min/+};Dnmt1^{loxP/loxP};VillinCreERT2$ mutant intestine exhibited crypt expansion, surprisingly, I also detected many areas that displayed a drastic loss of crypt and villus epithelium (Figure 4.6 C-D). When I assessed proliferation by performing immunofluorescent staining for Ki67, the $Apc^{Min/+};Dnmt1^{loxP/loxP};VillinCreERT2$ mutant intestine contained many crypts that had little to no Ki67 staining (compare Figure 4.6 L to 4.6 K), while crypts in $Dnmt1^{loxP/loxP};VillinCreERT2$ intestine had an obvious increase in the proliferative zone (Figure 4.6 I-J). Additionally, I performed TUNEL staining to assess levels of apoptosis in $Apc^{Min/+};Dnmt1^{loxP/loxP};VillinCreERT2$

mutants and control siblings (Figure 4.6 M-P). Interestingly, I observed increased levels of crypt cell apoptosis in *Apc*$^{Min/+}$*;Dnmt1*$^{loxP/loxP}$*;VillinCreERT2* (Figure 4.6 P) relative to all other conditions. These data indicate that loss of *Dnmt1* on the *Apc*$^{Min/+}$ background causes a severe acute phenotype of crypt loss not present in the *Apc*$^{+/+}$, *Dnmt1*-deficient intestine.

Apc$^{Min/+}$ mice display increased sensitivity to DNA damage, including damage induced by ionizing radiation (Tao, Tang et al. 2015), and are also noted to have defects in epithelial cell migration (Mahmoud, Boolbol et al. 1997). I reasoned that loss of *Dnmt1* might induce genome instability that many epithelial cells in *Apc*$^{Min/+}$ mice are unable to repair. To determine basal levels of DNA damage in mice one week after tamoxifen administration, long before tumor formation has been initiated, I performed γH2AX staining (Figure 4.6 I-L). I discovered a dramatic increase in the fraction of γH2AX^{+} crypt cells in *Apc*$^{Min/+}$*;Dnmt1*$^{loxP/loxP}$*;VillinCreERT2* (Figure 4.6 L) versus *Apc*$^{Min/+}$ controls, which contained no γH2AX^{+} epithelial cells (Figure 4.6 K). These results demonstrate that genomic instability in *Apc*$^{Min/+}$*;Dnmt1*$^{loxP/loxP}$*;VillinCreERT2* mice occurs prior to accelerated tumorigenesis. *Dnmt1*$^{loxP/loxP}$*;VillinCreERT2* mutants also displayed low levels of γH2AX^{+} crypt cells, indicating that Dnmt1 is required to maintain genomic stability in proliferating intestinal cells (Figure 4.6 I,J).

DNA methylation dynamics following Dnmt1 *deletion*

Despite the striking acute phenotype I observed following *Dnmt1* deletion in the adult *Apc*$^{Min/+}$ intestinal epithelium, *Apc*$^{Min/+}$*;Dnmt1*$^{loxP/loxP}$*;VillinCreERT2* mutant mice survive to three months of age. I hypothesized that the dramatic loss of global DNA methylation following *Dnmt1* ablation precipitates acute genome instability, and that animal survival to three months correlates with recovery of DNA methylation levels. To test this hypothesis, I performed targeted bisulfite sequencing of the Long Interspersed Nucleotide Element 1 (LINE1) to estimate global DNA methylation levels, and of the H19 imprinting control region (ICR) to determine DNA methylation maintenance (Lane, Dean et al. 2003, Yang, Estécio et al. 2004, Samuel, Suzuki et al. 2009).

I employed laser capture microdissection to collect crypts from *Apc*$^{Min/+}$*;Dnmt1*$^{loxP/loxP}$*;VillinCreERT2* mutant and *Apc*$^{Min/+}$*;Dnmt1*$^{loxP/loxP}$ control intestines one week following tamoxifen treatment (see schema in Figure 4.1). Strikingly, within one week following *Dnmt1* deletion, I observed a 50% reduction in DNA methylation at the LINE1 loci in mutant crypts compared to control crypt epithelium (Figure 4.7 A). In contrast, methylation of the *H19* imprinting control region was maintained, indicating that maintenance methylation of imprinted loci was preserved in *Apc*$^{Min/+}$*;Dnmt1*$^{loxP/loxP}$*;VillinCreERT2* intestinal epithelium (Figure 4.8 A).

To assess recovery of global DNA methylation with time, I implemented laser capture microdissection to isolate the neoplastic and normal intestinal epithelia from *Apc*$^{Min/+}$*;Dnmt1*$^{loxP/loxP}$*;VillinCreERT2* mutant and *Apc*$^{Min/+}$*;Dnmt1*$^{loxP/loxP}$ control intestines at three months of age, two months after tamoxifen administration. Surprisingly, I found no differences in methylation levels in all conditions tested, demonstrating that DNA methylation had been fully restored after acute loss following *Dnmt1* ablation (Figure 4.7 B). I excluded the trivial explanation that *Dnmt1*-positive 'Cre-escaper' cells had repopulated the neoplastic epithelium by performing immunohistochemistry for Dnmt1 protein, confirming that these tumors were *Dnmt1*-negative (compare Figure 4.9 B to 4.9 A).

I surmised that the *de novo* methyltransferases might compensate for the loss of Dnmt1, and performed immunofluorescent staining for both Dnmt3a and Dnmt3b one week following *Dnmt1* deletion. While I observed no change in Dnmt3a levels by immunofluorescence (Figure 4.10 A,B), I found Dnmt3b protein levels increased in five-week old *Apc*$^{Min/+}$*;Dnmt1*$^{loxP/loxP}$*;VillinCreERT2* crypts compared to sibling controls (Figure 4.10 C,D). Overall, these data suggest a mechanism in which Dnmt3b is activated to compensate for loss of Dnmt1 in the intestinal epithelium. I next aimed to test this proposed compensation mechanism using mouse genetics.

Dnmt3b is required to maintain DNA methylation and epithelial integrity in the absence of Dnmt1

To directly test the requirement for *Dnmt3b* in maintaining DNA methylation in the *Apc*$^{Min/+}$*;Dnmt1*$^{loxP/loxP}$*;VillinCreERT2* intestinal epithelium, I bred the *Dnmt3b*$^{loxP/loxP}$ allele (Lin, Yamada et al. 2006) onto the mutant genotype, producing *Apc*$^{Min/+}$*;Dnmt1*$^{loxP/loxP}$*;Dnmt3b*$^{loxP/loxP}$*;VillinCreERT2* mice, along with *Apc*$^{Min/+}$*;Dnmt1*$^{loxP/loxP}$*;Dnmt3b*$^{loxP/loxP}$ siblings as controls. In these cohorts of mice, I injected tamoxifen at four weeks of age to induce simultaneous ablation of *Dnmt1* and *Dnmt3b.* I isolated small intestines one week following tamoxifen administration for phenotypic analysis.

Histological examination revealed a grossly altered epithelium in the *Apc*$^{Min/+}$*;Dnmt1;Dnmt3b* mutant mice, with many areas lacking villi and/or crypts completely (compare Figure 4.11 B to 4.11 A). I performed immunohistochemistry for Dnmt1 and Dnmt3b to confirm loss of both proteins in the majority of the epithelium (Figure 4.11 C-F). Many crypts in mutants were completely Ki67-negative (Figure 4.11 H), and harbored extensive DNA damage as indicated by γH2AX foci (compare Figure 4.11 H versus 4.11 G). TUNEL staining revealed increased crypt cell apoptosis in *Apc*$^{Min/+}$*;Dnmt1;Dnmt3b* mutants compared to sibling controls (Figure 4.11 J versus 4.11 I). Hyper-proliferative crypts often escaped Cre-mediated *Dnmt3b* deletion (data not shown), consistent with my hypothesis that *Dnmt3b* is required to preserve epithelial integrity in the absence of *Dnmt1*.

To assess the overall requirement for *Dnmt3b* in *Apc*$^{Min/+}$*;Dnmt1*$^{loxP/loxP}$*;VillinCreERT2* survival, I injected tamoxifen into groups of *Apc*$^{Min/+}$*;Dnmt1*$^{loxP/loxP}$*;Dnmt3b*$^{loxP/loxP}$*;VillinCreERT2* mutants and littermate controls at four weeks of age, and weighed mice each day following CreERT2 induction. All *Apc*$^{Min/+}$*;Dnmt1;Dnmt3b* mutant mice became severely morbid within three weeks following tamoxifen administration and had to be euthanized (Figure 4.11 K). In contrast, 96% of *Apc*$^{Min/+}$*;Dnmt1*$^{loxP/loxP}$*;VillinCreERT2* mutant mice survived to three weeks following tamoxifen injection (Figure 4.11 K), demonstrating that loss of *Dnmt1* alone is non-lethal in the

mature intestinal epithelium. I conclude that *Dnmt3b* is crucial for epithelial survival in the *Apc*$^{Min/+}$*;Dnmt1*$^{loxP/loxP}$*;VillinCreERT2* mouse model (Figure 4.12 G-I).

Discussion

The results presented above have major implications for the fields of DNA methylation and intestinal cancer biology. I show that loss of the DNA methyltransferase Dnmt1 in the *Apc*$^{Min/+}$ cancer model results in acute hypomethylation and DNA damage (see summary model in Figure 4.12). I posit that this decreased genomic stability accelerates loss of heterozygosity (LOH) at the *Apc* locus, resulting in increased tumorigenesis and larger tumors (Figure 4.12 F). DNA methylation has been linked to genomic instability in multiple contexts, in both cell lines and in disease. In the HCT116 colorectal cancer cell line, ablation of catalytically active DNMT1 causes cell cycle arrest and apoptosis due to increased chromosomal instability (Chen, Hevi et al. 2007, Spada, Haemmer et al. 2007). Global hypomethylation in mice results in chromosome duplications and invasive T-cell lymphomas at four months of age (Gaudet, Hodgson et al. 2003), and in mouse ES cells, loss of Dnmt1 also causes global hypomethylation and increased mutation rates (Chen, Pettersson et al. 1998). In mouse embryonic fibroblasts (MEFs), ablation of Dnmt1 causes gradual hypomethylation, deregulated gene expression, and cell death (Jackson-Grusby, Beard et al. 2001). My work adds to this body of evidence that implicates a crucial role for Dnmt1 and DNA methylation in maintaining genome stability.

Importantly, my study shows increased intestinal adenoma formation after deletion of *Dnmt1*. My experimental paradigm results in intestine-specific, temporal loss of *Dnmt1* and acute hypomethylation, followed by recovery of global genome DNA methylation, in contrast to prior work, which had employed germline hypomorphic *Dnmt1* alleles (Laird, Jackson-Grusby et al. 1995, Cormier and Dove 2000, Eads, Nickel et al. 2002, Trasler, Deng et al. 2003, Yamada, Jackson-Grusby et al. 2005). These previous studies thus differed both in the timing of *Dnmt1* deletion and in lack of tissue specificity. Early intestinal development requires Wnt signaling to a lesser degree than the established adult stem cell niche (Korinek, Barker et al. 1998, Kim, Mao et al. 2007, Mustata, Vasile et al. 2013). In addition, deletion of *Dnmt1* during crypt establishment has different consequences on global DNA methylation than ablation in mature crypts, and causes cell death (Elliott, Sheaffer et al. 2015). Indeed, Laird and colleagues noted that tumor

suppression in their model only occurred if hypomethylation was induced early in life (1995). Therefore, deletion of *Dnmt1* during crypt establishment may lead to decreased cell proliferation and a decreased opportunity for tumor initiation. After crypts are established, ablation of *Dnmt1* results in increased proliferation and decreased genome stability, causing accelerated loss of $Apc^{Min/+}$ heterozygosity and adenoma formation (Figure 4.12 D-F).

Current dogma holds that deletion of *Dnmt1* is lethal in all dividing somatic cells (Liao, Karnik et al. 2015); however, I find that the rapidly dividing intestinal epithelium can survive without *Dnmt1*. I describe the first *in vivo* mouse model in which *Dnmt3b* compensates for loss of *Dnmt1* in somatic cells. Following *Dnmt1* ablation in the adult intestine and acute loss of Dnmt1, Dnmt3b activity is induced, and methylation of repetitive elements is restored. However, if *Dnmt3b* is ablated concurrently with *Dnmt1,* restoration of DNA methylation is prevented, resulting in massive DNA damage, and cell death (Figure 4.12 G-I). These results provide convincing evidence that Dnmt3b can contribute to maintenance DNA methylation in somatic tissues, and strongly suggest that the categories of '*de novo*' (Dnmt3a and 3b) versus 'maintenance' (Dnmt1) methylation are more plastic than traditionally thought.

In conclusion, I show that deletion of *Dnmt1* in the adult intestinal epithelium of $Apc^{Min/+}$ mice causes accelerated formation of adenomas. Loss of *Dnmt1* results in short-term hypomethylation, genomic instability, and apoptosis. Dnmt3b is upregulated in response to deletion of *Dnmt1* in the adult intestine, and is required to recover DNA methylation and epithelial integrity. Dnmt1-deficient adenomas maintain global DNA methylation, but continue to display increased genomic instability, indicating a fundamental role for Dnmt1 in preserving genomic integrity in the intestinal epithelium.

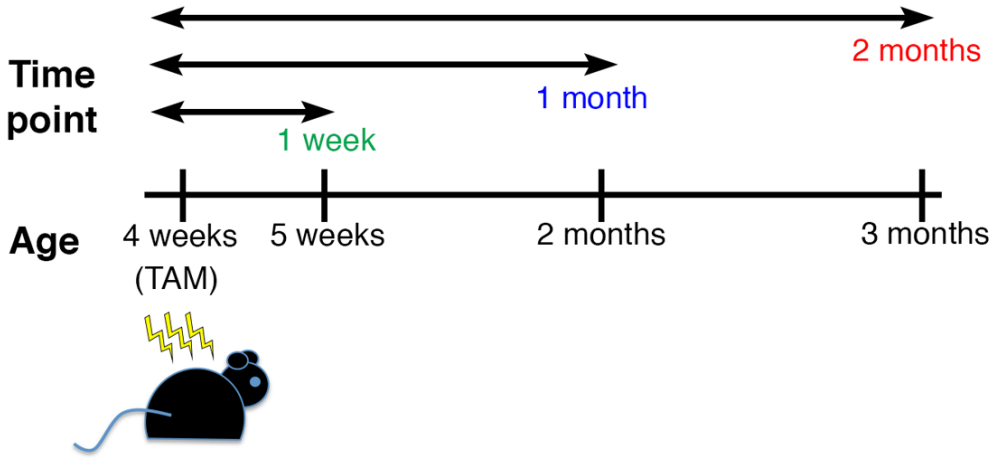

Figure 4.1. Analysis of *Apc*$^{Min/+}$;*Dnmt1*$^{loxP/loxP}$;*VillinCreERT2* mice.

Figure 4.1. Analysis of *Apc$^{Min/+}$;Dnmt1$^{loxP/loxP}$;VillinCreERT2* mice.

VillinCreERT2 activity was induced with three daily intraperitoneal injections of 1.6mg tamoxifen (TAM) in four-week old *Apc$^{Min/+}$;Dnmt1$^{loxP/loxP}$;VillinCreERT2* mutant and *Apc$^{Min/+}$;Dnmt1$^{loxP/loxP}$* control mice. To evaluate tumor development, the small intestine and colon were harvested at one month and two months following tamoxifen injections, corresponding to two months and three months of age, respectively. Acute effects of *Dnmt1* ablation were analyzed by harvesting the small intestine and colon one week following tamoxifen administration, at five weeks of age.

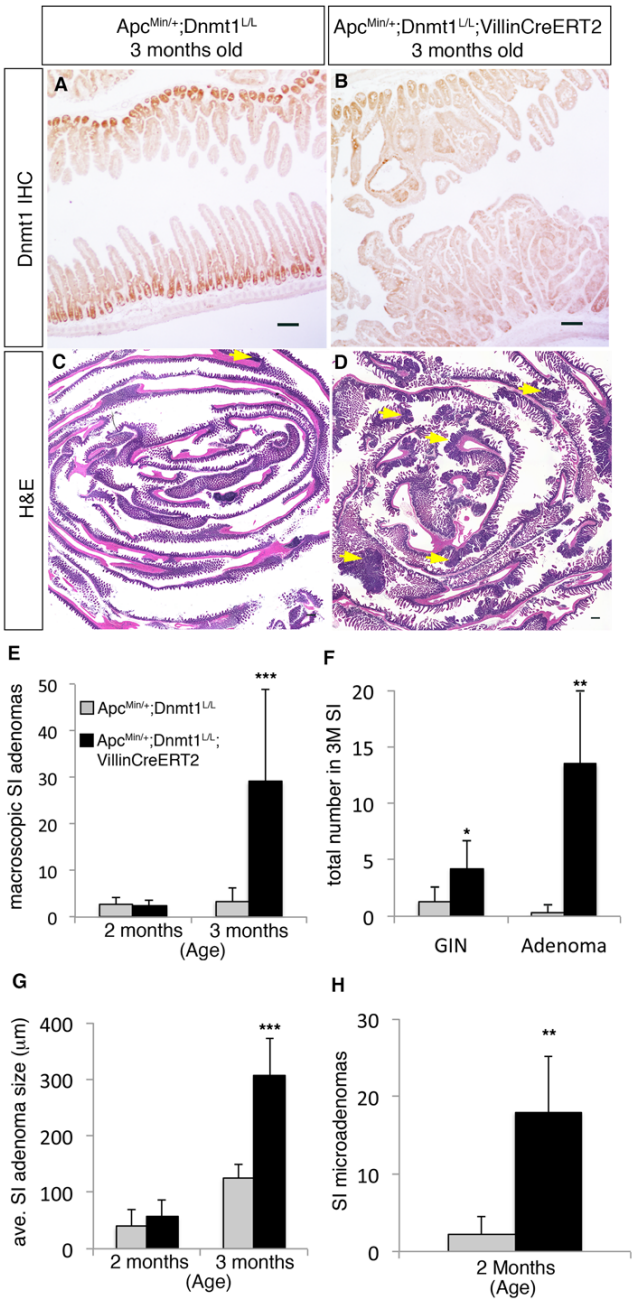

Figure 4.2. Deletion of *Dnmt1* in adult *Apc*$^{Min/+}$ mice accelerates adenoma initiation.

Figure 4.2. Deletion of *Dnmt1* in adult *Apc$^{Min/+}$* mice accelerates adenoma initiation.

Apc$^{Min/+}$;Dnmt1$^{loxP/loxP}$ mice and *Apc$^{Min/+}$;Dnmt1$^{loxP/loxP}$;VillinCreERT2* mice were injected with tamoxifen at 4 weeks of age. Intestines were harvested two months or one month following tamoxifen treatment, corresponding to three months and two months of age, respectively.

(A,B) *Dnmt1* deletion is maintained two months after tamoxifen treatment in the adult mouse small intestinal epithelium. Immunohistochemical staining of Dnmt1 protein is evident in the crypts of *Apc$^{Min/+}$;Dnmt1$^{loxP/loxP}$* (A) but absent in *Apc$^{Min/+}$;Dnmt1$^{loxP/loxP}$;VillinCreERT2* (B) mice.

(C,D) Dramatic increase in tumor formation observed in the three-month old *Dnmt1*-deficient small intestine. Hematoxylin and Eosin staining shows disruption of normal intestinal epithelial morphology throughout the entire length of the small intestine in tamoxifen-treated *Apc$^{Min/+}$;Dnmt1$^{loxP/loxP}$;VillinCreERT2* mice (D) compared to *Apc$^{Min/+}$;Dnmt1$^{loxP/loxP}$* mice (C). Arrows point to adenomas.

(E) *Dnmt1* deletion causes increased incidence of macroscopic tumors in three-month old mice. Total number of macroscopic tumors was counted throughout the entire small intestine in tamoxifen-treated *Apc$^{Min/+}$;Dnmt1$^{loxP/loxP}$* mice and *Apc$^{Min/+}$;Dnmt1$^{loxP/loxP}$;VillinCreERT2* mice at two (n≥5) and three (n≥17) months of age.

(F) Neoplastic lesions found in *Dnmt1*-deficient mice are predominantly adenomas. Total number of lesions displaying gastrointestinal intraepithelial neoplasia (GIN) and adenoma as determined by histopathological scoring were counted in three-month old mice (n=3-8 per group).

(G) *Dnmt1* deletion causes increased size of neoplastic lesions in the small intestine at three months of age. Neoplastic lesions were measured in tamoxifen-treated *Apc$^{Min/+}$;Dnmt1$^{loxP/loxP}$* mice and *Apc$^{min/+}$;Dnmt1$^{loxP/loxP}$;VillinCreERT2* mice at two (n≥24) and three (n≥9) months of age.

(H) Increased number of microadenomas in the two-month old Dnmt1-deficient small intestine. Total numbers of microadenomas were counted throughout the entire small intestine in tamoxifen-treated *Apc$^{Min/+}$;Dnmt1$^{loxP/loxP}$* mice and *Apc$^{Min/+}$;Dnmt1$^{loxP/loxP}$;VillinCreERT2* mice at two months of age (n≥5 per group). For all graphs, data are presented as average±SEM; **P*<0.05, ***P*<0.01, ****P*<0.001 by two-tailed Student's *t*-test. Scale bars are 50μm.

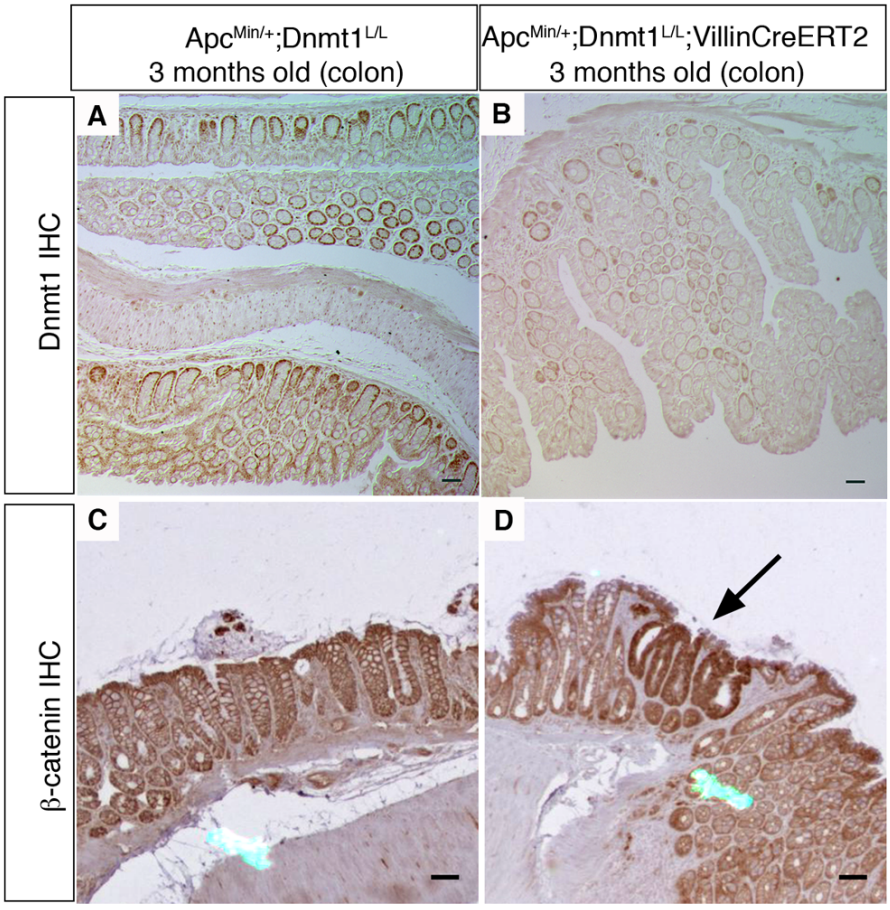

Figure 4.3. *Dnmt1* deletion causes increased incidence of microadenomas in the colon at three months.

Figure 4.3. *Dnmt1* deletion causes increased incidence of microadenomas in the colon at three months.

(A,B) *Dnmt1* deletion was maintained two months after tamoxifen treatment in the adult mouse colonic epithelium. Immunohistochemical staining of Dnmt1 protein is evident in the crypts of *Apc*$^{Min/+}$*;Dnmt1*$^{loxP/loxP}$ colonic epithelia (A), but is completely absent in *Apc*$^{Min/+}$*;Dnmt1*$^{loxP/loxP}$*;VillinCreERT2* mutant colon (B).

(C,D) Increased incidence of neoplastic crypts observed in three-month old *Dnmt1*-deficient colons. β-catenin staining shows an example of a microadenoma (arrow) with nuclear accumulation of β-catenin in *Apc*$^{Min/+}$*;Dnmt1*$^{loxP/loxP}$*;Villin-Cre-ERT2* mice (D) compared to localization on the cell membrane in the nontransformed colonic epithelia of *Apc*$^{Min/+}$*;Dnmt1*$^{loxP/loxP}$ mice (C). Scale bars are 50μm.

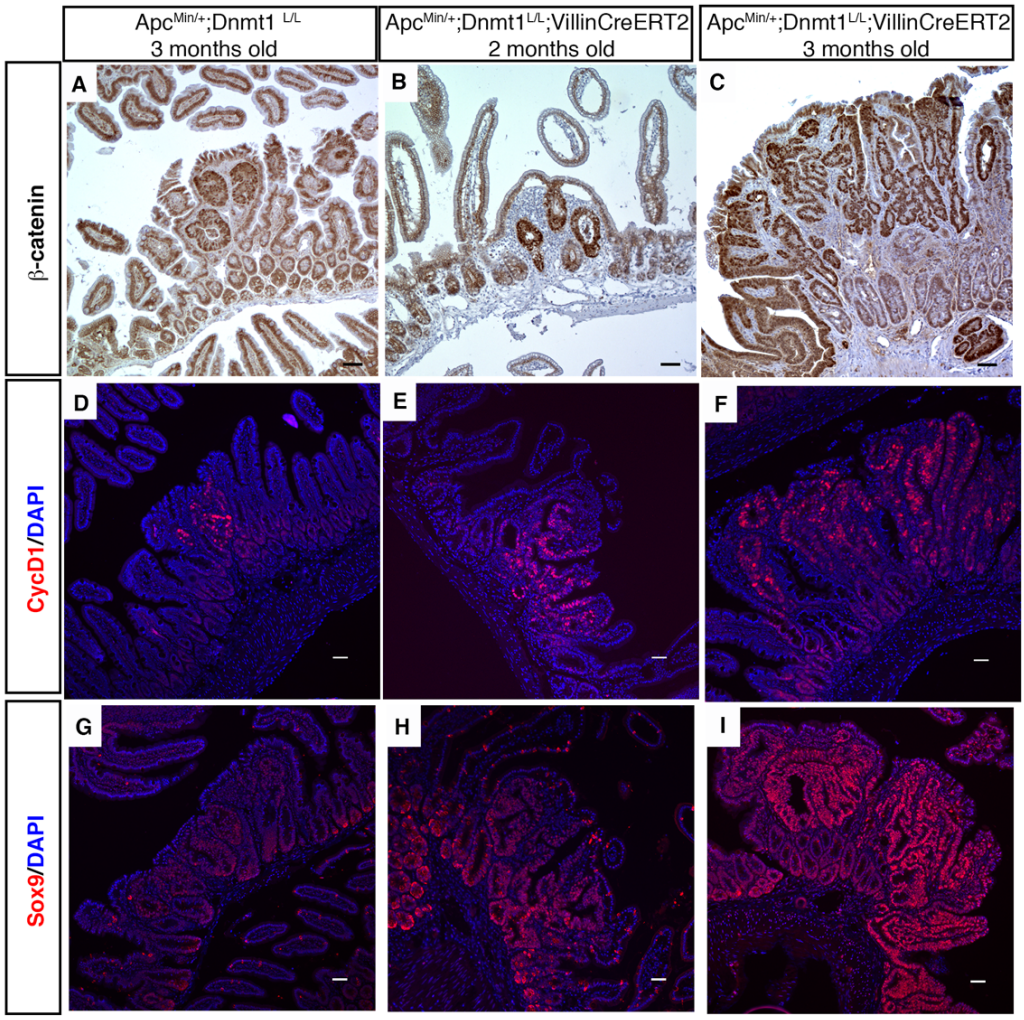

Figure 4.4. *Dnmt1*-deficient tumors display increased Wnt signaling.

Figure 4.4. *Dnmt1*-deficient tumors display increased Wnt signaling.

The small intestine was collected from three-month and two-month old *Apc*$^{Min/+}$*;Dnmt1*$^{loxP/loxP}$*;VillinCreERT2* mutants and *Apc*$^{Min/+}$*;Dnmt1*$^{loxP/loxP}$ controls, which were tamoxifen-treated at four weeks of age. Immunostaining for several Wnt targets was performed to characterize Wnt pathway activation in mutant compared to control tumors. At two months, *Dnmt1*-deficient tumors already exhibit increased Wnt signaling in tumors (B,E,F) relative to control tumors at three months (A,D,G).

(A-C) Immunohistochemical staining reveals increased nuclear β-catenin in three-month old *Apc*$^{Min/+}$*;Dnmt1*$^{loxP/loxP}$*;VillinCreERT2* mutant (C) compared to *Apc*$^{Min/+}$*;Dnmt1*$^{loxP/loxP}$ control small intestine (A). *Apc*$^{Min/+}$*;Dnmt1*$^{loxP/loxP}$*;VillinCreERT2* mutant tumors at two months of age (B) show similar levels of nuclear β-catenin compared to *Apc*$^{Min/+}$*;Dnmt1*$^{loxP/loxP}$ (A) tumors at three months.

(D-I) Wnt signaling target CycD1 is increased in three-month old *Dnmt1*-deficient tumors (F) relative to control tumors (D). Similarly sized tumors express comparable levels of CycD1 (compare D to E). CycD1 (red), DAPI (blue).

(G-I) Three-month old *Dnmt1*-deficient tumors exhibit increased Sox9 levels (I) compared to control tumors (G). Similarly sized tumors display comparable levels of Sox9 (compare G to H). Sox9 (red), DAPI (blue). Scale bars are 50μm.

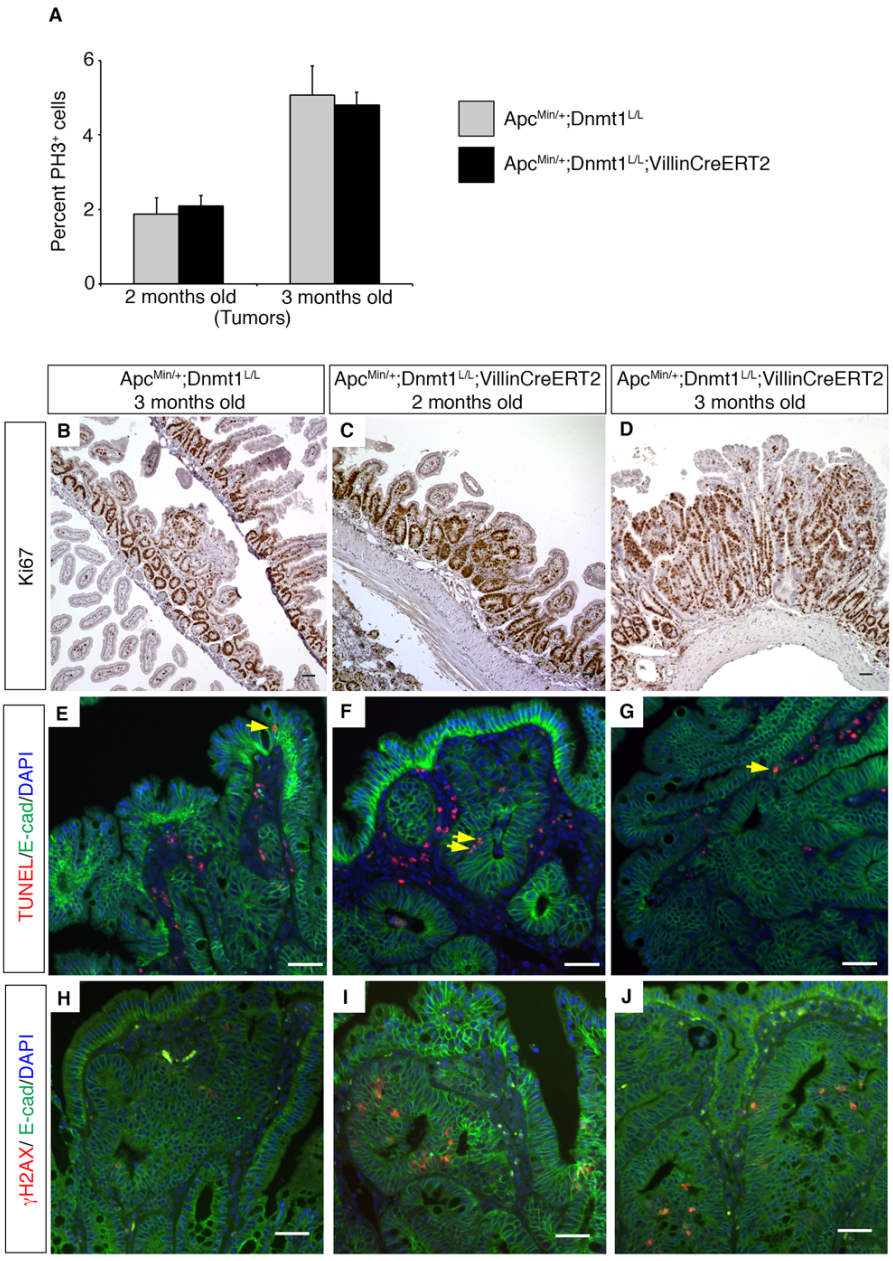

Figure 4.5. Loss of *Dnmt1* affects genome stability, but not tumor cell proliferation.

Figure 4.5. Loss of *Dnmt1* affects genome stability, but not tumor cell proliferation.

(A) Percentage of cells in mitosis was determined by immunostaining and counting of the phospho-H3 positive ($pH3^+$) nuclei in tumors at two months and three months of age. At both time points, tamoxifen-treated $Apc^{Min/+};Dnmt1^{loxP/loxP};VillinCreERT2$ and $Apc^{Min/+};Dnmt1^{loxP/loxP}$ displayed comparable percentages of $pH3^+$ cells, indicating that loss of *Dnmt1* does not affect mitotic rates in the small intestine.

(B-D) Cell proliferation, as visualized by immunohistochemical staining of Ki67, is similar in tamoxifen-treated $Apc^{Min/+};Dnmt1^{loxP/loxP};VillinCreERT2$ (C,D) compared to $Apc^{Min/+};Dnmt1^{loxP/loxP}$ (B) small intestine.

(E-G) Neoplastic epithelia contain TUNEL-positive cells at low frequency (yellow arrows) in $Apc^{Min/+};Dnmt1^{loxP/loxP}$ mice (E), which is unchanged in tamoxifen-treated $Apc^{Min/+};Dnmt1^{loxP/loxP};VillinCreERT2$ mice (F,G). TUNEL (red), E-cadherin (green), DAPI (blue).

(H-J) The number of neoplastic epithelial cells positive for DNA double-strand breaks, as visualized by immunofluorescence staining of γH2AX, is increased in tamoxifen-treated $Apc^{Min/+};Dnmt1^{loxP/loxP};VillinCreERT2$ mice (I,J) compared to $Apc^{Min/+};Dnmt1^{loxP/loxP}$ (H) small intestines. This is not due to accelerated growth, because similarly sized tumors also show increased γH2AX in $Apc^{Min/+};Dnmt1^{loxP/loxP};VillinCreERT2$ (I) compared to $Apc^{Min/+};Dnmt1^{loxP/loxP}$ (H). All scale bars: 50μm.

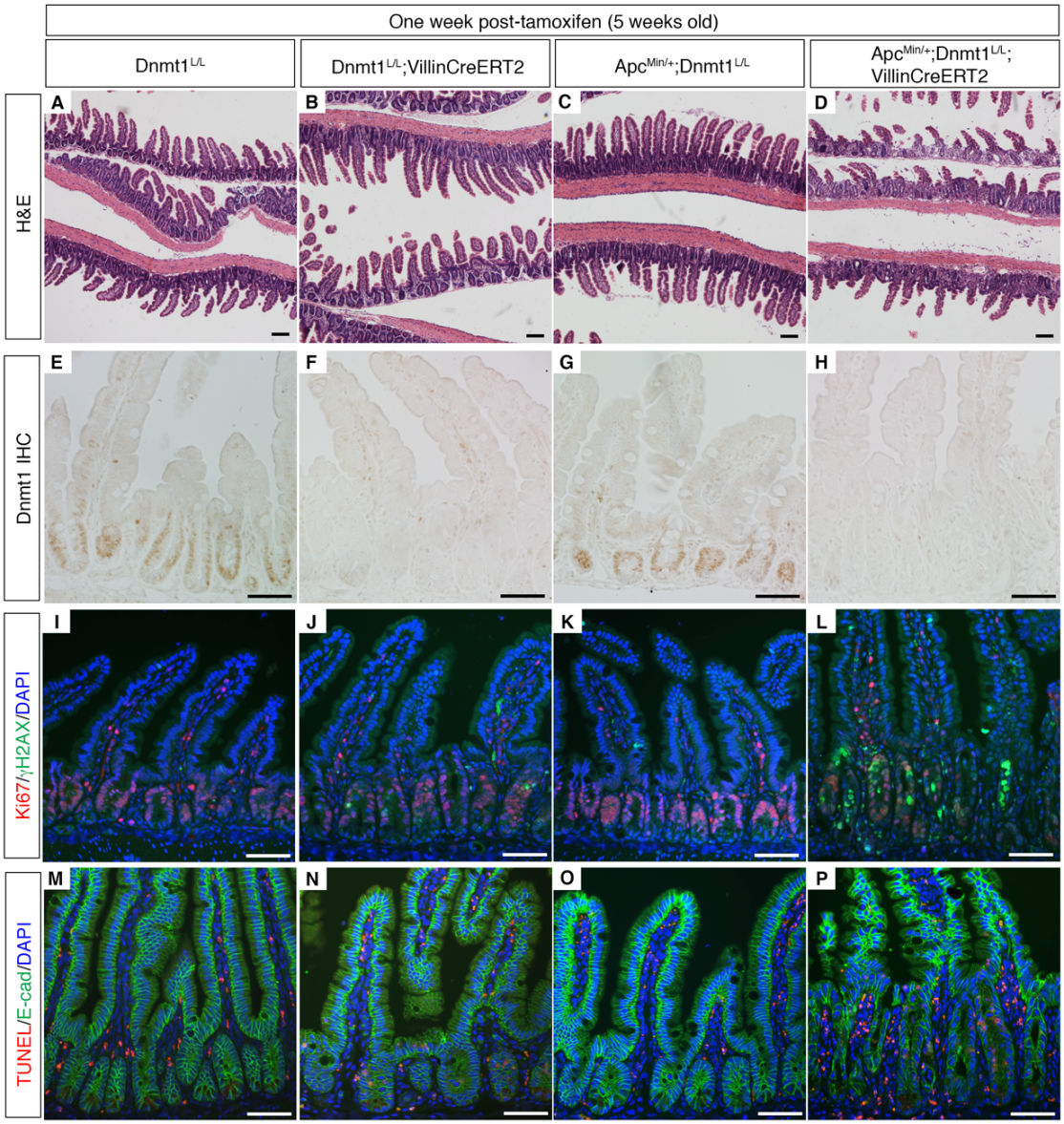

Figure 4.6. *Dnmt1* deletion in *Apc*$^{Min/+}$ mice causes massive epithelial remodeling within one week.

Figure 4.6. *Dnmt1* deletion in *Apc*$^{Min/+}$ mice causes massive epithelial remodeling within one week.

Dnmt1$^{loxP/loxP}$ (A), *Dnmt1*$^{loxP/loxP}$*;VillinCreERT2* (B), *Apc*$^{Min/+}$*;Dnmt1*$^{loxP/loxP}$ (C), and *Apc*$^{Min/+}$*;Dnmt1*$^{loxP/loxP}$*;VillinCreERT2* (D) intestinal epithelium one week after tamoxifen injection. Hematoxylin and Eosin staining demonstrates increased severity of the *Dnmt1* mutant phenotype on the *Apc*$^{Min/+}$ background (D) versus control (B).

(E-H) Immunohistochemistry for Dnmt1 confirms loss of protein in both tamoxifen-treated *Dnmt1*$^{loxP/loxP}$*;VillinCreERT2* (F) and *Apc*$^{Min/+}$*;Dnmt1*$^{loxP/loxP}$*;VillinCreERT2* mutants (H).

(I-L) Co-staining for Ki67 (red), a marker of proliferation, and γH2AX (green), which marks DNA double-stranded breaks. Both control genotypes (I,K) have minimal γH2AX foci. *Dnmt1*$^{loxP/loxP}$*;VillinCreERT2* mutants have increased proliferation (J), as previously reported (Sheaffer, Kim et al. 2014). *Apc*$^{Min/+}$*;Dnmt1*$^{loxP/loxP}$*;VillinCreERT2* mutants (L) have regions with decreased levels of Ki67 and display an increased number of γH2AX foci, reflecting elevated genomic instability immediately following *Dnmt1* ablation. See also Figure S1.

(M-P) TUNEL staining to detect apoptosis (red) with E-cadherin (green) to outline the epithelium. Controls display no apoptotic nuclei in crypt cells (M,O). Both *Dnmt1*-mutant genotypes (N,P) display increased apoptosis, although there are noticeably more apoptotic nuclei in *Apc*$^{Min/+}$*;Dnmt1*$^{loxP/loxP}$*;VillinCreERT2* crypts (P) compared to *Dnmt1*$^{loxP/loxP}$*;VillinCreERT2* crypts (N).

Scale bars in (A-D) are 100μm. Scale bars in (E-P) are 50μm.

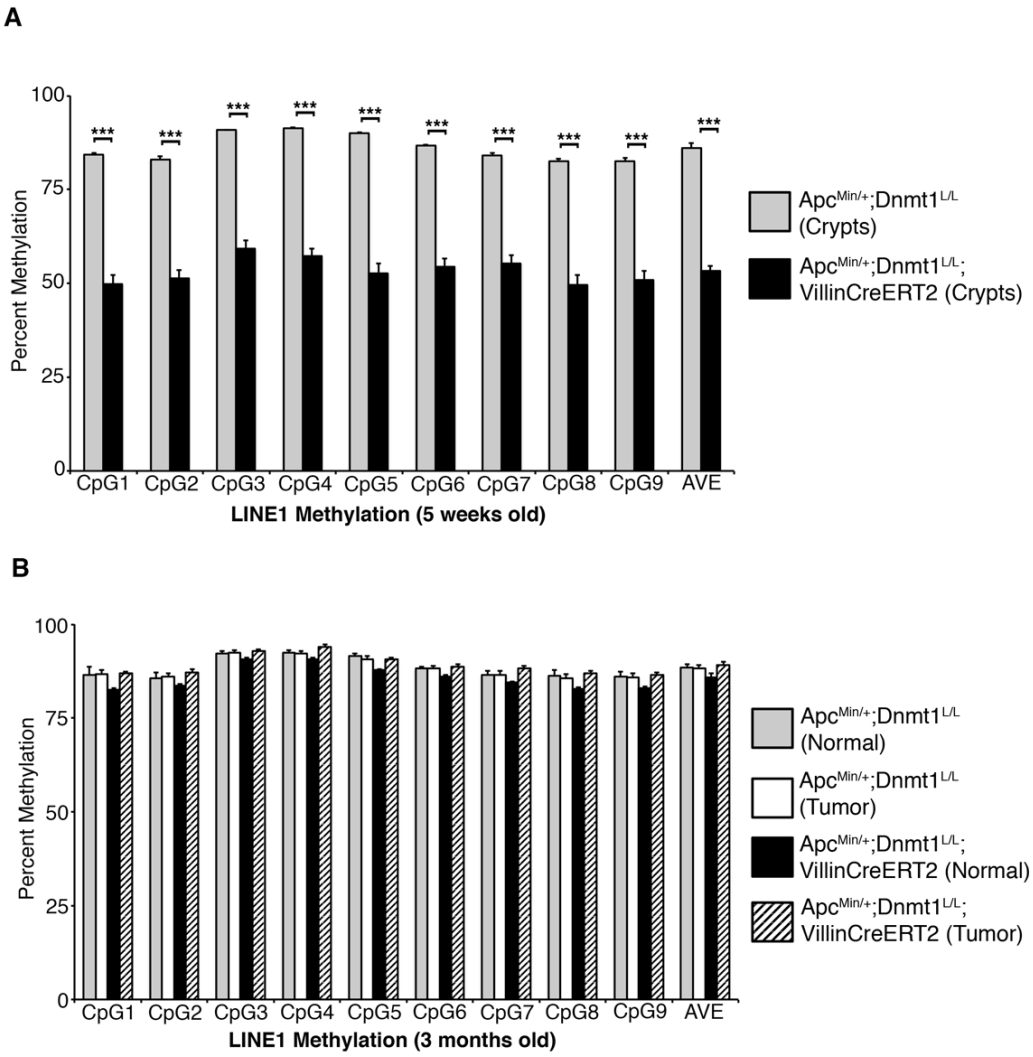

Figure 4.7. DNA methylation dynamics after acute *Dnmt1* deletion.

Figure 4.7. DNA methylation dynamics after acute *Dnmt1* deletion.

Apc$^{Min/+}$*;Dnmt1*$^{loxP/loxP}$*;VillinCreERT2* mice and *Apc*$^{Min/+}$*;Dnmt1*$^{loxP/loxP}$ controls were tamoxifen-treated at four weeks of age. The intestines were harvested at five weeks (A) or three months (B) of age, corresponding to one week and two months post-tamoxifen treatment, respectively. Crypt epithelium (A,B) or visible adenomas (B) were isolated by laser capture microdissection. Targeted bisulfite sequencing of nine CpGs in the LINE1 repetitive elements was performed to estimate global methylation levels.

(A) Five-week old *Apc*$^{Min/+}$*;Dnmt1*$^{loxP/loxP}$*;VillinCreERT2* intestinal crypts exhibit significantly reduced LINE1 methylation levels compared to *Dnmt1*$^{loxP/loxP}$*;Apc*$^{Min/+}$ control crypts (n=3-4 per group).

(B) No difference in methylation at the LINE elements was detected in normal and tumor cells from three-month old *Apc*$^{Min/+}$*;Dnmt1*$^{loxP/loxP}$ and *Apc*$^{Min/+}$*;Dnmt1*$^{loxP/loxP}$*; VillinCreERT2* mice treated with tamoxifen at four weeks of age (n=3-11 per group).

For all graphs, data are presented as average±SEM. ***P<0.001 by two-tailed Student's t-test.

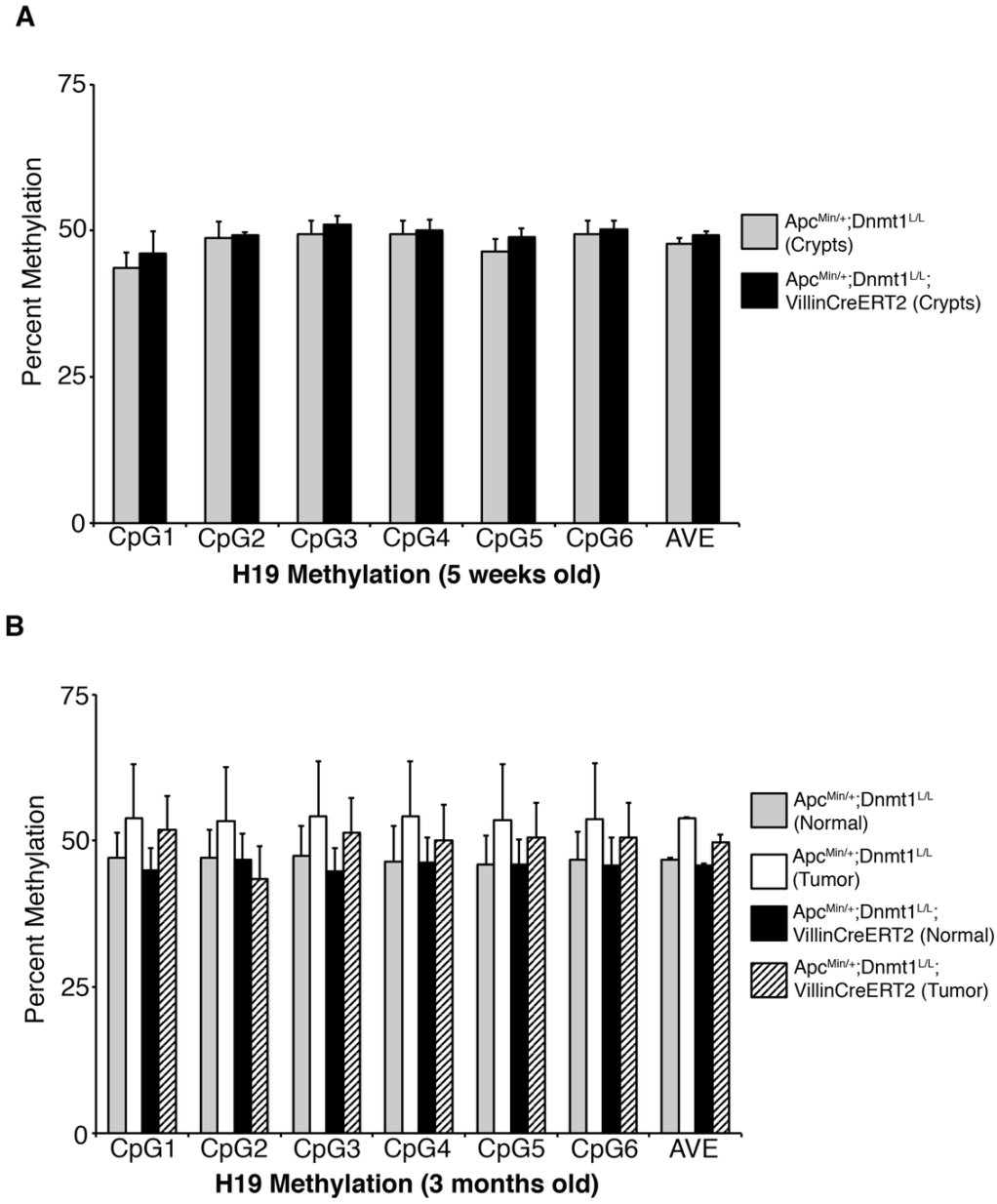

Figure 4.8. Methylation profiling of *H19* ICR following *Dnmt1* ablation.

Figure 4.8. Methylation profiling of *H19* ICR following *Dnmt1* ablation.

Apc$^{Min/+}$*;Dnmt1*$^{loxP/loxP}$*;VillinCreERT2* mice and *Apc*$^{Min/+}$*;Dnmt1*$^{loxP/loxP}$ controls were tamoxifen-treated at four weeks of age. Intestine was harvested at five weeks (A) or three months (B) of age, corresponding to one week and two months post-tamoxifen treatment, respectively. Crypt epithelium or visible adenomas were isolated by laser capture microdissection. Targeted bisulfite sequencing of six CpGs in the *H19* imprinting control region (ICR) was performed to estimate maintenance methylation.

(A) *H19* ICR methylation is preserved in five-week old *Dnmt1*-mutant *Apc*$^{Min/+}$ crypts, similar to *Dnmt1*$^{loxP/loxP}$*;Apc*$^{Min/+}$ control crypts. Average±SEM; (n=3-4).

(B) No change in *H19* ICR methylation is detected in normal and tumor cells from tamoxifen-treated, three-month old *Apc*$^{Min/+}$*;Dnmt1*$^{loxP/loxP}$ and *Apc*$^{Min/+}$*;Dnmt1*$^{loxP/loxP}$*;VillinCreERT2* mice. Average±SEM; (n=3-11).

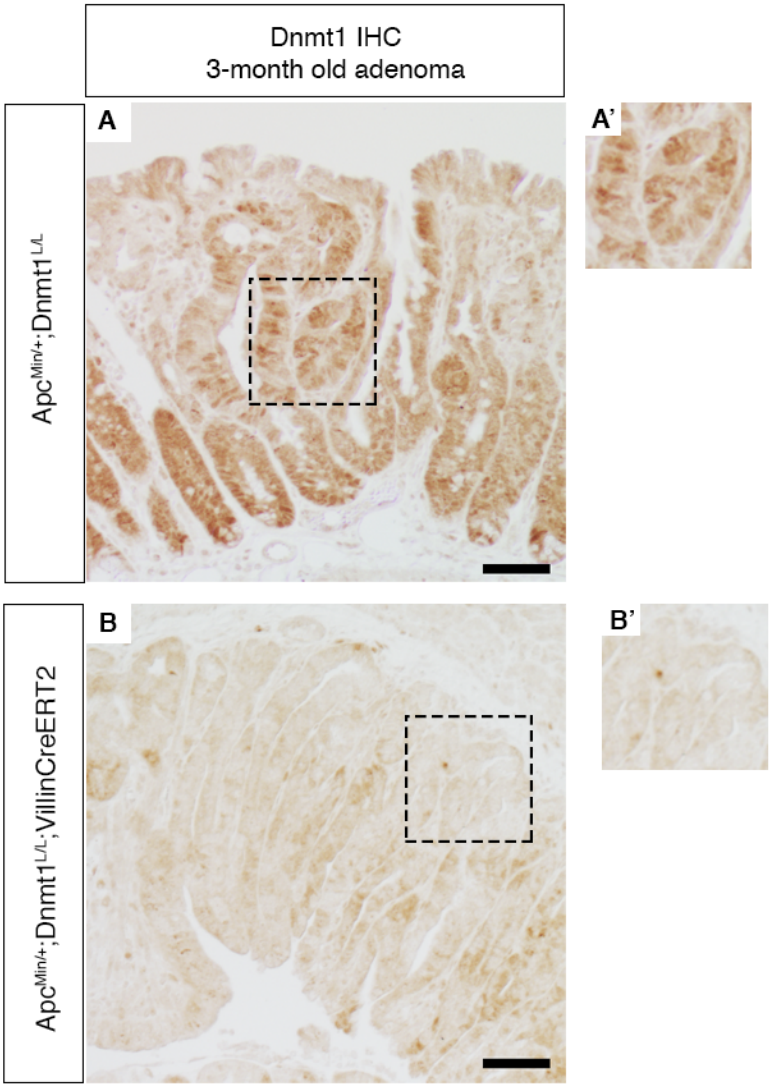

Figure 4.9. *Dnmt1*-deficient tumors do not express Dnmt1 protein.

Figure 4.9. *Dnmt1*-deficient tumors do not express Dnmt1 protein.

Apc$^{Min/+}$*;Dnmt1*$^{loxP/loxP}$*;VillinCreERT2* and *Apc*$^{Min/+}$*;Dnmt1*$^{loxP/loxP}$ mice were tamoxifen-treated at four weeks of age. Dnmt1 immunohistochemistry was performed in three-month old intestines to confirm ablation of *Dnmt1* in *Apc*$^{Min/+}$*;Dnmt1*$^{loxP/loxP}$*;VillinCreERT2* intestinal tumors (B and B'), relative to controls (A and A'). Dnmt1 is expressed in control three-month old adenomas (A, see inset in A'), and is not present in age-matched Dnmt1-deficient adenomas (B, see inset B'). Scale bars are 50μm.

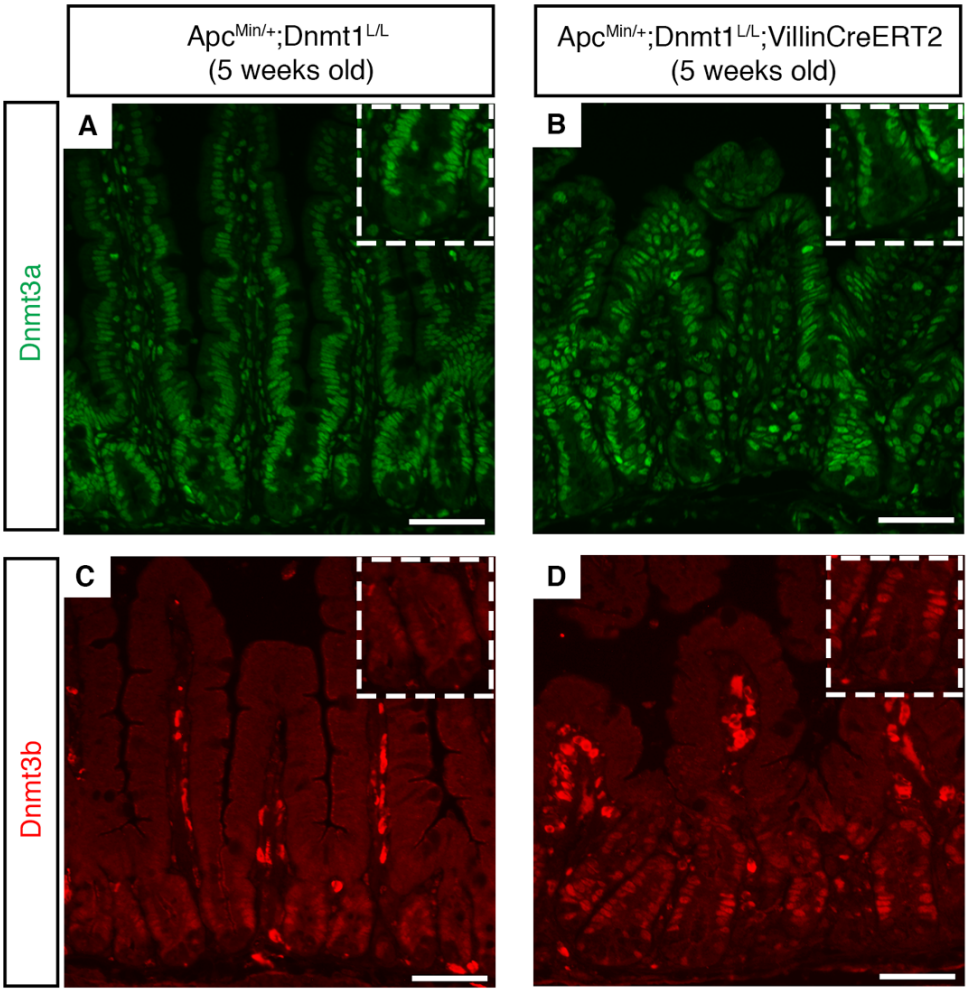

Figure 4.10. Dnmt3b is upregulated one week following *Dnmt1* ablation.

Figure 4.10. Dnmt3b is upregulated one week following *Dnmt1* ablation.

Dnmt3a (A,B) and Dnmt3b (C,D) immunofluorescent staining in *Apc*$^{Min/+}$*;Dnmt1*$^{loxP/loxP}$*;VillinCreERT2* mutant and *Apc*$^{Min/+}$*;Dnmt1*$^{loxP/loxP}$ control intestinal epithelium at one week post-tamoxifen injection. Inset shows 20X image of stained crypt epithelium. Dnmt3a levels in mutants (B) are similar to controls (A). Dnmt3b protein levels are increased in mutant crypts (D) compared to control crypts (C). Scale bars are 50μm.

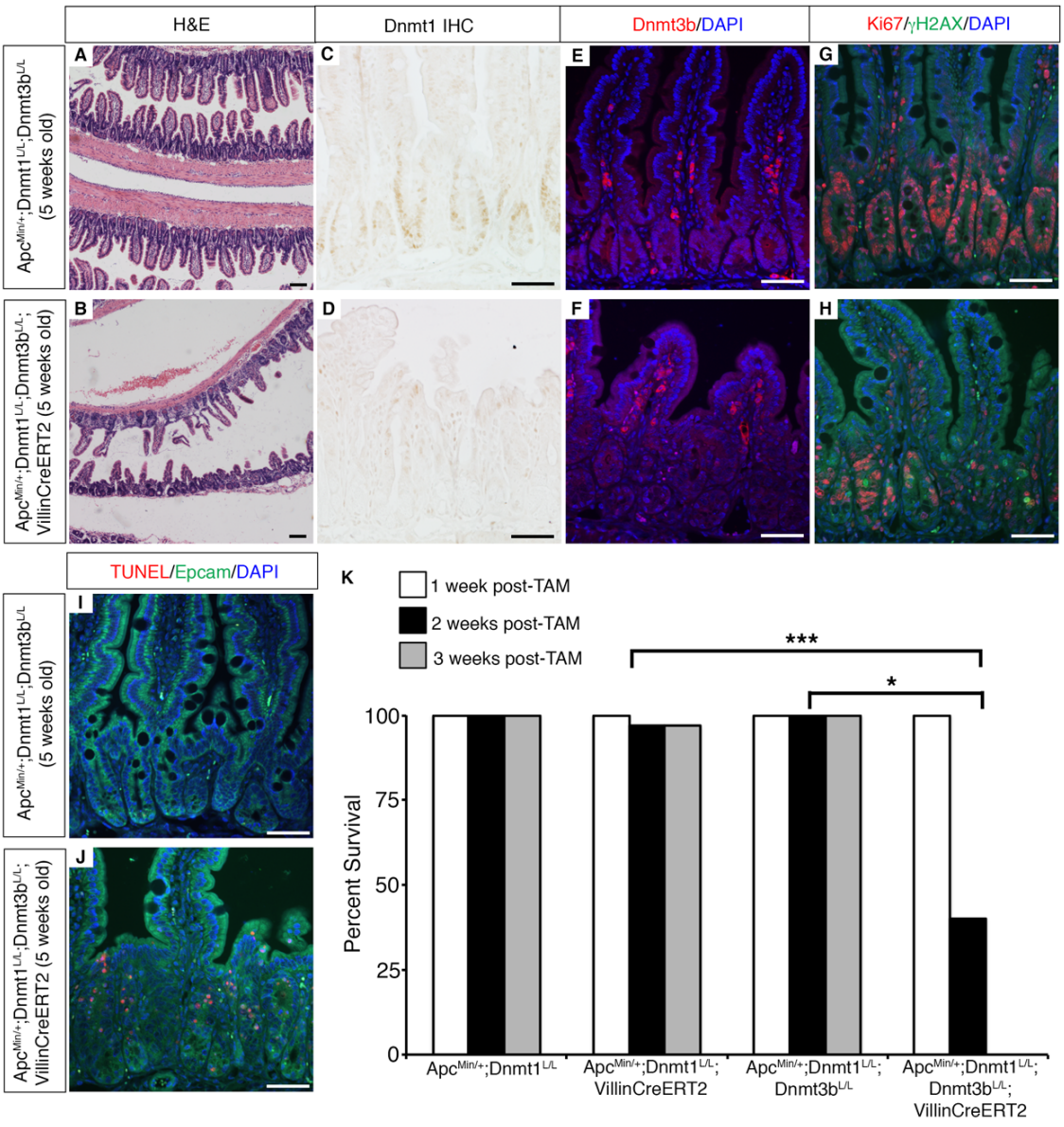

Figure 4.11. Dnmt3b is required to maintain DNA methylation and epithelial integrity in the absence of Dnmt1.

Figure 4.11. Dnmt3b is required to maintain DNA methylation and epithelial integrity in the absence of Dnmt1.

Loss of *Dnmt1* and *Dnmt3b* in *Apc*$^{Min/+}$ mice causes increased apoptosis and is not compatible with life.

(A,B) Hematoxylin and eosin staining reveals increased epithelial disorganization one week after tamoxifen injection in *Apc*$^{Min/+}$*;Dnmt1*$^{loxP/loxP}$*;Dnmt3b*$^{loxP/loxP}$*;VillinCreERT2* mutants compared to *Apc*$^{Min/+}$*;Dnmt1*$^{loxP/loxP}$*;Dnmt3b*$^{loxP/loxP}$ controls.

(C,D) Dnmt1 and (E,F) Dnmt3b protein staining confirms ablation of respective proteins in the intestinal epithelium of five-week old *Apc*$^{Min/+}$*;Dnmt1*$^{loxP/loxP}$*;Dnmt3b*$^{loxP/loxP}$*;VillinCreERT2* mutants.

(G,H) Co-staining for Ki67 (red), a marker of proliferation, and γH2AX (green), which marks DNA double-strand breaks. *Apc*$^{Min/+}$*;Dnmt1;Dnmt3b;VillinCreERT2* mutants (H) have decreased Ki67 staining and increased γH2AX foci compared to controls (G).

(I,J) Costaining of TUNEL (red), to mark apoptotic nuclei, and Epcam (green) to outline the epithelium. *Apc*$^{Min/+}$*;Dnmt1;Dnmt3b;VillinCreERT2* mutants (J) have increased apoptosis compared to controls (I). Scale bars are 50μm.

(K) Dnmt1; Dnmt3b deficient *Apc*$^{Min/+}$ mice are not viable. Percent survival of mice of the indicated genotypes following tamoxifen injection (TAM) at four weeks of age. **P*<0.05, ****P*<0.00001, by log rank test (n≥7 per group).

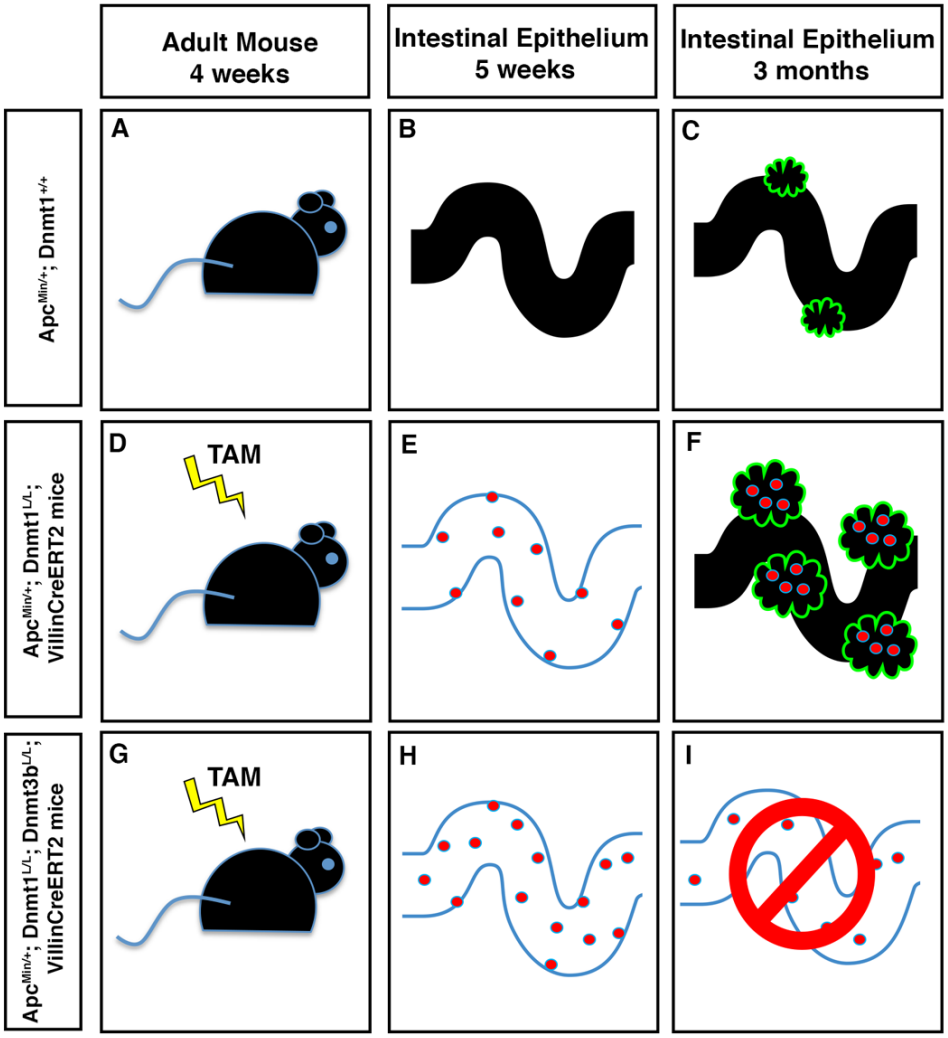

Figure 4.12. Functional analyses of DNA methylation in *Apc*$^{Min/+}$ cancer development.

Figure 4.12. Functional analyses of DNA methylation in *Apc*$^{Min/+}$ cancer development.

Mice and intestinal epithelium in (A-D,F,G) are shown in black, representing normal DNA methylation levels. The intestinal epithelium in (E,H) is white, indicating acute hypomethylation.

(A-C) *Apc*$^{Min/+}$*;Dnmt1*$^{loxP/loxP}$ control mice maintain DNA methylation in all tissues, including the intestinal epithelium. At five weeks, mice display normal DNA methylation levels, and no tumor formation (B). At three months of age, *Apc*$^{Min/+}$*;Dnmt1*$^{loxP/loxP}$ intestine has preserved DNA methylation, and harbors multiple adenomas (C, adenomas are outlined in green).

(D-F) In the current study, intestine-specific ablation of *Dnmt1* was induced in four-week old *Apc*$^{Min/+}$*;Dnmt1*$^{loxP/loxP}$*;VillinCreERT2* mice (D). Mice displayed acute global hypomethylation and increased genome instability in the intestine at five weeks of age (E, red circles indicate DNA damage). At three months of age, mice had recovered global DNA methylation, but exhibited significantly more tumors compared to controls (F, large adenomas outlined in green). These tumors also displayed increased genomic instability (F), distinct from control tumors at the same time point (C).

(G-I) Loss of both *Dnmt3b* and *Dnmt1* in the adult intestinal epithelium was induced using *Apc*$^{Min/+}$*;Dnmt1*$^{loxP/loxP}$*;Dnmt3b*$^{loxP/loxP}$*;VillinCreERT2* mice (G). Five-week old mice displayed severe hypomethylation and genome instability (H). Mice failed to recover and died within 21 days of *Dnmt1*/*Dnmt3b* ablation (I).

Chapter 5

Conclusions and Future Directions

Summary and Conclusions

I have shown that Dnmt1 is an essential regulator of genomic stability in the murine intestinal epithelium. Loss of *Dnmt1* in the neonatal intestine causes hypomethylation, irreparable DNA damage, and apoptosis of progenitor cells. As a result, these mice do not compete well for maternal resources, and die before weaning. *Dnmt1* ablation in the adult intestinal epithelium also results in acute DNA hypomethylation and DNA damage. However, the adult $Apc^{Min/+}$ intestine compensates for these aberrations by increased Dnmt3b activity, and recovers normal DNA methylation levels within two months of *Dnmt1* ablation. These results have implications for several fields of research, which I outline below.

Neonatal intestinal progenitors and adult intestinal stem cells are distinct cell populations, with differing requirements for Dnmt1

I have demonstrated that Dnmt1 is required to varying degrees in the intestinal epithelium, dependent on the stage of intestinal maturity. *Dnmt1* is required to maintain progenitor cells in the neonatal intestinal epithelium, and loss of *Dnmt1* during intestinal development results in perinatal lethality. *Dnmt1* ablation in the adult intestinal epithelium also results in acute DNA hypomethylation and DNA damage, but is not essential for intestinal epithelial survival, as reported previously (Sheaffer, Kim et al. 2014). Interestingly, the adult intestine recovers DNA methylation following the immediate effects of Dnmt1 deletion, indicating a distinct difference in the requirement of Dnmt1 in the developing, in comparison to mature, intestinal epithelium. The distinct adult and perinatal *Dnmt1*-mutant phenotypes are not an artifact of differential *Cre* transgene activity, because tamoxifen-treated $Dnmt1^{loxP/loxP}$*;VillinCreERT2* neonatal mice also exhibit decreased viability (data not shown). Therefore, these data indicate important differences in proliferative processes in the developing versus adult intestinal epithelium.

It is important to consider that the murine neonatal intestine is comparable to ~10 week-old human fetal intestine (Montgomery, Mulberg et al. 1999). Thus, the mouse intestine at birth is not fully mature, and the intestinal stem cell niche is not equivalent to the crypts found in adult

intestinal epithelium. Indeed, I discovered that the rate of proliferation in the perinatal intestine is dramatically increased compared to adult intestinal epithelium, similar to that reported by other groups (Figure 3.13; (Itzkovitz, Blat et al. 2012)). Wnt signaling, which is required to maintain proliferation in adult intestinal epithelial crypts, is not necessary in the developing intestine until after nascent villus formation at E15.5 (Korinek, Barker et al. 1998). Recent studies of intestinal organoid cultures derived from late-gestation and neonatal mouse intestine have further supported the notion that intervillus progenitors in the neonate are distinct from the crypt-based-columnar stem cell population in the adult (Fordham, Yui et al. 2013, Mustata, Vasile et al. 2013). *In vitro*, mature crypts form organoids with budding outgrowths that are anomalous to intestinal crypts *in vivo*. Although progenitors from embryonic and neonatal intestinal epithelium also form budding organoids *in vitro*, nearly half of late gestation intestinal progenitors form spheroids (Fordham, Yui et al. 2013, Mustata, Vasile et al. 2013). Spheroids are small cysts of proliferative intestinal cells, which do not produce buds during prolonged culture. Expression of Wnt signaling factors correlates with progenitor maturation and budding-organoid formation: in contrast to organoids derived from adult crypts, progenitors isolated from embryonic stages prior to E18.5 express low levels of Wnt, and form spheroids in culture (Fordham, Yui et al. 2013). Differing requirements for Wnt signaling during development indicate distinct regulation of proliferation and progenitor cell expression programs.

The differential requirement for Dnmt1 and DNA methylation during development relative to fully mature organs may be a global event not limited to the intestinal epithelium. In the developing pancreas, Dnmt1 is required to prevent p53-dependent apoptosis (Georgia et al), whereas in the mature pancreas, Dnmt1-mediated methylation is required to maintain endocrine β-cell identity (Dhawan et al Dev Cell 2011). It will be interesting to determine the requirements for Dnmt1 in other organs, both during development and in the adult organ, which will help elucidate the mechanisms underlying tissue-specific epigenetic regulation.

Dnmt1 and DNA methylation are essential for genomic stability in the intestinal epithelium

My results indicate that loss of *Dnmt1* in the perinatal, adult, and cancer-prone *Apc*$^{Min/+}$ intestinal epithelia causes an increase in double strand breaks, demonstrating that Dnmt1 is essential for maintaining genome integrity in the small intestine. Deletion of *Dnmt1* induces hypomethylation and genomic instability in various cell types *in vitro*, including mouse ES cells, mouse embryonic fibroblasts, and human HCT116 colorectal cancer cell lines. *Dnmt1* hypomorphic mice exhibit increased chromosomal duplications and rearrangements, and develop invasive T-cell lymphomas at approximately four months of age. It is important to note that these effects are not restricted to DNMT1 deficiency. Loss of *Dnmt3b* also induces hypomethylation and chromosomal instability in mouse embryonic fibroblasts (Dodge, Okano et al. 2005), suggesting that both Dnmt1 and Dnmt3b are crucial for maintaining DNA methylation and preserving genome integrity. Mutations in *DNMT3B* underlie Immunodeficiency, Centromeric region instability, and Facial anomalies (ICF) syndrome and cause hypomethylation at centromere-adjacent heterochromatin, leading to chromosomal translocations and deletions (Hansen, Wijmenga et al. 1999, Xu, Bestor et al. 1999). My studies corroborate these findings, further establishing that DNA methylation is crucial to maintaining genomic stability.

Chromosomal instability also correlates with DNA hypomethylation in sporadic human colorectal cancer (CRC) (Lengauer, Kinzler et al. 1997, Rodriguez, Frigola et al. 2006). Although hypomethylation occurs early in human CRC development (Feinberg and Vogelstein 1983, Gama-Sosa, Slagel et al. 1983, Goelz, Vogelstein et al. 1985, Feinberg, Gehrke et al. 1988), it is largely unknown to what extent loss of DNA methylation contributes to tumor progression. The majority of DNA methylation CRC research has focused on the hypermethylation of tumor suppressor gene promoters, which is known to cause decreased expression of genes important for mismatch repair and cell cycle control (Esteller 2005). These early studies suggested that tumor suppressor gene hypermethylation is a key step in tumor progression, in both human CRC and relevant mouse models (Esteller, Corn et al. 2001, Eads, Nickel et al. 2002).

The *Apc*$^{Min/+}$ mouse recapitulates the human familial adenomatous polyposis (FAP) syndrome (Moser, Pitot et al. 1990, Su, Kinzler et al. 1992), and is commonly utilized as an *in vivo* model for human CRC. FAP patients and *Apc*$^{Min/+}$ mice have only one functional copy of the *Apc* gene. Apc is a critical component of the cytoplasmic β-catenin destruction complex, and loss of Apc allows increased nuclear β-catenin localization, Wnt pathway stimulation, and uncontrolled cell proliferation (Pinto, Gregorieff et al. 2003, Sansom, Reed et al. 2004). Thus, loss of heterozygosity (LOH) at the *Apc* locus triggers tumor development (Su, Kinzler et al. 1992, Luongo, Moser et al. 1994). *Apc*$^{Min/+}$ mice develop multiple tumors in the small intestine by three months of age (Moser, Pitot et al. 1990, Su, Kinzler et al. 1992), and have served as an efficient model for *in vivo* studies of intestinal tumor development and progression.

Several studies have employed global hypomorphic *Dnmt1* alleles in *Apc*$^{Min/+}$ mice, and report that Dnmt1 is required for tumor progression in the *Apc*$^{Min/+}$ model (Laird, Jackson-Grusby et al. 1995, Cormier and Dove 2000, Eads, Nickel et al. 2002, Trasler, Deng et al. 2003, Yamada, Jackson-Grusby et al. 2005). These reports are ultimately inconclusive due to possible intestine-independent or developmental effects of decreased Dnmt1 expression. Indeed, my own work demonstrates that Dnmt1 is essential for maintenance of perinatal intestinal progenitor cells. Our lab also found that global loss of the mesenchymal transcription factor Foxl1 increases intestinal tumor load in *Apc*$^{Min/+}$ mice (Perreault, Sackett et al. 2005), demonstrating that *Apc*$^{Min/+}$ tumor multiplicity is influenced by factors not expressed in the intestinal epithelium. The reduced tumorigenesis phenotypes previously described in *Dnmt1*-hypomorphic *Apc*$^{Min/+}$ mice are likely due to decreased proliferation of progenitor cells in the neonatal intestine, which would provide fewer opportunities for tumor initiation. Alternatively, increased genomic instability in these mice from early development onward may actually prohibit tumor progression via increased levels of apoptosis in damaged cell populations (Halazonetis, Gorgoulis et al. 2008). In the adult intestinal epithelium, inducible deletion of *Dnmt1* causes acute hypomethylation of intestinal stem cell genes and two-fold expansion of the proliferative crypt zone (Sheaffer, Kim et al. 2014), which suggests that hypomethylation promotes proliferative processes in the intestinal epithelium.

Intestinal tumor progression could be due in part to the incomplete differentiation caused by hypomethylation, and ablation of *Dnmt1* may exacerbate this process.

To directly determine the function of epithelial Dnmt1 in intestinal tumorigenesis, I employed an intestine-specific, inducible ablation model to delete *Dnmt1* in $Apc^{Min/+}$ mice. In stark contrast to the previously published studies, I observed increased tumorigenesis two months following intestinal epithelial-specific ablation of *Dnmt1* in four-week old $Apc^{Min/+}$ mice. As predicted by my preceding work, *Dnmt1*-ablated tumors displayed multiple γH2AX foci, a marker of DNA double-strand breaks and genomic instability. I also noted increased microadenoma formation, indicating an accelerated rate of tumor initiation, although the proliferation rate of neoplastic cells was not altered relative to controls. To determine the underlying mechanism of this increased tumor load, I analyzed mice one week following *Dnmt1* deletion, and observed global hypomethylation and increased levels of DNA damage and crypt cell apoptosis relative to controls. $Apc^{Min/+}$ mice have weakened responses to stressors, such as irradiation (Tao, Tang et al. 2015), and I show that loss of *Dnmt1* in $Apc^{Min/+}$ mice precipitates massive epithelial damage and remodeling. Previously, Yamada and colleagues reported that *Dnmt1*-hypomorphic $Apc^{Min/+}$ mice displayed an increased number of microadenomas (2005). They concluded that loss of *Dnmt1* augmented LOH at the *Apc* locus, but did not provide a satisfying mechanism to explain this phenotype. I propose that the genomic instability induced following loss of *Dnmt1* increases LOH, resulting in accelerated tumorigenesis and ultimately larger tumors.

My results indicate that hypomethylation is a strong instigator of tumor development, as hypomethylation causes genomic instability, driving accelerated LOH at the *Apc* locus and increased tumorigenesis. As global hypomethylation correlates with chromosomal instability in CRC (Lengauer, Kinzler et al. 1997, Rodriguez, Frigola et al. 2006), and loss of Dnmt1 leads to increased chromosomal translocations and instability in several contexts (discussed above), it is possible that early genomic hypomethylation induces genomic instability. Thus, loss of Dnmt1 could contribute to the accumulation of multiple mutations during development from adenoma to carcinoma. Future work will determine the precise function of DNA hypomethylation in early tumor

formation, using both *in vivo* mouse models and patient-derived *in vitro* organoids. The CRISPR-Cas9 genome editing technology has been optimized for human intestinal organoid culture, and was utilized to mutate genes with putative roles in CRC development (Matano, Date et al. 2015). Mutated organoids were engrafted under the kidney capsule in immune-deficient mice to test tumor formation *in vivo* (Matano, Date et al. 2015). These models can be utilized and combined with next-generation sequencing technologies to precisely assess how hypomethylation contributes to genomic instability at different stages of CRC, and if genomic hypomethylation in mouse models has the same effect as in human CRC.

***Dnmt3b can compensate for Dnmt1 in the intestinal epithelium* in vivo**

Strikingly, by two months post-*Dnmt1* ablation, DNA methylation levels at repetitive elements in *Dnmt1*-deficient $Apc^{Min/+}$ tumors and adjacent epithelia were comparable to controls. These results were also confirmed by immunofluorescent staining with a 5-methylcytosine antibody (data not shown). I hypothesized that the *de novo* methyltransferases (Dnmt3a and Dnmt3b) become activated following *Dnmt1* deletion, and are necessary for remethylation of the genome and phenotypic recovery. Indeed, I observed increased Dnmt3b protein levels in *Dnmt1*-deficient $Apc^{Min/+}$ intestinal crypts, relative to $Apc^{Min/+}$ controls. Accordingly, I tested the requirement for Dnmt3b in the survival of $Apc^{Min/+}$;$Dnmt1^{loxP/loxP}$;*VillinCreERT2* tamoxifen-treated mice. Strikingly, when I deleted *Dnmt1* and *Dnmt3b* concurrently in the $Apc^{Min/+}$ intestinal epithelium, these mice were unable to recover, and died within three weeks of tamoxifen administration. Compared to *Dnmt1*-mutant $Apc^{Min/+}$ mice, *Dnmt1;Dnmt3b*-deficient $Apc^{Min/+}$ mice displayed extensive DNA damage and high levels of crypt cell apoptosis. These results clearly demonstrate that Dnmt3b is required to recover and maintain DNA methylation in the intestinal epithelium of *Dnmt1*-deficient $Apc^{Min/+}$ mice. Importantly, my data directly contradict the current DNA methylation dogma, and provide a novel *in vivo* model for Dnmt1 compensation by a *de novo* methyltransferase.

In the field of DNA methylation, it is standard to refer to Dnmt1 as the 'maintenance' methyltransferase, whereas Dnmt3a and Dnmt3b are termed the '*de novo*' methyltransferases. My data strongly suggest that these definitions need to be revised to better reflect the current body of literature. It has been suggested that all replicating somatic cells require Dnmt1 for cell survival (Liao, Karnik et al. 2015). I demonstrate that this is not the case in the mature intestinal epithelium, one of the most highly self-renewing tissues in mammals. My work corroborates *in vitro* evidence showing that loss of Dnmt1 does not lead to complete hypomethylation (Li, Bestor et al. 1992). In some cases, de novo methyltransferases are essential for methylation of certain elements or enhancers, and cannot be compensated for by Dnmt1. For example, hematopoietic stem cells (HSCs) require Dnmt3a for normal self-renewal and differentiation processes (Challen, Sun et al. 2012). Loss of Dnmt3a in HSCs causes demethylation at essential stem cell genes, inducing hyper-proliferation and reducing differentiation rates (Challen, Sun et al. 2012). Dnmt3b also contributes to silencing of germline genes in somatic cells (Velasco, Hubé et al. 2010), and maintenance methylation in ES cells (Liang, Chan et al. 2002, Chen, Ueda et al. 2003). My results provide additional evidence that the *de novo* methyltransferase Dntm3b can perform maintenance methylation *in vivo*.

In the future, to determine by which molecular mechanism Dnmt3b is functioning as a 'maintenance' methyltransferase, I could take advantage of the mouse models described in Chapter 4, in which *Dnmt1* is inducibly ablated in the adult $Apc^{Min/+}$ intestinal epithelium. In these experiments, $Apc^{Min/+};Dnmt1^{loxP/loxP};VillinCreERT2$ (mutant) and $Apc^{Min/+};Dnmt1^{loxP/loxP}$ (control) mice are tamoxifen-treated at four weeks of age to induce *Dnmt1* deletion, and intestinal crypts are harvested one week and two months following tamoxifen injection. These time points enable observation of acute DNA hypomethylation immediately following *Dnmt1* ablation compared to the long-term recovery of DNA methylation, which requires Dnmt3b. Whole-genome bisulfite sequencing from control and mutant intestinal crypts at these two time points following *Dnmt1* deletion would reveal how methylation patterns are decreased and subsequently recovered over time. ChIP-Seq for Dnmt1 and Dnmt3b from these cohorts of mice would allow me to characterize

compensation by Dnm3b in mutant crypts. At one week following *Dnmt1* ablation, I would predict to see loss of Dnmt1 localization in mutant crypts, and normal Dnmt3b distribution, relative to respective ChIP-Seq of control crypts. Following recovery of DNA methylation at two months post *Dnmt1* deletion, I would expect Dnmt3b ChIP-Seq profiles from mutants to mimic Dnmt1 ChIP-Seq profiles in control crypts. To elucidate the mechanism underlying Dnmt3b maintenance methylation, I could perform immunoprecipitation of Dnmt3b, followed by mass spectrometry to identify the protein complexes associated with Dnmt3b in mutant crypts, compared to controls. Mutant crypts may exhibit differential Dnmt3b binding at two months post-*Dnmt1* ablation, compared to control crypts and mutant crypts at one week following tamoxifen treatment. These experiments would define how DNA methylation and Dnmt binding profiles change during the course of DNA methylation loss and recovery, and provide an exciting model to analyze drastic chromatin alterations *in vivo*.

Future Directions: An Epigenetic Map of Intestinal Differentiation

My research has significance in multiple fields. In intestinal biology, my work strongly suggests distinct differences between developing and mature crypts. Understanding crypt development is essential for developing new cancer therapeutics targeting aberrant stem cell activity. Since the $Lgr5^{+}$, CBC stem cell population is touted as being the cell of origin in colorectal cancers (Barker, Ridgway et al. 2009, Merlos-Suárez, Barriga et al. 2011, Barker, van Oudenaarden et al. 2012), understanding how these cells develop within the context of the intestinal crypt is crucial to advancing intestinal disease research. Recent studies employing the organoid mini-gut model system has also shown that embryonic and fetal intestinal progenitors have distinct expression profiles, and form unique cyst-structures in culture (Fordham, Yui et al. 2013, Mustata, Vasile et al. 2013). Use of organoid model systems to enrich for homogenous populations of specific cell types will be useful in studying progenitors during intestinal development, as well as epigenetic changes that occur during mature intestinal differentiation.

The intestinal epithelium is a remarkable system due to the high rate of cell turnover and diversity of cell types within the compact crypt-villus architecture. Indeed, the crypt-villus subunit is an ideal *in vivo* model of adult intestinal stem cell proliferation, renewal, and differentiation. However, to fully understand how epigenetic marks interact and influence this process, we must isolate and characterize multiple marks and transcription factor binding profiles of stem, progenitor, and differentiated cell populations. In the past decade, many markers for specific cell types in the intestinal epithelium have been defined, the vast majority of which label stem cells, such as the $Lgr5^{+}$ crypt-based-columnar stem cells (CBC) (Barker, van Es et al. 2007). Fluorescent-activated cell sorting (FACS) isolation of CBCs is feasible by utilization of knock-in mice, which express fluorescent proteins downstream of stem cell gene promoters (Barker, van Es et al. 2007). This has enabled transcriptome sequencing, whole-genome bisulfite sequencing, and ChIP-Seq analysis of the CBC stem cell population (Merlos-Suárez, Barriga et al. 2011, Kaaij, van de Wetering et al. 2013, Kim, Li et al. 2014, Sheaffer, Kim et al. 2014). Progenitor cell populations can also be isolated using genetic mouse models. For instance, Notch-deficient mice display increased secretory progenitors in crypts; these crypt cells can be isolated using EDTA dissociation methods (Kim, Li et al. 2014). Differentiated cells can be selected for using similar genetic methods, such as loss of *Atoh1* to enrich for enterocytes in villi (Kim, Li et al. 2014).

These methods have been utilized in several reports that describe differences in epigenetic marks and transcription factor binding between CBC, progenitor, and differentiated cells (Verzi, Shin et al. 2013, Kim, Li et al. 2014, Sheaffer, Kim et al. 2014). These studies have indicated a major role for transcription factors, such as Cdx2, in maintenance of chromatin profiles during intestinal differentiation (Verzi, Shin et al. 2013, Kim, Li et al. 2014), and a function for DNA methylation in restricting the proliferative cell region (Sheaffer, Kim et al. 2014). Interestingly, all of these reports found that the most dynamic regions of epigenetic control are associated with enhancer marks, including H3K27ac and H3K4me2. Although many epigenetic marks have been profiled in intestinal cells, a broad study profiling multiple repressive (H3K27me3, H3K9me3) and activating marks (H3K4me3, H3K79me2, H3K36me3) in all of the

intestinal cell sub-populations has not yet been published. A complete and detailed epigenomic map of intestinal differentiation will be an invaluable tool in the study of intestinal development, homeostasis, and disease.

Chapter 6

Bibliography

Aaltonen, L. A., P. Peltomäki, F. S. Leach, P. Sistonen, L. Pylkkänen, J. P. Mecklin, H. Järvinen, S. M. Powell, J. Jen and S. R. Hamilton (1993). "Clues to the pathogenesis of familial colorectal cancer." Science **260**(5109): 812-816.

Ahuja, N., A. L. Mohan, Q. Li, J. M. Stolker, J. G. Herman, S. R. Hamilton, S. B. Baylin and J. P. Issa (1997). "Association between CpG island methylation and microsatellite instability in colorectal cancer." Cancer Res **57**(16): 3370-3374.

Al-Nafussi, A. I. and N. A. Wright (1982). "Cell kinetics in the mouse small intestine during immediate postnatal life." Virchows Arch B Cell Pathol Incl Mol Pathol **40**(1): 51-62.

Allan, L. A., T. Duhig, M. Read and M. Fried (2000). "The p21(WAF1/CIP1) promoter is methylated in Rat-1 cells: stable restoration of p53-dependent p21(WAF1/CIP1) expression after transfection of a genomic clone containing the p21(WAF1/CIP1) gene." Mol Cell Biol **20**(4): 1291-1298.

Ashburner, M., C. A. Ball, J. A. Blake, D. Botstein, H. Butler, J. M. Cherry, A. P. Davis, K. Dolinski, S. S. Dwight, J. T. Eppig, M. A. Harris, D. P. Hill, L. Issel-Tarver, A. Kasarskis, S. Lewis, J. C. Matese, J. E. Richardson, M. Ringwald, G. M. Rubin and G. Sherlock (2000). "Gene ontology: tool for the unification of biology. The Gene Ontology Consortium." Nat Genet **25**(1): 25-29.

Barker, N., R. A. Ridgway, J. H. van Es, M. van de Wetering, H. Begthel, M. van den Born, E. Danenberg, A. R. Clarke, O. J. Sansom and H. Clevers (2009). "Crypt stem cells as the cells-of-origin of intestinal cancer." Nature **457**(7229): 608-611.

Barker, N., J. H. van Es, J. Kuipers, P. Kujala, M. van den Born, M. Cozijnsen, A. Haegebarth, J. Korving, H. Begthel, P. J. Peters and H. Clevers (2007). "Identification of stem cells in small intestine and colon by marker gene Lgr5." Nature **449**(7165): 1003-1007.

Barker, N., A. van Oudenaarden and H. Clevers (2012). "Identifying the stem cell of the intestinal crypt: strategies and pitfalls." Cell Stem Cell **11**(4): 452-460.

Barski, A., S. Cuddapah, K. Cui, T. Y. Roh, D. E. Schones, Z. Wang, G. Wei, I. Chepelev and K. Zhao (2007). "High-resolution profiling of histone methylations in the human genome." Cell **129**(4): 823-837.

Bartolomei, M. S., S. Zemel and S. M. Tilghman (1991). "Parental imprinting of the mouse H19 gene." Nature **351**(6322): 153-155.

Batts, L. E., D. B. Polk, R. N. Dubois and H. Kulessa (2006). "Bmp signaling is required for intestinal growth and morphogenesis." Dev Dyn **235**(6): 1563-1570.

Baubonis, W. and B. Sauer (1993). "Genomic targeting with purified Cre recombinase." Nucleic Acids Res **21**(9): 2025-2029.

Berger, S. L. (2007). "The complex language of chromatin regulation during transcription." Nature **447**(7143): 407-412.

Berger, S. L., T. Kouzarides, R. Shiekhattar and A. Shilatifard (2009). "An operational definition of epigenetics." Genes Dev **23**(7): 781-783.

Berman, B. P., D. J. Weisenberger, J. F. Aman, T. Hinoue, Z. Ramjan, Y. Liu, H. Noushmehr, C. P. Lange, C. M. van Dijk, R. A. Tollenaar, D. Van Den Berg and P. W. Laird (2012). "Regions of focal DNA hypermethylation and long-range hypomethylation in colorectal cancer coincide with nuclear lamina-associated domains." Nat Genet **44**(1): 40-46.

Bevins, C. L. and N. H. Salzman (2011). "Paneth cells, antimicrobial peptides and maintenance of intestinal homeostasis." Nat Rev Microbiol **9**(5): 356-368.

Bilodeau, S., M. H. Kagey, G. M. Frampton, P. B. Rahl and R. A. Young (2009). "SetDB1 contributes to repression of genes encoding developmental regulators and maintenance of ES cell state." Genes Dev **23**(21): 2484-2489.

Blache, P., M. van de Wetering, I. Duluc, C. Domon, P. Berta, J. N. Freund, H. Clevers and P. Jay (2004). "SOX9 is an intestine crypt transcription factor, is regulated by the Wnt pathway, and represses the CDX2 and MUC2 genes." J Cell Biol **166**(1): 37-47.

Boivin, G. P., K. Washington, K. Yang, J. M. Ward, T. P. Pretlow, R. Russell, D. G. Besselsen, V. L. Godfrey, T. Doetschman, W. F. Dove, H. C. Pitot, R. B. Halberg, S. H. Itzkowitz, J. Groden and

R. J. Coffey (2003). "Pathology of mouse models of intestinal cancer: consensus report and recommendations." Gastroenterology **124**(3): 762-777.

Boyer, L. A., K. Plath, J. Zeitlinger, T. Brambrink, L. A. Medeiros, T. I. Lee, S. S. Levine, M. Wernig, A. Tajonar, M. K. Ray, G. W. Bell, A. P. Otte, M. Vidal, D. K. Gifford, R. A. Young and R. Jaenisch (2006). "Polycomb complexes repress developmental regulators in murine embryonic stem cells." Nature **441**(7091): 349-353.

Brenner, C., R. Deplus, C. Didelot, A. Loriot, E. Viré, C. De Smet, A. Gutierrez, D. Danovi, D. Bernard, T. Boon, P. G. Pelicci, B. Amati, T. Kouzarides, Y. de Launoit, L. Di Croce and F. Fuks (2005). "Myc represses transcription through recruitment of DNA methyltransferase corepressor." EMBO J **24**(2): 336-346.

Bry, L., P. Falk, K. Huttner, A. Ouellette, T. Midtvedt and J. I. Gordon (1994). "Paneth cell differentiation in the developing intestine of normal and transgenic mice." Proc Natl Acad Sci U S A **91**(22): 10335-10339.

Bunz, F., A. Dutriaux, C. Lengauer, T. Waldman, S. Zhou, J. P. Brown, J. M. Sedivy, K. W. Kinzler and B. Vogelstein (1998). "Requirement for p53 and p21 to sustain G2 arrest after DNA damage." Science **282**(5393): 1497-1501.

Cahill, D. P., C. Lengauer, J. Yu, G. J. Riggins, J. K. Willson, S. D. Markowitz, K. W. Kinzler and B. Vogelstein (1998). "Mutations of mitotic checkpoint genes in human cancers." Nature **392**(6673): 300-303.

Carulli, A. J., T. M. Keeley, E. S. Demitrack, J. Chung, I. Maillard and L. C. Samuelson (2015). "Notch receptor regulation of intestinal stem cell homeostasis and crypt regeneration." Dev Biol **402**(1): 98-108.

Challen, G. A., D. Sun, M. Jeong, M. Luo, J. Jelinek, J. S. Berg, C. Bock, A. Vasanthakumar, H. Gu, Y. Xi, S. Liang, Y. Lu, G. J. Darlington, A. Meissner, J. P. Issa, L. A. Godley, W. Li and M. A. Goodell (2012). "Dnmt3a is essential for hematopoietic stem cell differentiation." Nat Genet **44**(1): 23-31.

Chang, B. D., K. Watanabe, E. V. Broude, J. Fang, J. C. Poole, T. V. Kalinichenko and I. B. Roninson (2000). "Effects of p21Waf1/Cip1/Sdi1 on cellular gene expression: implications for carcinogenesis, senescence, and age-related diseases." Proc Natl Acad Sci U S A **97**(8): 4291-4296.

Chen, P. Y., S. J. Cokus and M. Pellegrini (2010). "BS Seeker: precise mapping for bisulfite sequencing." BMC Bioinformatics **11**: 203.

Chen, Q., X. Zhang, W. M. Li, Y. Q. Ji, H. Z. Cao and P. Zheng (2014). "Prognostic value of LGR5 in colorectal cancer: a meta-analysis." PLoS One **9**(9): e107013.

Chen, R. Z., U. Pettersson, C. Beard, L. Jackson-Grusby and R. Jaenisch (1998). "DNA hypomethylation leads to elevated mutation rates." Nature **395**(6697): 89-93.

Chen, T., S. Hevi, F. Gay, N. Tsujimoto, T. He, B. Zhang, Y. Ueda and E. Li (2007). "Complete inactivation of DNMT1 leads to mitotic catastrophe in human cancer cells." Nat Genet **39**(3): 391-396.

Chen, T., Y. Ueda, J. E. Dodge, Z. Wang and E. Li (2003). "Establishment and maintenance of genomic methylation patterns in mouse embryonic stem cells by Dnmt3a and Dnmt3b." Mol Cell Biol **23**(16): 5594-5605.

Cheng, H. and C. P. Leblond (1974). "Origin, differentiation and renewal of the four main epithelial cell types in the mouse small intestine. I. Columnar cell." Am J Anat **141**(4): 461-479.

Clapier, C. R. and B. R. Cairns (2009). "The biology of chromatin remodeling complexes." Annu Rev Biochem **78**: 273-304.

Cormier, R. T. and W. F. Dove (2000). "Dnmt1N/+ reduces the net growth rate and multiplicity of intestinal adenomas in C57BL/6-multiple intestinal neoplasia (Min)/+ mice independently of p53 but demonstrates strong synergy with the modifier of Min 1(AKR) resistance allele." Cancer Res **60**(14): 3965-3970.

Creyghton, M. P., A. W. Cheng, G. G. Welstead, T. Kooistra, B. W. Carey, E. J. Steine, J. Hanna, M. A. Lodato, G. M. Frampton, P. A. Sharp, L. A. Boyer, R. A. Young and R. Jaenisch (2010).

"Histone H3K27ac separates active from poised enhancers and predicts developmental state." Proc Natl Acad Sci U S A **107**(50): 21931-21936.

Cui, H., I. L. Horon, R. Ohlsson, S. R. Hamilton and A. P. Feinberg (1998). "Loss of imprinting in normal tissue of colorectal cancer patients with microsatellite instability." Nat Med **4**(11): 1276-1280.

Cummings, D. E. and J. Overduin (2007). "Gastrointestinal regulation of food intake." J Clin Invest **117**(1): 13-23.

Deng, C., P. Zhang, J. W. Harper, S. J. Elledge and P. Leder (1995). "Mice lacking p21CIP1/WAF1 undergo normal development, but are defective in G1 checkpoint control." Cell **82**(4): 675-684.

Dialynas, G. K., M. W. Vitalini and L. L. Wallrath (2008). "Linking Heterochromatin Protein 1 (HP1) to cancer progression." Mutat Res **647**(1-2): 13-20.

Dodge, J. E., M. Okano, F. Dick, N. Tsujimoto, T. Chen, S. Wang, Y. Ueda, N. Dyson and E. Li (2005). "Inactivation of Dnmt3b in mouse embryonic fibroblasts results in DNA hypomethylation, chromosomal instability, and spontaneous immortalization." J Biol Chem **280**(18): 17986-17991.

Durand, A., B. Donahue, G. Peignon, F. Letourneur, N. Cagnard, C. Slomianny, C. Perret, N. F. Shroyer and B. Romagnolo (2012). "Functional intestinal stem cells after Paneth cell ablation induced by the loss of transcription factor Math1 (Atoh1)." Proc Natl Acad Sci U S A **109**(23): 8965-8970.

Eads, C. A., K. D. Danenberg, K. Kawakami, L. B. Saltz, P. V. Danenberg and P. W. Laird (1999). "CpG island hypermethylation in human colorectal tumors is not associated with DNA methyltransferase overexpression." Cancer Res **59**(10): 2302-2306.

Eads, C. A., A. E. Nickel and P. W. Laird (2002). "Complete genetic suppression of polyp formation and reduction of CpG-island hypermethylation in Apc(Min/+) Dnmt1-hypomorphic Mice." Cancer Res **62**(5): 1296-1299.

Edgar, R., M. Domrachev and A. E. Lash (2002). "Gene Expression Omnibus: NCBI gene expression and hybridization array data repository." Nucleic Acids Res **30**(1): 207-210.

el Marjou, F., K. P. Janssen, B. H. Chang, M. Li, V. Hindie, L. Chan, D. Louvard, P. Chambon, D. Metzger and S. Robine (2004). "Tissue-specific and inducible Cre-mediated recombination in the gut epithelium." Genesis **39**(3): 186-193.

Elliott, E. N., K. L. Sheaffer, J. Schug, T. S. Stappenbeck and K. H. Kaestner (2015). "Dnmt1 is essential to maintain progenitors in the perinatal intestinal epithelium." Development **142**(12): 2163-2172.

Esteller, M. (2005). "Aberrant DNA methylation as a cancer-inducing mechanism." Annu Rev Pharmacol Toxicol **45**: 629-656.

Esteller, M., P. G. Corn, S. B. Baylin and J. G. Herman (2001). "A gene hypermethylation profile of human cancer." Cancer Res **61**(8): 3225-3229.

Estève, P. O., H. G. Chin, A. Smallwood, G. R. Feehery, O. Gangisetty, A. R. Karpf, M. F. Carey and S. Pradhan (2006). "Direct interaction between DNMT1 and G9a coordinates DNA and histone methylation during replication." Genes Dev **20**(22): 3089-3103.

Fan, G., C. Beard, R. Z. Chen, G. Csankovszki, Y. Sun, M. Siniaia, D. Biniszkiewicz, B. Bates, P. P. Lee, R. Kuhn, A. Trumpp, C. Poon, C. B. Wilson and R. Jaenisch (2001). "DNA hypomethylation perturbs the function and survival of CNS neurons in postnatal animals." J Neurosci **21**(3): 788-797.

Faust, C., A. Schumacher, B. Holdener and T. Magnuson (1995). "The eed mutation disrupts anterior mesoderm production in mice." Development **121**(2): 273-285.

Fearon, E. R. (2011). "Molecular genetics of colorectal cancer." Annu Rev Pathol **6**: 479-507.

Feinberg, A. P., C. W. Gehrke, K. C. Kuo and M. Ehrlich (1988). "Reduced genomic 5-methylcytosine content in human colonic neoplasia." Cancer Res **48**(5): 1159-1161.

Feinberg, A. P. and B. Vogelstein (1983). "Hypomethylation distinguishes genes of some human cancers from their normal counterparts." Nature **301**(5895): 89-92.

Fordham, R. P., S. Yui, N. R. Hannan, C. Soendergaard, A. Madgwick, P. J. Schweiger, O. H. Nielsen, L. Vallier, R. A. Pedersen, T. Nakamura, M. Watanabe and K. B. Jensen (2013).

"Transplantation of expanded fetal intestinal progenitors contributes to colon regeneration after injury." Cell Stem Cell **13**(6): 734-744.

Fre, S., M. Huyghe, P. Mourikis, S. Robine, D. Louvard and S. Artavanis-Tsakonas (2005). "Notch signals control the fate of immature progenitor cells in the intestine." Nature **435**(7044): 964-968.

Fre, S., S. K. Pallavi, M. Huyghe, M. Laé, K. P. Janssen, S. Robine, S. Artavanis-Tsakonas and D. Louvard (2009). "Notch and Wnt signals cooperatively control cell proliferation and tumorigenesis in the intestine." Proc Natl Acad Sci U S A **106**(15): 6309-6314.

Galiatsatos, P. and W. D. Foulkes (2006). "Familial adenomatous polyposis." Am J Gastroenterol **101**(2): 385-398.

Gama-Sosa, M. A., V. A. Slagel, R. W. Trewyn, R. Oxenhandler, K. C. Kuo, C. W. Gehrke and M. Ehrlich (1983). "The 5-methylcytosine content of DNA from human tumors." Nucleic Acids Res **11**(19): 6883-6894.

Gao, F., Y. Zhang, S. Wang, Y. Liu, L. Zheng, J. Yang, W. Huang, Y. Ye, W. Luo and D. Xiao (2014). "Hes1 is involved in the self-renewal and tumourigenicity of stem-like cancer cells in colon cancer." Sci Rep **4**: 3963.

Gao, N. and K. H. Kaestner (2010). "Cdx2 regulates endo-lysosomal function and epithelial cell polarity." Genes Dev **24**(12): 1295-1305.

Gao, N., P. White and K. H. Kaestner (2009). "Establishment of intestinal identity and epithelial-mesenchymal signaling by Cdx2." Dev Cell **16**(4): 588-599.

Gaudet, F., J. G. Hodgson, A. Eden, L. Jackson-Grusby, J. Dausman, J. W. Gray, H. Leonhardt and R. Jaenisch (2003). "Induction of tumors in mice by genomic hypomethylation." Science **300**(5618): 489-492.

Georgia, S., M. Kanji and A. Bhushan (2013). "DNMT1 represses p53 to maintain progenitor cell survival during pancreatic organogenesis." Genes Dev **27**(4): 372-377.

Gerbe, F., B. Brulin, L. Makrini, C. Legraverend and P. Jay (2009). "DCAMKL-1 expression identifies Tuft cells rather than stem cells in the adult mouse intestinal epithelium." Gastroenterology **137**(6): 2179-2180; author reply 2180-2171.

Gerbe, F., C. Legraverend and P. Jay (2012). "The intestinal epithelium tuft cells: specification and function." Cell Mol Life Sci **69**(17): 2907-2917.

Gerbe, F., J. H. van Es, L. Makrini, B. Brulin, G. Mellitzer, S. Robine, B. Romagnolo, N. F. Shroyer, J. F. Bourgaux, C. Pignodel, H. Clevers and P. Jay (2011). "Distinct ATOH1 and Neurog3 requirements define tuft cells as a new secretory cell type in the intestinal epithelium." J Cell Biol **192**(5): 767-780.

Goelz, S. E., B. Vogelstein, S. R. Hamilton and A. P. Feinberg (1985). "Hypomethylation of DNA from benign and malignant human colon neoplasms." Science **228**(4696): 187-190.

Gupta, R. K., N. Gao, R. K. Gorski, P. White, O. T. Hardy, K. Rafiq, J. E. Brestelli, G. Chen, C. J. Stoeckert and K. H. Kaestner (2007). "Expansion of adult beta-cell mass in response to increased metabolic demand is dependent on HNF-4alpha." Genes Dev **21**(7): 756-769.

Halazonetis, T. D., V. G. Gorgoulis and J. Bartek (2008). "An oncogene-induced DNA damage model for cancer development." Science **319**(5868): 1352-1355.

Hall, P. A., P. J. Coates, B. Ansari and D. Hopwood (1994). "Regulation of cell number in the mammalian gastrointestinal tract: the importance of apoptosis." J Cell Sci **107 (Pt 12)**: 3569-3577.

Hansen, R. S., C. Wijmenga, P. Luo, A. M. Stanek, T. K. Canfield, C. M. Weemaes and S. M. Gartler (1999). "The DNMT3B DNA methyltransferase gene is mutated in the ICF immunodeficiency syndrome." Proc Natl Acad Sci U S A **96**(25): 14412-14417.

Haramis, A. P., H. Begthel, M. van den Born, J. van Es, S. Jonkheer, G. J. Offerhaus and H. Clevers (2004). "De novo crypt formation and juvenile polyposis on BMP inhibition in mouse intestine." Science **303**(5664): 1684-1686.

He, X. C., J. Zhang, W. G. Tong, O. Tawfik, J. Ross, D. H. Scoville, Q. Tian, X. Zeng, X. He, L. M. Wiedemann, Y. Mishina and L. Li (2004). "BMP signaling inhibits intestinal stem cell self-renewal through suppression of Wnt-beta-catenin signaling." Nat Genet **36**(10): 1117-1121.

.

Ho, L. L., A. Sinha, M. Verzi, K. M. Bernt, S. A. Armstrong and R. A. Shivdasani (2013). "DOT1L-mediated H3K79 methylation in chromatin is dispensable for Wnt pathway-specific and other intestinal epithelial functions." Mol Cell Biol **33**(9): 1735-1745.

Holliday, R. and J. E. Pugh (1975). "DNA modification mechanisms and gene activity during development." Science **187**(4173): 226-232.

Irizarry, R. A., C. Ladd-Acosta, B. Wen, Z. Wu, C. Montano, P. Onyango, H. Cui, K. Gabo, M. Rongione, M. Webster, H. Ji, J. B. Potash, S. Sabunciyan and A. P. Feinberg (2009). "The human colon cancer methylome shows similar hypo- and hypermethylation at conserved tissue-specific CpG island shores." Nat Genet **41**(2): 178-186.

Ishizuya-Oka, A., T. Hasebe, K. Shimizu, K. Suzuki and S. Ueda (2006). "Shh/BMP-4 signaling pathway is essential for intestinal epithelial development during Xenopus larval-to-adult remodeling." Dev Dyn **235**(12): 3240-3249.

Issa, J. P. (2004). "CpG island methylator phenotype in cancer." Nat Rev Cancer **4**(12): 988-993.

Itzkovitz, S., I. C. Blat, T. Jacks, H. Clevers and A. van Oudenaarden (2012). "Optimality in the development of intestinal crypts." Cell **148**(3): 608-619.

Jackson, M., A. Krassowska, N. Gilbert, T. Chevassut, L. Forrester, J. Ansell and B. Ramsahoye (2004). "Severe global DNA hypomethylation blocks differentiation and induces histone hyperacetylation in embryonic stem cells." Mol Cell Biol **24**(20): 8862-8871.

Jackson-Grusby, L., C. Beard, R. Possemato, M. Tudor, D. Fambrough, G. Csankovszki, J. Dausman, P. Lee, C. Wilson, E. Lander and R. Jaenisch (2001). "Loss of genomic methylation causes p53-dependent apoptosis and epigenetic deregulation." Nat Genet **27**(1): 31-39.

Jass, J. R. (2007). "Classification of colorectal cancer based on correlation of clinical, morphological and molecular features." Histopathology **50**(1): 113-130.

Jensen, J., E. E. Pedersen, P. Galante, J. Hald, R. S. Heller, M. Ishibashi, R. Kageyama, F. Guillemot, P. Serup and O. D. Madsen (2000). "Control of endodermal endocrine development by Hes-1." Nat Genet **24**(1): 36-44.

Jenuwein, T. and C. D. Allis (2001). "Translating the histone code." Science **293**(5532): 1074-1080.

Jones, P. A. and S. B. Baylin (2007). "The epigenomics of cancer." Cell **128**(4): 683-692.

Jones, P. A. and G. Liang (2009). "Rethinking how DNA methylation patterns are maintained." Nat Rev Genet **10**(11): 805-811.

Jones, P. A. and D. Takai (2001). "The role of DNA methylation in mammalian epigenetics." Science **293**(5532): 1068-1070.

Jones, P. L., G. J. Veenstra, P. A. Wade, D. Vermaak, S. U. Kass, N. Landsberger, J. Strouboulis and A. P. Wolffe (1998). "Methylated DNA and MeCP2 recruit histone deacetylase to repress transcription." Nat Genet **19**(2): 187-191.

Jones, S., M. Li, D. W. Parsons, X. Zhang, J. Wesseling, P. Kristel, M. K. Schmidt, S. Markowitz, H. Yan, D. Bigner, R. H. Hruban, J. R. Eshleman, C. A. Iacobuzio-Donahue, M. Goggins, A. Maitra, S. N. Malek, S. Powell, B. Vogelstein, K. W. Kinzler, V. E. Velculescu and N. Papadopoulos (2012). "Somatic mutations in the chromatin remodeling gene ARID1A occur in several tumor types." Hum Mutat **33**(1): 100-103.

Kaaij, L. T., M. van de Wetering, F. Fang, B. Decato, A. Molaro, H. J. van de Werken, J. H. van Es, J. Schuijers, E. de Wit, W. de Laat, G. J. Hannon, H. C. Clevers, A. D. Smith and R. F. Ketting (2013). "DNA methylation dynamics during intestinal stem cell differentiation reveals enhancers driving gene expression in the villus." Genome Biol **14**(5): R50.

Kabiri, Z., G. Greicius, B. Madan, S. Biechele, Z. Zhong, H. Zaribafzadeh, Edison, J. Aliyev, Y. Wu, R. Bunte, B. O. Williams, J. Rossant and D. M. Virshup (2014). "Stroma provides an intestinal stem cell niche in the absence of epithelial Wnts." Development **141**(11): 2206-2215.

Kaestner, K. H., S. C. Bleckmann, A. P. Monaghan, J. Schlöndorff, A. Mincheva, P. Lichter and G. Schütz (1996). "Clustered arrangement of winged helix genes fkh-6 and MFH-1: possible implications for mesoderm development." Development **122**(6): 1751-1758.

Kaestner, K. H., D. G. Silberg, P. G. Traber and G. Schütz (1997). "The mesenchymal winged helix transcription factor Fkh6 is required for the control of gastrointestinal proliferation and differentiation." Genes Dev **11**(12): 1583-1595.

Kaji, K., I. M. Caballero, R. MacLeod, J. Nichols, V. A. Wilson and B. Hendrich (2006). "The NuRD component Mbd3 is required for pluripotency of embryonic stem cells." Nat Cell Biol **8**(3): 285-292.

Karlsson, L., P. Lindahl, J. K. Heath and C. Betsholtz (2000). "Abnormal gastrointestinal development in PDGF-A and PDGFR-(alpha) deficient mice implicates a novel mesenchymal structure with putative instructive properties in villus morphogenesis." Development **127**(16): 3457-3466.

Kazanjian, A., T. Noah, D. Brown, J. Burkart and N. F. Shroyer (2010). "Atonal homolog 1 is required for growth and differentiation effects of notch/gamma-secretase inhibitors on normal and cancerous intestinal epithelial cells." Gastroenterology **139**(3): 918-928, 928.e911-916.

Kim, B. M., J. Mao, M. M. Taketo and R. A. Shivdasani (2007). "Phases of canonical Wnt signaling during the development of mouse intestinal epithelium." Gastroenterology **133**(2): 529-538.

Kim, T. H., L. O. Barrera, M. Zheng, C. Qu, M. A. Singer, T. A. Richmond, Y. Wu, R. D. Green and B. Ren (2005). "A high-resolution map of active promoters in the human genome." Nature **436**(7052): 876-880.

Kim, T. H., F. Li, I. Ferreiro-Neira, L. L. Ho, A. Luyten, K. Nalapareddy, H. Long, M. Verzi and R. A. Shivdasani (2014). "Broadly permissive intestinal chromatin underlies lateral inhibition and cell plasticity." Nature **506**(7489): 511-515.

Kim, T. H. and R. A. Shivdasani (2011). "Genetic evidence that intestinal Notch functions vary regionally and operate through a common mechanism of Math1 repression." J Biol Chem **286**(13): 11427-11433.

Knox, J. D., F. D. Araujo, P. Bigey, A. D. Slack, G. B. Price, M. Zannis-Hadjopoulos and M. Szyf (2000). "Inhibition of DNA methyltransferase inhibits DNA replication." J Biol Chem **275**(24): 17986-17990.

Korinek, V., N. Barker, P. Moerer, E. van Donselaar, G. Huls, P. J. Peters and H. Clevers (1998). "Depletion of epithelial stem-cell compartments in the small intestine of mice lacking Tcf-4." Nat Genet **19**(4): 379-383.

Kouzarides, T. (2007). "Chromatin modifications and their function." Cell **128**(4): 693-705.

Kreymann, B., G. Williams, M. A. Ghatei and S. R. Bloom (1987). "Glucagon-like peptide-1 7-36: a physiological incretin in man." Lancet **2**(8571): 1300-1304.

Krivtsov, A. V. and S. A. Armstrong (2007). "MLL translocations, histone modifications and leukaemia stem-cell development." Nat Rev Cancer **7**(11): 823-833.

Kuhnert, F., C. R. Davis, H. T. Wang, P. Chu, M. Lee, J. Yuan, R. Nusse and C. J. Kuo (2004). "Essential requirement for Wnt signaling in proliferation of adult small intestine and colon revealed by adenoviral expression of Dickkopf-1." Proc Natl Acad Sci U S A **101**(1): 266-271.

Laird, P. W., L. Jackson-Grusby, A. Fazeli, S. L. Dickinson, W. E. Jung, E. Li, R. A. Weinberg and R. Jaenisch (1995). "Suppression of intestinal neoplasia by DNA hypomethylation." Cell **81**(2): 197-205.

Lane, N., W. Dean, S. Erhardt, P. Hajkova, A. Surani, J. Walter and W. Reik (2003). "Resistance of IAPs to methylation reprogramming may provide a mechanism for epigenetic inheritance in the mouse." Genesis **35**(2): 88-93.

Leary, R. J., J. C. Lin, J. Cummins, S. Boca, L. D. Wood, D. W. Parsons, S. Jones, T. Sjöblom, B. H. Park, R. Parsons, J. Willis, D. Dawson, J. K. Willson, T. Nikolskaya, Y. Nikolsky, L. Kopelovich, N. Papadopoulos, L. A. Pennacchio, T. L. Wang, S. D. Markowitz, G. Parmigiani, K. W. Kinzler, B. Vogelstein and V. E. Velculescu (2008). "Integrated analysis of homozygous deletions, focal

amplifications, and sequence alterations in breast and colorectal cancers." Proc Natl Acad Sci U S A **105**(42): 16224-16229.

Lee, C. S. and K. H. Kaestner (2004). "Clinical endocrinology and metabolism. Development of gut endocrine cells." Best Pract Res Clin Endocrinol Metab **18**(4): 453-462.

Lengauer, C., K. W. Kinzler and B. Vogelstein (1997). "DNA methylation and genetic instability in colorectal cancer cells." Proc Natl Acad Sci U S A **94**(6): 2545-2550.

Lengauer, C., K. W. Kinzler and B. Vogelstein (1997). "Genetic instability in colorectal cancers." Nature **386**(6625): 623-627.

Leonhardt, H., A. W. Page, H. U. Weier and T. H. Bestor (1992). "A targeting sequence directs DNA methyltransferase to sites of DNA replication in mammalian nuclei." Cell **71**(5): 865-873.

Lessard, J., J. I. Wu, J. A. Ranish, M. Wan, M. M. Winslow, B. T. Staahl, H. Wu, R. Aebersold, I. A. Graef and G. R. Crabtree (2007). "An essential switch in subunit composition of a chromatin remodeling complex during neural development." Neuron **55**(2): 201-215.

Lessard, J. A. and G. R. Crabtree (2010). "Chromatin regulatory mechanisms in pluripotency." Annu Rev Cell Dev Biol **26**: 503-532.

Levy, D. B., K. J. Smith, Y. Beazer-Barclay, S. R. Hamilton, B. Vogelstein and K. W. Kinzler (1994). "Inactivation of both APC alleles in human and mouse tumors." Cancer Res **54**(22): 5953-5958.

Li, E., C. Beard and R. Jaenisch (1993). "Role for DNA methylation in genomic imprinting." Nature **366**(6453): 362-365.

Li, E., T. H. Bestor and R. Jaenisch (1992). "Targeted mutation of the DNA methyltransferase gene results in embryonic lethality." Cell **69**(6): 915-926.

Li, F., G. Mao, D. Tong, J. Huang, L. Gu, W. Yang and G. M. Li (2013). "The histone mark H3K36me3 regulates human DNA mismatch repair through its interaction with MutS α." Cell **153**(3): 590-600.

Liang, G., M. F. Chan, Y. Tomigahara, Y. C. Tsai, F. A. Gonzales, E. Li, P. W. Laird and P. A. Jones (2002). "Cooperativity between DNA methyltransferases in the maintenance methylation of repetitive elements." Mol Cell Biol **22**(2): 480-491.

Liao, J., R. Karnik, H. Gu, M. J. Ziller, K. Clement, A. M. Tsankov, V. Akopian, C. A. Gifford, J. Donaghey, C. Galonska, R. Pop, D. Reyon, S. Q. Tsai, W. Mallard, J. K. Joung, J. L. Rinn, A. Gnirke and A. Meissner (2015). "Targeted disruption of DNMT1, DNMT3A and DNMT3B in human embryonic stem cells." Nat Genet **47**(5): 469-478.

Lin, H., Y. Yamada, S. Nguyen, H. Linhart, L. Jackson-Grusby, A. Meissner, K. Meletis, G. Lo and R. Jaenisch (2006). "Suppression of intestinal neoplasia by deletion of Dnmt3b." Mol Cell Biol **26**(8): 2976-2983.

Linhart, H. G., H. Lin, Y. Yamada, E. Moran, E. J. Steine, S. Gokhale, G. Lo, E. Cantu, M. Ehrich, T. He, A. Meissner and R. Jaenisch (2007). "Dnmt3b promotes tumorigenesis in vivo by gene-specific de novo methylation and transcriptional silencing." Genes Dev **21**(23): 3110-3122.

Lister, R., M. Pelizzola, R. H. Dowen, R. D. Hawkins, G. Hon, J. Tonti-Filippini, J. R. Nery, L. Lee, Z. Ye, Q. M. Ngo, L. Edsall, J. Antosiewicz-Bourget, R. Stewart, V. Ruotti, A. H. Millar, J. A. Thomson, B. Ren and J. R. Ecker (2009). "Human DNA methylomes at base resolution show widespread epigenomic differences." Nature **462**(7271): 315-322.

Long, M. A. and F. M. Rossi (2009). "Silencing inhibits Cre-mediated recombination of the Z/AP and Z/EG reporters in adult cells." PLoS One **4**(5): e5435.

Loughery, J. E., P. D. Dunne, K. M. O'Neill, R. R. Meehan, J. R. McDaid and C. P. Walsh (2011). "DNMT1 deficiency triggers mismatch repair defects in human cells through depletion of repair protein levels in a process involving the DNA damage response." Hum Mol Genet **20**(16): 3241-3255.

Luco, R. F., Q. Pan, K. Tominaga, B. J. Blencowe, O. M. Pereira-Smith and T. Misteli (2010). "Regulation of alternative splicing by histone modifications." Science **327**(5968): 996-1000.

Luger, K., A. W. Mäder, R. K. Richmond, D. F. Sargent and T. J. Richmond (1997). "Crystal structure of the nucleosome core particle at 2.8 A resolution." Nature **389**(6648): 251-260.

Luo, Y., C. J. Wong, A. M. Kaz, S. Dzieciatkowski, K. T. Carter, S. M. Morris, J. Wang, J. E. Willis, K. W. Makar, C. M. Ulrich, J. D. Lutterbaugh, M. J. Shrubsole, W. Zheng, S. D. Markowitz and W. M. Grady (2014). "Differences in DNA methylation signatures reveal multiple pathways of progression from adenoma to colorectal cancer." Gastroenterology **147**(2): 418-429.e418.

Luongo, C., A. R. Moser, S. Gledhill and W. F. Dove (1994). "Loss of Apc+ in intestinal adenomas from Min mice." Cancer Res **54**(22): 5947-5952.

Lynch, H. T. and A. de la Chapelle (2003). "Hereditary colorectal cancer." N Engl J Med **348**(10): 919-932.

Madison, B. B., K. Braunstein, E. Kuizon, K. Portman, X. T. Qiao and D. L. Gumucio (2005). "Epithelial hedgehog signals pattern the intestinal crypt-villus axis." Development **132**(2): 279-289.

Madison, B. B., L. Dunbar, X. T. Qiao, K. Braunstein, E. Braunstein and D. L. Gumucio (2002). "Cis elements of the villin gene control expression in restricted domains of the vertical (crypt) and horizontal (duodenum, cecum) axes of the intestine." J Biol Chem **277**(36): 33275-33283.

Madison, B. B., L. B. McKenna, D. Dolson, D. J. Epstein and K. H. Kaestner (2009). "FoxF1 and FoxL1 link hedgehog signaling and the control of epithelial proliferation in the developing stomach and intestine." J Biol Chem **284**(9): 5936-5944.

Mahmoud, N. N., S. K. Boolbol, R. T. Bilinski, C. Martucci, A. Chadburn and M. M. Bertagnolli (1997). "Apc gene mutation is associated with a dominant-negative effect upon intestinal cell migration." Cancer Res **57**(22): 5045-5050.

Mahmoudi, T., S. F. Boj, P. Hatzis, V. S. Li, N. Taouatas, R. G. Vries, H. Teunissen, H. Begthel, J. Korving, S. Mohammed, A. J. Heck and H. Clevers (2010). "The leukemia-associated Mllt10/Af10-Dot1l are Tcf4/β-catenin coactivators essential for intestinal homeostasis." PLoS Biol **8**(11): e1000539.

Margueron, R. and D. Reinberg (2010). "Chromatin structure and the inheritance of epigenetic information." Nat Rev Genet **11**(4): 285-296.

Margueron, R. and D. Reinberg (2011). "The Polycomb complex PRC2 and its mark in life." Nature **469**(7330): 343-349.

Matano, M., S. Date, M. Shimokawa, A. Takano, M. Fujii, Y. Ohta, T. Watanabe, T. Kanai and T. Sato (2015). "Modeling colorectal cancer using CRISPR-Cas9-mediated engineering of human intestinal organoids." Nat Med **21**(3): 256-262.

May, R., T. E. Riehl, C. Hunt, S. M. Sureban, S. Anant and C. W. Houchen (2008). "Identification of a novel putative gastrointestinal stem cell and adenoma stem cell marker, doublecortin and CaM kinase-like-1, following radiation injury and in adenomatous polyposis coli/multiple intestinal neoplasia mice." Stem Cells **26**(3): 630-637.

Merlos-Suárez, A., F. M. Barriga, P. Jung, M. Iglesias, M. V. Céspedes, D. Rossell, M. Sevillano, X. Hernando-Momblona, V. da Silva-Diz, P. Muñoz, H. Clevers, E. Sancho, R. Mangues and E. Batlle (2011). "The intestinal stem cell signature identifies colorectal cancer stem cells and predicts disease relapse." Cell Stem Cell **8**(5): 511-524.

Michel, L. S., V. Liberal, A. Chatterjee, R. Kirchwegger, B. Pasche, W. Gerald, M. Dobles, P. K. Sorger, V. V. Murty and R. Benezra (2001). "MAD2 haplo-insufficiency causes premature anaphase and chromosome instability in mammalian cells." Nature **409**(6818): 355-359.

Miyoshi, H., R. Ajima, C. T. Luo, T. P. Yamaguchi and T. S. Stappenbeck (2012). "Wnt5a potentiates TGF-β signaling to promote colonic crypt regeneration after tissue injury." Science **338**(6103): 108-113.

Mojsov, S., G. C. Weir and J. F. Habener (1987). "Insulinotropin: glucagon-like peptide I (7-37) co-encoded in the glucagon gene is a potent stimulator of insulin release in the perfused rat pancreas." J Clin Invest **79**(2): 616-619.

Montgomery, R. K., A. E. Mulberg and R. J. Grand (1999). "Development of the human gastrointestinal tract: twenty years of progress." Gastroenterology **116**(3): 702-731.

Mortusewicz, O., L. Schermelleh, J. Walter, M. C. Cardoso and H. Leonhardt (2005). "Recruitment of DNA methyltransferase I to DNA repair sites." Proc Natl Acad Sci U S A **102**(25): 8905-8909.

Moser, A. R., W. F. Dove, K. A. Roth and J. I. Gordon (1992). "The Min (multiple intestinal neoplasia) mutation: its effect on gut epithelial cell differentiation and interaction with a modifier system." J Cell Biol **116**(6): 1517-1526.

Moser, A. R., H. C. Pitot and W. F. Dove (1990). "A dominant mutation that predisposes to multiple intestinal neoplasia in the mouse." Science **247**(4940): 322-324.

Mustata, R. C., G. Vasile, V. Fernandez-Vallone, S. Strollo, A. Lefort, F. Libert, D. Monteyne, D. Pérez-Morga, G. Vassart and M. I. Garcia (2013). "Identification of Lgr5-independent spheroid-generating progenitors of the mouse fetal intestinal epithelium." Cell Rep **5**(2): 421-432.

Nakamura, N. and K. Takenaga (1998). "Hypomethylation of the metastasis-associated S100A4 gene correlates with gene activation in human colon adenocarcinoma cell lines." Clin Exp Metastasis **16**(5): 471-479.

Nakanishi, Y., H. Seno, A. Fukuoka, T. Ueo, Y. Yamaga, T. Maruno, N. Nakanishi, K. Kanda, H. Komekado, M. Kawada, A. Isomura, K. Kawada, Y. Sakai, M. Yanagita, R. Kageyama, Y. Kawaguchi, M. M. Taketo, S. Yonehara and T. Chiba (2013). "Dclk1 distinguishes between tumor and normal stem cells in the intestine." Nat Genet **45**(1): 98-103.

Nan, X., H. H. Ng, C. A. Johnson, C. D. Laherty, B. M. Turner, R. N. Eisenman and A. Bird (1998). "Transcriptional repression by the methyl-CpG-binding protein MeCP2 involves a histone deacetylase complex." Nature **393**(6683): 386-389.

Network, C. G. A. (2012). "Comprehensive molecular characterization of human colon and rectal cancer." Nature **487**(7407): 330-337.

Nguyen, A. T. and Y. Zhang (2011). "The diverse functions of Dot1 and H3K79 methylation." Genes Dev **25**(13): 1345-1358.

Nichols, J. and A. Smith (2009). "Naive and primed pluripotent states." Cell Stem Cell **4**(6): 487-492.

Noah, T. K. and N. F. Shroyer (2013). "Notch in the intestine: regulation of homeostasis and pathogenesis." Annu Rev Physiol **75**: 263-288.

Nosho, K., K. Shima, N. Irahara, S. Kure, Y. Baba, G. J. Kirkner, L. Chen, S. Gokhale, A. Hazra, D. Spiegelman, E. L. Giovannucci, R. Jaenisch, C. S. Fuchs and S. Ogino (2009). "DNMT3B expression might contribute to CpG island methylator phenotype in colorectal cancer." Clin Cancer Res **15**(11): 3663-3671.

O'Carroll, D., S. Erhardt, M. Pagani, S. C. Barton, M. A. Surani and T. Jenuwein (2001). "The polycomb-group gene Ezh2 is required for early mouse development." Mol Cell Biol **21**(13): 4330-4336.

Okada, Y., Q. Feng, Y. Lin, Q. Jiang, Y. Li, V. M. Coffield, L. Su, G. Xu and Y. Zhang (2005). "hDOT1L links histone methylation to leukemogenesis." Cell **121**(2): 167-178.

Okano, M., D. W. Bell, D. A. Haber and E. Li (1999). "DNA methyltransferases Dnmt3a and Dnmt3b are essential for de novo methylation and mammalian development." Cell **99**(3): 247-257.

Okano, M., S. Xie and E. Li (1998). "Cloning and characterization of a family of novel mammalian DNA (cytosine-5) methyltransferases." Nat Genet **19**(3): 219-220.

Ong, C. T. and V. G. Corces (2011). "Enhancer function: new insights into the regulation of tissue-specific gene expression." Nat Rev Genet **12**(4): 283-293.

Pasini, D., A. P. Bracken, J. B. Hansen, M. Capillo and K. Helin (2007). "The polycomb group protein Suz12 is required for embryonic stem cell differentiation." Mol Cell Biol **27**(10): 3769-3779.

Pellegrinet, L., V. Rodilla, Z. Liu, S. Chen, U. Koch, L. Espinosa, K. H. Kaestner, R. Kopan, J. Lewis and F. Radtke (2011). "Dll1- and dll4-mediated notch signaling are required for homeostasis of intestinal stem cells." Gastroenterology **140**(4): 1230-1240.e1231-1237.

Perreault, N., S. D. Sackett, J. P. Katz, E. E. Furth and K. H. Kaestner (2005). "Foxl1 is a mesenchymal Modifier of Min in carcinogenesis of stomach and colon." Genes Dev **19**(3): 311-315.

Peters, A. H., S. Kubicek, K. Mechtler, R. J. O'Sullivan, A. A. Derijck, L. Perez-Burgos, A. Kohlmaier, S. Opravil, M. Tachibana, Y. Shinkai, J. H. Martens and T. Jenuwein (2003).

"Partitioning and plasticity of repressive histone methylation states in mammalian chromatin." Mol Cell **12**(6): 1577-1589.

Pino, M. S. and D. C. Chung (2010). "The chromosomal instability pathway in colon cancer." Gastroenterology **138**(6): 2059-2072.

Pinto, D., A. Gregorieff, H. Begthel and H. Clevers (2003). "Canonical Wnt signals are essential for homeostasis of the intestinal epithelium." Genes Dev **17**(14): 1709-1713.

Plasschaert, R. N. and M. S. Bartolomei (2014). "Genomic imprinting in development, growth, behavior and stem cells." Development **141**(9): 1805-1813.

Portela, A. and M. Esteller (2010). "Epigenetic modifications and human disease." Nat Biotechnol **28**(10): 1057-1068.

Porter, E. M., C. L. Bevins, D. Ghosh and T. Ganz (2002). "The multifaceted Paneth cell." Cell Mol Life Sci **59**(1): 156-170.

Rajagopalan, H., M. A. Nowak, B. Vogelstein and C. Lengauer (2003). "The significance of unstable chromosomes in colorectal cancer." Nat Rev Cancer **3**(9): 695-701.

Ramalho-Santos, M., D. A. Melton and A. P. McMahon (2000). "Hedgehog signals regulate multiple aspects of gastrointestinal development." Development **127**(12): 2763-2772.

Reisman, D., S. Glaros and E. A. Thompson (2009). "The SWI/SNF complex and cancer." Oncogene **28**(14): 1653-1668.

Reynolds, N., M. Salmon-Divon, H. Dvinge, A. Hynes-Allen, G. Balasooriya, D. Leaford, A. Behrens, P. Bertone and B. Hendrich (2012). "NuRD-mediated deacetylation of H3K27 facilitates recruitment of Polycomb Repressive Complex 2 to direct gene repression." EMBO J **31**(3): 593-605.

Riccio, O., M. E. van Gijn, A. C. Bezdek, L. Pellegrinet, J. H. van Es, U. Zimber-Strobl, L. J. Strobl, T. Honjo, H. Clevers and F. Radtke (2008). "Loss of intestinal crypt progenitor cells owing to inactivation of both Notch1 and Notch2 is accompanied by derepression of CDK inhibitors p27Kip1 and p57Kip2." EMBO Rep **9**(4): 377-383.

Roberts, D. J., R. L. Johnson, A. C. Burke, C. E. Nelson, B. A. Morgan and C. Tabin (1995). "Sonic hedgehog is an endodermal signal inducing Bmp-4 and Hox genes during induction and regionalization of the chick hindgut." Development **121**(10): 3163-3174.

Roberts, D. J., D. M. Smith, D. J. Goff and C. J. Tabin (1998). "Epithelial-mesenchymal signaling during the regionalization of the chick gut." Development **125**(15): 2791-2801.

Rodriguez, J., J. Frigola, E. Vendrell, R. A. Risques, M. F. Fraga, C. Morales, V. Moreno, M. Esteller, G. Capellà, M. Ribas and M. A. Peinado (2006). "Chromosomal instability correlates with genome-wide DNA demethylation in human primary colorectal cancers." Cancer Res **66**(17): 8462-9468.

Samuel, M. S., H. Suzuki, M. Buchert, T. L. Putoczki, N. C. Tebbutt, T. Lundgren-May, A. Christou, M. Inglese, M. Toyota, J. K. Heath, R. L. Ward, P. M. Waring and M. Ernst (2009). "Elevated Dnmt3a activity promotes polyposis in Apc(Min) mice by relaxing extracellular restraints on Wnt signaling." Gastroenterology **137**(3): 902-913, 913.e901-911.

San Roman, A. K., C. D. Jayewickreme, L. C. Murtaugh and R. A. Shivdasani (2014). "Wnt secretion from epithelial cells and subepithelial myofibroblasts is not required in the mouse intestinal stem cell niche in vivo." Stem Cell Reports **2**(2): 127-134.

Sansom, O. J., K. R. Reed, A. J. Hayes, H. Ireland, H. Brinkmann, I. P. Newton, E. Batlle, P. Simon-Assmann, H. Clevers, I. S. Nathke, A. R. Clarke and D. J. Winton (2004). "Loss of Apc in vivo immediately perturbs Wnt signaling, differentiation, and migration." Genes Dev **18**(12): 1385-1390.

Sato, T., J. H. van Es, H. J. Snippert, D. E. Stange, R. G. Vries, M. van den Born, N. Barker, N. F. Shroyer, M. van de Wetering and H. Clevers (2011). "Paneth cells constitute the niche for Lgr5 stem cells in intestinal crypts." Nature **469**(7330): 415-418.

Sato, T., R. G. Vries, H. J. Snippert, M. van de Wetering, N. Barker, D. E. Stange, J. H. van Es, A. Abo, P. Kujala, P. J. Peters and H. Clevers (2009). "Single Lgr5 stem cells build crypt-villus structures in vitro without a mesenchymal niche." Nature **459**(7244): 262-265.

Saxonov, S., P. Berg and D. L. Brutlag (2006). "A genome-wide analysis of CpG dinucleotides in the human genome distinguishes two distinct classes of promoters." Proc Natl Acad Sci U S A **103**(5): 1412-1417.

Schneider, C. A., W. S. Rasband and K. W. Eliceiri (2012). "NIH Image to ImageJ: 25 years of image analysis." Nat Methods **9**(7): 671-675.

Schuettengruber, B., A. M. Martinez, N. Iovino and G. Cavalli (2011). "Trithorax group proteins: switching genes on and keeping them active." Nat Rev Mol Cell Biol **12**(12): 799-814.

Sheaffer, K. L. and K. H. Kaestner (2012). "Transcriptional networks in liver and intestinal development." Cold Spring Harb Perspect Biol **4**(9): a008284.

Sheaffer, K. L., R. Kim, R. Aoki, E. N. Elliott, J. Schug, L. Burger, D. Schübeler and K. H. Kaestner (2014). "DNA methylation is required for the control of stem cell differentiation in the small intestine." Genes Dev **28**(6): 652-664.

Shen, X., Y. Liu, Y. J. Hsu, Y. Fujiwara, J. Kim, X. Mao, G. C. Yuan and S. H. Orkin (2008). "EZH1 mediates methylation on histone H3 lysine 27 and complements EZH2 in maintaining stem cell identity and executing pluripotency." Mol Cell **32**(4): 491-502.

Shroyer, N. F., M. A. Helmrath, V. Y. Wang, B. Antalffy, S. J. Henning and H. Y. Zoghbi (2007). "Intestine-specific ablation of mouse atonal homolog 1 (Math1) reveals a role in cellular homeostasis." Gastroenterology **132**(7): 2478-2488.

Siegel, R., C. Desantis and A. Jemal (2014). "Colorectal cancer statistics, 2014." CA Cancer J Clin **64**(2): 104-117.

Smallwood, A., P. O. Estève, S. Pradhan and M. Carey (2007). "Functional cooperation between HP1 and DNMT1 mediates gene silencing." Genes Dev **21**(10): 1169-1178.

Smith, Z. D. and A. Meissner (2013). "DNA methylation: roles in mammalian development." Nat Rev Genet **14**(3): 204-220.

Spada, F., A. Haemmer, D. Kuch, U. Rothbauer, L. Schermelleh, E. Kremmer, T. Carell, G. Längst and H. Leonhardt (2007). "DNMT1 but not its interaction with the replication machinery is required for maintenance of DNA methylation in human cells." J Cell Biol **176**(5): 565-571.

Stadler, M. B., R. Murr, L. Burger, R. Ivanek, F. Lienert, A. Schöler, E. van Nimwegen, C. Wirbelauer, E. J. Oakeley, D. Gaidatzis, V. K. Tiwari and D. Schübeler (2011). "DNA-binding factors shape the mouse methylome at distal regulatory regions." Nature **480**(7378): 490-495.

Stanger, B. Z., R. Datar, L. C. Murtaugh and D. A. Melton (2005). "Direct regulation of intestinal fate by Notch." Proc Natl Acad Sci U S A **102**(35): 12443-12448.

Su, L. K., K. W. Kinzler, B. Vogelstein, A. C. Preisinger, A. R. Moser, C. Luongo, K. A. Gould and W. F. Dove (1992). "Multiple intestinal neoplasia caused by a mutation in the murine homolog of the APC gene." Science **256**(5057): 668-670.

Sukegawa, A., T. Narita, T. Kameda, K. Saitoh, T. Nohno, H. Iba, S. Yasugi and K. Fukuda (2000). "The concentric structure of the developing gut is regulated by Sonic hedgehog derived from endodermal epithelium." Development **127**(9): 1971-1980.

Suzuki, H., D. N. Watkins, K. W. Jair, K. E. Schuebel, S. D. Markowitz, W. D. Chen, T. P. Pretlow, B. Yang, Y. Akiyama, M. Van Engeland, M. Toyota, T. Tokino, Y. Hinoda, K. Imai, J. G. Herman and S. B. Baylin (2004). "Epigenetic inactivation of SFRP genes allows constitutive WNT signaling in colorectal cancer." Nat Genet **36**(4): 417-422.

Takai, D. and P. A. Jones (2002). "Comprehensive analysis of CpG islands in human chromosomes 21 and 22." Proc Natl Acad Sci U S A **99**(6): 3740-3745.

Takeda, N., R. Jain, M. R. LeBoeuf, Q. Wang, M. M. Lu and J. A. Epstein (2011). "Interconversion between intestinal stem cell populations in distinct niches." Science **334**(6061): 1420-1424.

Tao, S., D. Tang, Y. Morita, T. Sperka, O. Omrani, A. Lechel, V. Sakk, J. Kraus, H. A. Kestler, M. Kühl and K. L. Rudolph (2015). "Wnt activity and basal niche position sensitize intestinal stem and progenitor cells to DNA damage." EMBO J **34**(5): 624-640.

Tate, P. H. and A. P. Bird (1993). "Effects of DNA methylation on DNA-binding proteins and gene expression." Curr Opin Genet Dev **3**(2): 226-231.

Thirman, M. J., H. J. Gill, R. C. Burnett, D. Mbangkollo, N. R. McCabe, H. Kobayashi, S. Ziemin-van der Poel, Y. Kaneko, R. Morgan and A. A. Sandberg (1993). "Rearrangement of the MLL

gene in acute lymphoblastic and acute myeloid leukemias with 11q23 chromosomal translocations." N Engl J Med **329**(13): 909-914.

Tian, H., B. Biehs, C. Chiu, C. W. Siebel, Y. Wu, M. Costa, F. J. de Sauvage and O. D. Klein (2015). "Opposing activities of notch and wnt signaling regulate intestinal stem cells and gut homeostasis." Cell Rep **11**(1): 33-42.

Tian, H., B. Biehs, S. Warming, K. G. Leong, L. Rangell, O. D. Klein and F. J. de Sauvage (2011). "A reserve stem cell population in small intestine renders Lgr5-positive cells dispensable." Nature **478**(7368): 255-259.

Tie, F., R. Banerjee, C. A. Stratton, J. Prasad-Sinha, V. Stepanik, A. Zlobin, M. O. Diaz, P. C. Scacheri and P. J. Harte (2009). "CBP-mediated acetylation of histone H3 lysine 27 antagonizes Drosophila Polycomb silencing." Development **136**(18): 3131-3141.

Toyota, M., N. Ahuja, M. Ohe-Toyota, J. G. Herman, S. B. Baylin and J. P. Issa (1999). "CpG island methylator phenotype in colorectal cancer." Proc Natl Acad Sci U S A **96**(15): 8681-8686.

Trapnell, C., A. Roberts, L. Goff, G. Pertea, D. Kim, D. R. Kelley, H. Pimentel, S. L. Salzberg, J. L. Rinn and L. Pachter (2012). "Differential gene and transcript expression analysis of RNA-seq experiments with TopHat and Cufflinks." Nat Protoc **7**(3): 562-578.

Trasler, J., L. Deng, S. Melnyk, I. Pogribny, F. Hiou-Tim, S. Sibani, C. Oakes, E. Li, S. J. James and R. Rozen (2003). "Impact of Dnmt1 deficiency, with and without low folate diets, on tumor numbers and DNA methylation in Min mice." Carcinogenesis **24**(1): 39-45.

Tremblay, K. D., J. R. Saam, R. S. Ingram, S. M. Tilghman and M. S. Bartolomei (1995). "A paternal-specific methylation imprint marks the alleles of the mouse H19 gene." Nat Genet **9**(4): 407-413.

Troughton, W. D. and J. S. Trier (1969). "Paneth and goblet cell renewal in mouse duodenal crypts." J Cell Biol **41**(1): 251-268.

Tsumura, A., T. Hayakawa, Y. Kumaki, S. Takebayashi, M. Sakaue, C. Matsuoka, K. Shimotohno, F. Ishikawa, E. Li, H. R. Ueda, J. Nakayama and M. Okano (2006). "Maintenance of

self-renewal ability of mouse embryonic stem cells in the absence of DNA methyltransferases Dnmt1, Dnmt3a and Dnmt3b." Genes Cells **11**(7): 805-814.

Unterberger, A., S. D. Andrews, I. C. Weaver and M. Szyf (2006). "DNA methyltransferase 1 knockdown activates a replication stress checkpoint." Mol Cell Biol **26**(20): 7575-7586.

van de Wetering, M., E. Sancho, C. Verweij, W. de Lau, I. Oving, A. Hurlstone, K. van der Horn, E. Batlle, D. Coudreuse, A. P. Haramis, M. Tjon-Pon-Fong, P. Moerer, M. van den Born, G. Soete, S. Pals, M. Eilers, R. Medema and H. Clevers (2002). "The beta-catenin/TCF-4 complex imposes a crypt progenitor phenotype on colorectal cancer cells." Cell **111**(2): 241-250.

van der Flier, L. G. and H. Clevers (2009). "Stem cells, self-renewal, and differentiation in the intestinal epithelium." Annu Rev Physiol **71**: 241-260.

van der Flier, L. G., A. Haegebarth, D. E. Stange, M. van de Wetering and H. Clevers (2009). "OLFM4 is a robust marker for stem cells in human intestine and marks a subset of colorectal cancer cells." Gastroenterology **137**(1): 15-17.

van Es, J. H., N. de Geest, M. van de Born, H. Clevers and B. A. Hassan (2010). "Intestinal stem cells lacking the Math1 tumour suppressor are refractory to Notch inhibitors." Nat Commun **1**: 18.

van Es, J. H., T. Sato, M. van de Wetering, A. Lyubimova, A. N. Nee, A. Gregorieff, N. Sasaki, L. Zeinstra, M. van den Born, J. Korving, A. C. Martens, N. Barker, A. van Oudenaarden and H. Clevers (2012). "Dll1+ secretory progenitor cells revert to stem cells upon crypt damage." Nat Cell Biol **14**(10): 1099-1104.

van Es, J. H., M. E. van Gijn, O. Riccio, M. van den Born, M. Vooijs, H. Begthel, M. Cozijnsen, S. Robine, D. J. Winton, F. Radtke and H. Clevers (2005). "Notch/gamma-secretase inhibition turns proliferative cells in intestinal crypts and adenomas into goblet cells." Nature **435**(7044): 959-963.

Vandesompele, J., K. De Preter, F. Pattyn, B. Poppe, N. Van Roy, A. De Paepe and F. Speleman (2002). "Accurate normalization of real-time quantitative RT-PCR data by geometric averaging of multiple internal control genes." Genome Biol **3**(7): RESEARCH0034.

VanDussen, K. L., A. J. Carulli, T. M. Keeley, S. R. Patel, B. J. Puthoff, S. T. Magness, I. T. Tran, I. Maillard, C. Siebel, Å. Kolterud, A. S. Grosse, D. L. Gumucio, S. A. Ernst, Y. H. Tsai, P. J.

Dempsey and L. C. Samuelson (2012). "Notch signaling modulates proliferation and differentiation of intestinal crypt base columnar stem cells." Development **139**(3): 488-497.

VanDussen, K. L. and L. C. Samuelson (2010). "Mouse atonal homolog 1 directs intestinal progenitors to secretory cell rather than absorptive cell fate." Dev Biol **346**(2): 215-223.

Velasco, G., F. Hubé, J. Rollin, D. Neuillet, C. Philippe, H. Bouzinba-Segard, A. Galvani, E. Viegas-Péquignot and C. Francastel (2010). "Dnmt3b recruitment through E2F6 transcriptional repressor mediates germ-line gene silencing in murine somatic tissues." Proc Natl Acad Sci U S A **107**(20): 9281-9286.

Venkatesh, S., M. Smolle, H. Li, M. M. Gogol, M. Saint, S. Kumar, K. Natarajan and J. L. Workman (2012). "Set2 methylation of histone H3 lysine 36 suppresses histone exchange on transcribed genes." Nature **489**(7416): 452-455.

Venolia, L. and S. M. Gartler (1983). "Comparison of transformation efficiency of human active and inactive X-chromosomal DNA." Nature **302**(5903): 82-83.

Verzi, M. P., H. Shin, H. H. He, R. Sulahian, C. A. Meyer, R. K. Montgomery, J. C. Fleet, M. Brown, X. S. Liu and R. A. Shivdasani (2010). "Differentiation-specific histone modifications reveal dynamic chromatin interactions and partners for the intestinal transcription factor CDX2." Dev Cell **19**(5): 713-726.

Verzi, M. P., H. Shin, L. L. Ho, X. S. Liu and R. A. Shivdasani (2011). "Essential and redundant functions of caudal family proteins in activating adult intestinal genes." Mol Cell Biol **31**(10): 2026-2039.

Verzi, M. P., H. Shin, A. K. San Roman, X. S. Liu and R. A. Shivdasani (2013). "Intestinal master transcription factor CDX2 controls chromatin access for partner transcription factor binding." Mol Cell Biol **33**(2): 281-292.

Vilar, E. and S. B. Gruber (2010). "Microsatellite instability in colorectal cancer-the stable evidence." Nat Rev Clin Oncol **7**(3): 153-162.

Viré, E., C. Brenner, R. Deplus, L. Blanchon, M. Fraga, C. Didelot, L. Morey, A. Van Eynde, D. Bernard, J. M. Vanderwinden, M. Bollen, M. Esteller, L. Di Croce, Y. de Launoit and F. Fuks

(2006). "The Polycomb group protein EZH2 directly controls DNA methylation." Nature **439**(7078): 871-874.

Vogelstein, B., E. R. Fearon, S. R. Hamilton, S. E. Kern, A. C. Preisinger, M. Leppert, Y. Nakamura, R. White, A. M. Smits and J. L. Bos (1988). "Genetic alterations during colorectal-tumor development." N Engl J Med **319**(9): 525-532.

Waddington, C. H. (2012). "The epigenotype. 1942." Int J Epidemiol **41**(1): 10-13.

Wade, P. A., A. Gegonne, P. L. Jones, E. Ballestar, F. Aubry and A. P. Wolffe (1999). "Mi-2 complex couples DNA methylation to chromatin remodelling and histone deacetylation." Nat Genet **23**(1): 62-66.

Waterston, R. H., K. Lindblad-Toh, E. Birney, J. Rogers, J. F. Abril, P. Agarwal, R. Agarwala, R. Ainscough, M. Alexandersson, P. An, S. E. Antonarakis, J. Attwood, R. Baertsch, J. Bailey, K. Barlow, S. Beck, E. Berry, B. Birren, T. Bloom, P. Bork, M. Botcherby, N. Bray, M. R. Brent, D. G. Brown, S. D. Brown, C. Bult, J. Burton, J. Butler, R. D. Campbell, P. Carninci, S. Cawley, F. Chiaromonte, A. T. Chinwalla, D. M. Church, M. Clamp, C. Clee, F. S. Collins, L. L. Cook, R. R. Copley, A. Coulson, O. Couronne, J. Cuff, V. Curwen, T. Cutts, M. Daly, R. David, J. Davies, K. D. Delehaunty, J. Deri, E. T. Dermitzakis, C. Dewey, N. J. Dickens, M. Diekhans, S. Dodge, I. Dubchak, D. M. Dunn, S. R. Eddy, L. Elnitski, R. D. Emes, P. Eswara, E. Eyras, A. Felsenfeld, G. A. Fewell, P. Flicek, K. Foley, W. N. Frankel, L. A. Fulton, R. S. Fulton, T. S. Furey, D. Gage, R. A. Gibbs, G. Glusman, S. Gnerre, N. Goldman, L. Goodstadt, D. Grafham, T. A. Graves, E. D. Green, S. Gregory, R. Guigó, M. Guyer, R. C. Hardison, D. Haussler, Y. Hayashizaki, L. W. Hillier, A. Hinrichs, W. Hlavina, T. Holzer, F. Hsu, A. Hua, T. Hubbard, A. Hunt, I. Jackson, D. B. Jaffe, L. S. Johnson, M. Jones, T. A. Jones, A. Joy, M. Kamal, E. K. Karlsson, D. Karolchik, A. Kasprzyk, J. Kawai, E. Keibler, C. Kells, W. J. Kent, A. Kirby, D. L. Kolbe, I. Korf, R. S. Kucherlapati, E. J. Kulbokas, D. Kulp, T. Landers, J. P. Leger, S. Leonard, I. Letunic, R. Levine, J. Li, M. Li, C. Lloyd, S. Lucas, B. Ma, D. R. Maglott, E. R. Mardis, L. Matthews, E. Mauceli, J. H. Mayer, M. McCarthy, W. R. McCombie, S. McLaren, K. McLay, J. D. McPherson, J. Meldrim, B. Meredith, J. P. Mesirov, W. Miller, T. L. Miner, E. Mongin, K. T. Montgomery, M. Morgan, R. Mott,

J. C. Mullikin, D. M. Muzny, W. E. Nash, J. O. Nelson, M. N. Nhan, R. Nicol, Z. Ning, C. Nusbaum, M. J. O'Connor, Y. Okazaki, K. Oliver, E. Overton-Larty, L. Pachter, G. Parra, K. H. Pepin, J. Peterson, P. Pevzner, R. Plumb, C. S. Pohl, A. Poliakov, T. C. Ponce, C. P. Ponting, S. Potter, M. Quail, A. Reymond, B. A. Roe, K. M. Roskin, E. M. Rubin, A. G. Rust, R. Santos, V. Sapojnikov, B. Schultz, J. Schultz, M. S. Schwartz, S. Schwartz, C. Scott, S. Seaman, S. Searle, T. Sharpe, A. Sheridan, R. Shownkeen, S. Sims, J. B. Singer, G. Slater, A. Smit, D. R. Smith, B. Spencer, A. Stabenau, N. Stange-Thomann, C. Sugnet, M. Suyama, G. Tesler, J. Thompson, D. Torrents, E. Trevaskis, J. Tromp, C. Ucla, A. Ureta-Vidal, J. P. Vinson, A. C. Von Niederhausern, C. M. Wade, M. Wall, R. J. Weber, R. B. Weiss, M. C. Wendl, A. P. West, K. Wetterstrand, R. Wheeler, S. Whelan, J. Wierzbowski, D. Willey, S. Williams, R. K. Wilson, E. Winter, K. C. Worley, D. Wyman, S. Yang, S. P. Yang, E. M. Zdobnov, M. C. Zody, E. S. Lander and M. G. S. Consortium (2002). "Initial sequencing and comparative analysis of the mouse genome." Nature **420**(6915): 520-562.

Weisenberger, D. J., K. D. Siegmund, M. Campan, J. Young, T. I. Long, M. A. Faasse, G. H. Kang, M. Widschwendter, D. Weener, D. Buchanan, H. Koh, L. Simms, M. Barker, B. Leggett, J. Levine, M. Kim, A. J. French, S. N. Thibodeau, J. Jass, R. Haile and P. W. Laird (2006). "CpG island methylator phenotype underlies sporadic microsatellite instability and is tightly associated with BRAF mutation in colorectal cancer." Nat Genet **38**(7): 787-793.

Westphalen, C. B., S. Asfaha, Y. Hayakawa, Y. Takemoto, D. J. Lukin, A. H. Nuber, A. Brandtner, W. Setlik, H. Remotti, A. Muley, X. Chen, R. May, C. W. Houchen, J. G. Fox, M. D. Gershon, M. Quante and T. C. Wang (2014). "Long-lived intestinal tuft cells serve as colon cancer-initiating cells." J Clin Invest **124**(3): 1283-1295.

Widschwendter, M., H. Fiegl, D. Egle, E. Mueller-Holzner, G. Spizzo, C. Marth, D. J. Weisenberger, M. Campan, J. Young, I. Jacobs and P. W. Laird (2007). "Epigenetic stem cell signature in cancer." Nat Genet **39**(2): 157-158.

Wood, L. D., D. W. Parsons, S. Jones, J. Lin, T. Sjöblom, R. J. Leary, D. Shen, S. M. Boca, T. Barber, J. Ptak, N. Silliman, S. Szabo, Z. Dezso, V. Ustyanksky, T. Nikolskaya, Y. Nikolsky, R.

Karchin, P. A. Wilson, J. S. Kaminker, Z. Zhang, R. Croshaw, J. Willis, D. Dawson, M. Shipitsin, J. K. Willson, S. Sukumar, K. Polyak, B. H. Park, C. L. Pethiyagoda, P. V. Pant, D. G. Ballinger, A. B. Sparks, J. Hartigan, D. R. Smith, E. Suh, N. Papadopoulos, P. Buckhaults, S. D. Markowitz, G. Parmigiani, K. W. Kinzler, V. E. Velculescu and B. Vogelstein (2007). "The genomic landscapes of human breast and colorectal cancers." Science **318**(5853): 1108-1113.

Xu, G. L., T. H. Bestor, D. Bourc'his, C. L. Hsieh, N. Tommerup, M. Bugge, M. Hulten, X. Qu, J. J. Russo and E. Viegas-Péquignot (1999). "Chromosome instability and immunodeficiency syndrome caused by mutations in a DNA methyltransferase gene." Nature **402**(6758): 187-191.

Xue, Y., J. Wong, G. T. Moreno, M. K. Young, J. Côté and W. Wang (1998). "NURD, a novel complex with both ATP-dependent chromatin-remodeling and histone deacetylase activities." Mol Cell **2**(6): 851-861.

Yamada, Y., L. Jackson-Grusby, H. Linhart, A. Meissner, A. Eden, H. Lin and R. Jaenisch (2005). "Opposing effects of DNA hypomethylation on intestinal and liver carcinogenesis." Proc Natl Acad Sci U S A **102**(38): 13580-13585.

Yang, A. S., M. R. Estécio, K. Doshi, Y. Kondo, E. H. Tajara and J. P. Issa (2004). "A simple method for estimating global DNA methylation using bisulfite PCR of repetitive DNA elements." Nucleic Acids Res **32**(3): e38.

Yang, Q., N. A. Bermingham, M. J. Finegold and H. Y. Zoghbi (2001). "Requirement of Math1 for secretory cell lineage commitment in the mouse intestine." Science **294**(5549): 2155-2158.

Zee, B. M., R. S. Levin, B. Xu, G. LeRoy, N. S. Wingreen and B. A. Garcia (2010). "In vivo residue-specific histone methylation dynamics." J Biol Chem **285**(5): 3341-3350.

Zhang, Y., H. H. Ng, H. Erdjument-Bromage, P. Tempst, A. Bird and D. Reinberg (1999). "Analysis of the NuRD subunits reveals a histone deacetylase core complex and a connection with DNA methylation." Genes Dev **13**(15): 1924-1935.

Zheng, X., K. Tsuchiya, R. Okamoto, M. Iwasaki, Y. Kano, N. Sakamoto, T. Nakamura and M. Watanabe (2011). "Suppression of hath1 gene expression directly regulated by hes1 via notch

signaling is associated with goblet cell depletion in ulcerative colitis." Inflamm Bowel Dis **17**(11): 2251-2260.

Zhu, W. G., K. Srinivasan, Z. Dai, W. Duan, L. J. Druhan, H. Ding, L. Yee, M. A. Villalona-Calero, C. Plass and G. A. Otterson (2003). "Methylation of adjacent CpG sites affects Sp1/Sp3 binding and activity in the p21(Cip1) promoter." Mol Cell Biol **23**(12): 4056-4065.

Ziller, M. J., H. Gu, F. Müller, J. Donaghey, L. T. Tsai, O. Kohlbacher, P. L. De Jager, E. D. Rosen, D. A. Bennett, B. E. Bernstein, A. Gnirke and A. Meissner (2013). "Charting a dynamic DNA methylation landscape of the human genome." Nature **500**(7463): 477-481.